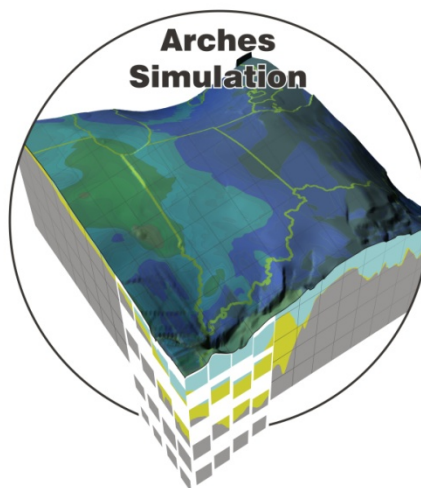


VARIABLE DENSITY FLOW MODELING FOR SIMULATION FRAMEWORK FOR REGIONAL GEOLOGIC CO₂ STORAGE ALONG ARCHES PROVINCE OF MIDWESTERN UNITED STATES

TOPICAL REPORT



October 2011

Reporting Period: October 1, 2010 - September 30, 2011

DOE Award Number: DE-FE0001034

Ohio Department of Development Grant Agreement: CDO/D-10-03

Principal Investigator: Joel Sminchak
Energy Systems & Carbon Management
Battelle Memorial Institute
505 King Avenue
Columbus, OH 43201



This report was prepared as an account of work sponsored by an agency of the United States Government. Neither the United States Government nor any agency thereof, nor any of their employees, makes any warranty, express or implied, or assumes any legal liability or responsibility for the accuracy, completeness, or usefulness of any information, apparatus, product, or process disclosed, or represents that its use would not infringe privately owned rights. Reference herein to any specific commercial product, process, or service by trade name, trademark, manufacturer, or otherwise does not necessarily constitute or imply its endorsement, recommendation, or favoring by the United States Government or any agency thereof. The views and opinions of authors expressed herein do not necessarily state or reflect those of the United States Government or any agency thereof.

ABSTRACT

The Arches Province in the Midwestern U.S. has been identified as a major area for carbon dioxide (CO₂) storage applications because of the intersection of Mt. Simon sandstone reservoir thickness and permeability. To better understand large-scale CO₂ storage infrastructure requirements in the Arches Province, variable density scoping level modeling was completed. Three main tasks were completed for the variable density modeling:

- Single-phase, variable density groundwater flow modeling,
- Scoping level multi-phase simulations, and
- Preliminary basin-scale multi-phase simulations.

The variable density modeling task was successful in evaluating appropriate input data for the Arches Province numerical simulations. Data from the geocellular model developed earlier in the project were translated into preliminary numerical models. These models were calibrated to observed conditions in the Mt. Simon, suggesting a suitable geologic depiction of the system. The initial models were used to assess boundary conditions, calibrate to reservoir conditions, examine grid dimensions, evaluate upscaling items, and develop regional storage field scenarios. The task also provided practical information on items related to CO₂ storage applications in the Arches Province such as pressure buildup estimates, well spacing limitations, and injection field arrangements.

The Arches Simulation project is a three-year effort and part of the United States Department of Energy (U.S. DOE)/National Energy Technology Laboratory (NETL) program on innovative and advanced technologies and protocols for monitoring/verification/accounting (MVA), simulation, and risk assessment of CO₂ sequestration in geologic formations. The overall objective of the project is to develop a simulation framework for regional geologic CO₂ storage infrastructure along the Arches Province of the Midwestern U.S. The project is supported by U.S. DOE/NETL under agreement DE-FE0001034 and Ohio Department of Development under agreement CDO/D-10-03.

TABLE OF CONTENTS

ABSTRACT	iii
LIST OF FIGURES	iv
LIST OF TABLES	vi
LIST OF ACRONYMS	vii
EXECUTIVE SUMMARY	viii
Section 1.0: INTRODUCTION	1
1.1 Background	1
1.2 Objectives	1
1.3 Methods	2
1.4 Previous Work	2
1.5 Assumptions/Limitations	2
Section 2.0: SINGLE-PHASE FLOW SIMULATIONS	4
2.1 MODFLOW/SEAWAT Overview	4
2.2 Model Setup	5
2.3 Simulation Scenarios	9
2.4 Results	11
Section 3.0: SCOPING SIMULATIONS	24
3.1 Scoping Simulations Overview	24
3.2 Model Setup – Generic Case	24
3.3 Scenarios – Generic Case	26
3.4 Results – Generic Case	26
3.5 Summary – Generic Case	30
3.6 Model Setup – Site-specific Case	30
3.7 Scenarios – Site-Specific Case	35
3.8 Results – Site-Specific Case	35
3.9 Summary – Site-specific Case	38
3.10 CO ₂ Storage Capacity Analysis	38
Section 4.0: PRELIMINARY BASIN SCALE SIMULATIONS	41
4.1 Basin Scale Simulation Overview	41
4.2 Model Setup	41
4.4 Simulation Results	51
Section 5.0: CONCLUSIONS	56
Section 6.0: REFERENCES	58

LIST OF FIGURES

Figure 2-1. 3D Image of SEAWAT Model Setup	7
Figure 2-2. SEAWAT Layers	7
Figure 2-3. SEAWAT Model Domain and Grid	8
Figure 2-4. Observed Reservoir Pressure Map for Mt. Simon Formation	9
Figure 2-5. On-Site and Regional Injection Field Scenario Location Map	11

Figure 2-6. SEAWAT Simulated Reservoir Pressure Map for Mt. Simon Formation	12
Figure 2-7. Calibration Map for SEAWAT Model Showing Observed vs. Simulated Pressure in the Mt. Simon Formation	13
Figure 2-8. Simulated Flow Vector Map for Mt. Simon Sandstone (Model Layer 4).....	15
Figure 2-9. Sensitivity Plot for 0.2X to 5.0X Permeability Scaling Factors.....	16
Figure 2-10. SEAWAT Simulated Delta Pressure 1×10 million metric tons/yr per well [7 Mt/yr total injection]	18
Figure 2-11. SEAWAT Simulated Delta Pressure 7×2 million metric tons/yr per well [14 Mt/yr total injection]	18
Figure 2-12. SEAWAT Simulated Delta Pressure 7×3 million metric tons/yr per well (21 Mt/yr total injection)	19
Figure 2-13. SEAWAT Simulated Delta Pressure 7×5 million metric tons/yr per well [35 Mt/yr total injection]	19
Figure 2-14. SEAWAT Simulated Delta Pressure 7×10 million metric tons/yr per well [70 Mt/yr total injection]	20
Figure 2-15. SEAWAT Simulation Showing Upward Migration of Low-Density Brine Fluid in Vertical Cross Section Through a Regional Injection Well Injecting at 1 Million Metric Tons CO ₂ Per Year after 20 Years of Injection.....	21
Figure 2-16. SEAWAT Simulated Delta Pressure- 10% On-Site Injection (25.6 Mt/yr total injection)...	22
Figure 2-17. SEAWAT Simulated Delta Pressure- 25% On-Site Injection (64 Mt/yr total injection).....	23
Figure 2-18. SEAWAT Simulated Delta Pressure- 50% On-Site Injection (128 Mt/yr total injection)....	23
Figure 3.1 Model Geometry, Generic Case	25
Figure 3-2. Pressure and Saturation Contours (25 mile site radius, 5×5 well array)	26
Figure 3-3. Pressure Buildup at Mid-point of Mt. Simon (25 mile site radius, 5×5 well array).....	27
Figure 3-4. Pressure and Saturation Contours (32 mile site radius, 6×6 well array)	28
Figure 3-5. Pressure Buildup at Mid-point of the Mt. Simon (32 mile site radius, 6×6 well array).....	28
Figure 3-6. Pressure and Saturation Contours (40 mile site radius, 7×7 well array)	28
Figure 3-7. Pressure Buildup at Mid-point of the Mt. Simon (40 mile site radius, 7×7 well array).....	29
Figure 3-8. Pressure Buildup as a Function of Site Radius and Well Array	29
Figure 3-9. Potential Regional Storage Field Locations	30
Figure 3-10. Stratigraphic Columns at Each Regional Site	31
Figure 3-11. Model Domain Simplification.....	32
Figure 3-12. Model Geometry (Site 7, Model A)	32
Figure 3-13. Averaged Porosity Profile (left panel) and Permeability Profile (right panel) at Site 7.....	33
Figure 3-14. Relative Permeability Curves (Case 1 [VG_Mualem] – left panel, and Case 2 [VG_Mualem_fit] – right panel).....	35
Figure 3-15. Pressure and Saturation Contours (Site 7, Model A, Case 1).....	36
Figure 3-16. Pressure and Saturation Contours (Site 7, Model A, Case 2).....	36
Figure 3-17. Injection Well Pressure Buildup (Site 7, Model A Case 1, Case 2).....	37
Figure 3-18. CO ₂ Mass Flux Integral across EC-MS Interface (Site 7, Model A, Case 1, Case 2).....	37
Figure 3-19. Calculated Plume Radii for Seven Regional Storage Sites in the Mt. Simon for 20 Year Injection at 10 and 20 MMT/yr with 1% and 4% Storage Efficiency Factors.....	39
Figure 3-20. Calculated Plume Radii for 50 Source-Located Storage Sites in the Mt. Simon for 20 Year Injection Using 25% and 50% CO ₂ Source Output with 1% and 4% Storage Efficiency Factors.....	40
Figure 4-1. Geocellular Model Porosity Distribution for the Eau Claire.....	42
Figure 4-2. Geocellular Porosity Distribution for the Mt. Simon	42
Figure 4-3. Geocellular Model Permeability Distribution for the Eau Claire.....	43
Figure 4-4. Geocellular Model Permeability Distribution for the Mt. Simon.....	43
Figure 4-5. Plan View Numerical Model Mesh Showing Injection Well Locations	44
Figure 4-6. Three-Dimensional Boundary Fitted Grid (Inactive Cells are Shown in Green).....	45
Figure 4-6. Schematic of a Boundary Fitted Cell	46

Figure 4-7. Schematic Showing the Data Cells (in black lines) and Simulation Cells (in blue lines) (The cells or the portion of the cells that fall within the boundary of a simulation cell are contributors for property upscaling.)	46
Figure 4-8. Porosity Distribution Upscaled to Boundary Fitted Simulation Mesh	47
Figure 4-9. Lateral Permeability Distribution Upscaled to Boundary Fitted Simulation Mesh.....	48
Figure 4-10. Vertical Permeability Distribution Upscaled to Boundary Fitted Simulation Mesh	49
Figure 4-11. Initial Reservoir Pressure Established from Steady-State Simulation	50
Figure 4-12. Initial Reservoir Temperature Established from Steady-State Simulation.....	51
Figure 4-13. Gas Pressure after 15 years of CO ₂ Injection	52
Figure 4-14. Gas Pressure in the Area Near Each Injection Location After 15 Years of CO ₂ Injection ..	53
Figure 4-15. Gas Saturation in the Area Near Each Injection Location After 15 Years of CO ₂ Injection ..	54
Figure 4-16. Intrinsic Permeability in the Area Near Each Injection Location	55

LIST OF TABLES

Table 2-1. Variable Density Simulation Input Parameters.....	6
Table 2-2. Comparison of Flow Budgets for Arches Province Simulation and Eberts and George Regional Aquifer System Analysis for Midwestern Basins and Arches	14
Table 2-3. SEAWAT Regional Storage Field Scenarios.....	17
Table 2-4. SEAWAT On-Site Injection Scenarios	22
Table 3.1 Model Parameters, Generic Case	25
Table 3.2. Model Dimensions and Injection Rate, Generic Case.....	26
Table 3-3. Capillary Pressure Curve Parameters, Case 1 and Case 2.....	35

LIST OF ACRONYMS

2D	two-dimensional
3D	three-dimensional
CO ₂	carbon dioxide
GIS	geographic information system
mD	millidarcy
MICP	mercury injection capillary pressure
MRCSP	Midwest Regional Carbon Sequestration Partnership
MVA	monitoring/verification/accounting
NETL	National Energy Technology Laboratory
psi	pounds per square inch
QA/QC	quality assurance/quality control
SCAL	special core analysis
STOMP	Subsurface Transport Over Multiple Phases
Ss	sub sea
U.S. DOE	U.S. Department of Energy

EXECUTIVE SUMMARY

This Topical Report presents a summary of preliminary variable density modeling completed for the Arches Province in the Midwestern U.S. The Arches Simulation project is designed to develop a simulation framework for regional geologic carbon dioxide (CO₂) storage infrastructure along the Arches Province through: 1) development of a geologic model, and 2) advanced reservoir simulations of large-scale CO₂ storage along the province. The goal of this project is to build a geologic model for the Arches Province and complete advanced reservoir simulations necessary for effective implementation of large-scale CO₂ storage in the region. The Arches Province in the Midwestern U.S. has been identified as a major area for CO₂ sequestration because of the intersection of reservoir thickness and permeability along the province. The province includes areas of Indiana, Kentucky, Michigan, and Ohio along several arch structures between the Appalachian, Illinois, and Michigan sedimentary basins. The main injection target is the Mt. Simon sandstone due to its depth, thickness, hydraulic properties, and brine salinity.

The Arches Simulation project is a three-year effort as part of the U.S. Department of Energy (DOE)/National Energy Technology Laboratory (NETL) program on monitoring/verification/accounting (MVA), simulation, and risk assessment of CO₂ sequestration in geologic formations. The project is supported by U.S. DOE/NETL under agreement DE-FE0001034 and Ohio Department of Development under agreement CDO/D-10-03. The project research team consists of Battelle Memorial Institute, Battelle Pacific Northwest Division, the Geological Surveys of Ohio, Indiana, and Kentucky, and Western Michigan University.

The objective of the variable density modeling was to evaluate model input for the full basin-scale simulations. Overall, the variable density modeling is an intermediate step to more complex simulations. The initial models were designed to assess boundary conditions, calibrate to reservoir conditions, examine grid dimensions, evaluate upscaling items, and develop regional storage field scenarios. The models also allowed review of the translation of the geocellular model into numerical flow models. The task also provided practical information on items related to CO₂ storage applications in the Arches Province such as pressure buildup estimates, well spacing limitations, and injection field arrangements.

The variable density modeling was divided into three main components:

- Single-phase groundwater flow modeling,
- Scoping level multi-phase simulations, and
- Preliminary basin-scale multi-phase simulations.

Each model was based on the geocellular model developed earlier with this project. The single-phase simulations were completed with a variable density flow model. These simulations were used for model calibration, examination of boundary conditions, and simulation of on-site and regional storage scenarios. The scoping level multi-phase simulations were completed to examine dynamics of regional storage field arrangements and key model input parameters such as relative permeability curves. The preliminary basin-scale multi-phase simulations were completed to investigate issues related to running complex numerical simulations across the large area included in the Arches Province.

The variable density models represent a simplified version of real CO₂ storage systems, because it does not incorporate CO₂ phase behavior or immiscibility with brine. Consequently, this simplified model has inherent assumptions and limitations related to simulating fluid flow processes. The variable density simulations were intended to provide general guidance for a large region of the Midwestern U.S. A site-specific CO₂ storage project would require field work such as seismic surveys, drilling, geophysical logging, reservoir tests, detailed reservoir modeling, and system design. The results of this report shall not be viewed or interpreted as a definitive assessment of suitability of candidate geologic CO₂ storage

formations, the presence of suitable caprocks, or sufficient injectivity to allow CO₂ sequestration to be carried out in an economic manner.

Initial single-phase flow simulations were developed for the Arches Province based on the geocellular model dataset. The single-phase flow simulations were completed with the computer codes MODFLOW (McDonald and Harbaugh, 1988) and SEAWAT (Langevin et al., 2007). These single-phase simulations helped provide guidance on input parameters for the more complex multiple-phase simulations. The model results indicate suitable calibration to observed reservoir pressure, flow budget, and flow vectors in the Mt. Simon.

The SEAWAT model suggests that fairly high resolution grid spacing is necessary around the injection wells to capture CO₂ injection processes. Grid cell spacing less than 500 m by 500 m X-Y is likely necessary around injection wells. Otherwise, the cells are too large to accurately simulate changes in saturation. Well modules are another option for simulating near-well processes. However, the coarser grid spacing appears sufficient to simulate pressure changes on a basin scale.

Scoping level simulations were run with the multi-phase code STOMP in two-dimensional (2D) mode. The first set of simulations was completed based on general conditions in the model domain for 5X5, 6X6, and 7X7 well clusters at several injection rates. Simulation results were analyzed for injection potential and pressure buildup. The second set of simulations was based on site-specific conditions at seven potential regional storage sites identified in the pipeline routing study. These simulations were used to evaluate the range of conditions expected within the Arches Province. The simulations were also used to assess effects of relative permeability curves based on Leverett J-function fit of mercury injection capillary pressure test data on Mt. Simon rock cores completed in association with the Arches Province. In general, the simulations seemed insensitive to capillary pressure relationships, suggesting these processes may not be critical for basin-scale models. The local-scale column models were useful for establishing the expected magnitude of plume movement and pressure buildup in the near-field. Furthermore, using representative columns from proposed regional storage sites aided in estimating plume size and pressure buildup at each site. The simulations also provided a basis for balancing injection rates across sites to maximize sweep efficiency and balance pressures in the near-field.

The preliminary basin-scale multi-phase simulations indicated that more grid refinement and material property evaluation were needed near the injection areas to capture the impacts of injecting a significant amount of mass into a regional reservoir. With the simplified model, the affects were too localized and probably not representative of the regional affect of multiple injection areas with large amounts of total injected mass. The next steps for full basin-scale model will be to refine the grid further, particularly in the vertical direction and use a number of wells within each injection area to inject the CO₂. A network of wells within each injection area will provide a more representative model and distribute the CO₂ more reasonably into the reservoir. In addition, the regional model will be used to establish boundary conditions for submodels where the grid resolution and injection scenarios can be constructed in a more realistic manner.

Section 1.0: INTRODUCTION

The Arches Simulation project is designed to develop a simulation framework for regional geologic carbon dioxide (CO₂) storage infrastructure along the Arches Province through development of a geologic model and advanced reservoir simulations of large-scale CO₂ storage along the province. This report presents a summary of the variable density modeling task.

1.1 Background

The Arches Province in the Midwestern U.S. has been identified as a major area for CO₂ sequestration because of the intersection of reservoir thickness and permeability along the province. The province includes areas of Indiana, Kentucky, Michigan, and Ohio along several arch structures between the Appalachian, Illinois, and Michigan sedimentary basins. The main injection target is the Mt. Simon sandstone due to its depth, thickness, hydraulic properties, and brine salinity. There are many existing CO₂ sources in proximity to the Arches Province, and the area is adjacent to the Ohio River Valley corridor of coal-fired power plants such that it may be feasible to access the area with a pipeline network.

The Arches Simulation project is a three-year effort as part of the United States Department of Energy (U.S. DOE)/National Energy Technology Laboratory (NETL) program on innovative and advanced technologies and protocols for monitoring/verification/accounting (MVA), simulation, and risk assessment of CO₂ sequestration in geologic formations. The project is supported by U.S. DOE/NETL under agreement DE-FE0001034 and Ohio Department of Development under agreement CDO/D-10-03. The work includes seven main tasks aimed at compiling hydrogeological information on the Mt. Simon sandstone and confining layers, development of model framework, preliminary variable density flow simulations, multiple-phase model runs of regional storage infrastructure scenarios, and analyzing implications for regional storage feasibility. The research team consists of Battelle Memorial Institute, Battelle Pacific Northwest Division, the Geological Surveys of Ohio, Indiana, and Kentucky, and Western Michigan University.

1.2 Objectives

The overall objective of this project is to develop a simulation framework for regional geologic CO₂ storage infrastructure along the Arches Province of the Midwestern U.S. The goal of this project is to build a geologic model for the Arches Province and complete advanced reservoir simulations necessary for effective implementation of large-scale CO₂ storage in the region. The project is focused on connecting a very strong set of existing field data to advanced simulation concepts and address key emerging issues in sequestration modeling. The work will represent applied simulation of CO₂ storage—the widespread application along a major, regional geologic structure in an area of the country with a dense concentration of large CO₂ sources.

The objective of the variable density modeling task was to evaluate model input for the full basin-scale simulations. Overall, the variable density modeling is an intermediate step to more complex simulations. These initial models can be completed in less time, so multiple runs may be completed to examine a wide array of input parameters. The initial models were designed to assess boundary conditions, calibrate to reservoir conditions, examine grid dimensions, evaluate upscaling items, and develop regional storage field scenarios. The models also allowed review of the translation of the geocellular model into numerical flow models. The task also provided practical information on items related to CO₂ storage applications in the Arches Province such as pressure buildup estimates, well spacing limitations, and injection field arrangements.

1.3 Methods

The variable density modeling was divided into three main components:

- Single-phase groundwater flow modeling,
- Scoping level multi-phase simulations, and
- Preliminary basin-scale multi-phase simulations.

Each model was based on the geocellular model developed earlier with this project. The single-phase simulations were completed with a variable density flow model. These simulations were used for model calibration, examination of boundary conditions, and simulation of on-site and regional storage scenarios. The scoping level multi-phase simulations were completed to examine dynamics of regional storage field arrangements and key model input parameters such as relative permeability curves. The preliminary basin-scale multi-phase simulations were completed to investigate issues related to running complex numerical simulations across the large area included in the Arches Province.

1.4 Previous Work

Initial work on the project involved compiling and interpreting information on the deep rock formations, Mt. Simon injection well operations, and geotechnical data. This information was summarized in the topical report *Data Package Summary Report: Simulation Framework for Regional Geologic CO₂ Storage Along Arches Province of the Midwest United States* (Battelle, 2010). Based on this information, a conceptual model was developed for the Arches Province that integrates geologic and hydrologic information on the Eau Claire and Mt. Simon formations into a geocellular model. The conceptual model describes the geologic setting, stratigraphy, geologic structures, hydrologic features, and distribution of key hydraulic parameters. The conceptual model is focused on the Mt. Simon sandstone and Eau Claire formations. The geocellular model depicts the parameters and conditions in a numerical array that may be imported into the numerical simulations of CO₂ storage. The conceptual model was designed to feed numerical simulations of large-scale CO₂ storage in the Arches Province region. The conceptual model was summarized in the topical report *Conceptual Model Summary Report Simulation Framework for Regional Geologic CO₂ Storage Infrastructure Along Arches Province of Midwestern United States* (Battelle, 2011).

1.5 Assumptions/Limitations

The variable density models are numerical representations of fluid flow processes in the subsurface. Consequently, the models have inherent assumptions and limitations related to depicting fluid flow processes. Major assumptions and limitations to the variable density simulations are listed as follows:

- Research was focused on the Arches Province. Adjacent areas in the Appalachian Basin, Illinois Basin, Michigan Basin, Ontario Province, and Wisconsin were not reviewed in detail.
- Since this is a basin-scale simulation study, it was necessary to generalize many trends in geology and input parameters. In general, any CO₂ storage project would require more detailed investigation of rock formations in the project area.
- The models are based on numerical equations that predict fluid flow through permeable media. These fundamental equations of fluid flow have been established in hydrogeology and reservoir engineering. However, they may not account for all the variations in natural systems.
- Model results were calibrated to available field data on the Mt. Simon and Eau Claire formations. These data are limited in many areas and may be influenced by field methods.

Implementation of a CO₂ storage project is a multi-year effort involving site screening, site assessment, characterization, testing, and system design. The variable density simulations were intended to provide general guidance for a large region of the Midwestern U.S. A site-specific CO₂ storage project would require field work such as seismic surveys, drilling, geophysical logging, reservoir tests, detailed reservoir modeling, and system design. The results of this report shall not be viewed or interpreted as a definitive assessment of suitability of candidate geologic CO₂ storage formations, the presence of suitable caprocks, or sufficient injectivity to allow CO₂ sequestration to be carried out in an economical manner.

Section 2.0: SINGLE-PHASE FLOW SIMULATIONS

This section describes the initial single-phase flow simulations completed for the Arches Province. The objective of single-phase simulations was to provide guidance on input parameters for the more complex multiple-phase simulations. The single-phase simulations were performed with variable density groundwater flow computer codes. These codes simulate brine flow and variable density effects. The models do not account for multi-phase behavior related to supercritical CO₂. Therefore, the models have limitations. However, the models allow rapid numerical solutions, and many different model iterations can be evaluated to determine a suitable model setup. By porting the single-phase flow simulation results to the multi-phase model, the modeling process will be streamlined and more effective.

2.1 MODFLOW/SEAWAT Overview

The single-phase flow simulations were completed with the computer codes MODFLOW (McDonald and Harbaugh, 1988) and SEAWAT (Langevin et al., 2007). MODFLOW is a modular finite-difference flow model computer code designed to simulate the flow of groundwater through aquifers. The code was developed by the United States Geological Survey (USGS) and is well accepted for scientific and industrial applications. The code is based on solution of the partial differential equation for fluid flow in three dimensions. The modular nature of the program has allowed addition of many specialized modules. Because the code does not simulate multiple-phase behavior of CO₂, MODFLOW has not been frequently used to simulate CO₂ sequestration. However, the code solves the same fundamental Darcy equation of fluid flow as other computer codes. Nicot et al. (2009) applied MODFLOW to investigate pressure buildup and fluid migration issues related to CO₂ sequestration operations in aquifer systems in the Texas Gulf Coast. The single-phase flow simulations in this project follow a similar process and objectives.

SEAWAT is a MODFLOW-based computer program designed to simulate variable density groundwater flow and solute transport. The program has been used to assess issues related to brine migration in aquifers and saltwater intrusion. The SEAWAT code simulates variable density flow processes based on numerical equations which account for relative density difference terms, solute mass accumulation terms, and conservation of mass. The main advantage of the SEAWAT code is that it provides a proxy for upward migration of CO₂. The code may also provide some indication of the CO₂ injection plume by way of solute proxy.

There are limitations related to simulating CO₂ storage with the SEAWAT program. The program does not address multiple-phase processes related to supercritical CO₂ and brine mixtures. The program does not address the low viscosity properties of super critical CO₂ injected into the rock formations. CO₂ dissolution into brine is also not accounted for in the code. The models do not have the capacity to completely model density changes of CO₂ related to temperature/pressure conditions. However, pressure and flow away from the CO₂/brine interface may be accurately portrayed by the codes. In addition, the model has the capability to accommodate complex arrangements of permeability, fluid density, boundary conditions, and other parameters. Consequently, the single-phase SEAWAT simulations are useful for examining overall model input and setup.

The MODFLOW/SEAWAT codes represent fluid heads in terms of head elevation because aquifers are typically monitored in relation to water level elevation. Conditions in deep reservoirs are typically measured in pressure units of pounds per square inch (psi). To allow easier comparison with observed pressure in the Mt. Simon sandstone, the results of the MODFLOW/SEAWAT simulations were converted into pressure based on average pressure gradient in the Mt. Simon. This conversion equates 70 m head to approximately 100 psi.

2.2 Model Setup

The numerical model was developed in MODFLOW/SEAWAT using a modeling package (Figure 2-1). Several model iterations were completed to determine appropriate model setup. Table 2-1 summarizes the final model input parameters. The model was specified with six layers from the Knox to the Precambrian formations (Figure 2-2). The Knox layer was included as a blank layer to assist in analysis of flux across layers. The Mt. Simon was represented by three layers to depict upward migration of low density fluid. The model was run in transient mode for 36,500 days, which allows for injection and post-injection periods. To facilitate numerical solution, cells in areas where the Mt. Simon is greater than approximately 2,100 m deep were designated as inactive (Figure 2-3). During model development, it was determined that higher grid resolution around injection wells was necessary to facilitate accurate model solution near the injection wells.

The Knox and Precambrian layers were specified as homogeneous permeability distributions. The Eau Claire was specified as a variable permeability distribution based on the average values across the formation in the geocellular model (Battelle, 2011). The Mt. Simon layers were also given a variable permeability distribution based on average values across the formation in the geocellular model. The same permeability distribution was assigned for all three Mt. Simon layers in the model. Therefore, there was no vertical heterogeneity represented in the permeability distribution. Uniform porosity and storage parameters were input for each model layer.

Several different boundary condition arrangements were evaluated during model development. Overall, the boundary conditions were assigned based on the reservoir pressure map for the Mt. Simon prepared as part of the conceptual model (Figure 2-4). The boundary conditions were input to match this pressure distribution and limit their influence in the central portion of the model. The effects of several different boundary condition arrangements were examined in the SEAWAT model. The final model was calibrated to Mt. Simon pressures based on specified heads in the western and eastern edges of the model. The model was set up with no flow boundaries in the northeast and southern areas. A zone of specified heads was also assigned in the central portion of the study area in the Knox layer to allow calibration. These boundary conditions were generally similar to previous work by Gupta and Bair (1997) and other simulation projects for the Illinois basin (Clifford, 1973; Person, et al., 2010; Zou et al., 2010).

Table 2-1. Variable Density Simulation Input Parameters

Parameter	Value	Comment
Flow model	MODFLOW/SEWAT	MODFLOW 2000, transient simulation, total simulation time = 36,500 days (100 years)
Domain	700 x 700 km	Inactive cells specified in areas where Mt. Simon is greater than 2,100 m deep or not present
Rows	163 - 262	Resolution increased near wells for injection scenarios
Columns	144 - 244	Resolution increased near wells for injection scenarios
Grid Spacing	10,000 x 10,000 m to 500 x 500 m	Variable grid spacing with grid increased grid resolution increased near injection wells
Layers	6	Variable thickness based on structure maps: Layer 1 = Knox Layer 2 = Eau Claire Layer 3 = Mt. Simon (upper 1/3 rd) Layer 4 = Mt. Simon (middle 1/3 rd) Layer 5 = Mt. Simon (lower 1/3 rd) Layer 6 = Precambrian
Permeability	Constant value for layers 1 and 6 Variable distribution for layers 2-5	Layer 1 (Knox) = 2.6 mD Layer 2 (Eau Claire) = based on geocellular model Layer 3-5 (Mt. Simon) = based on geocellular model Layer 6 (Precambrian) = 0.0008 mD
Porosity	Constant value for layers 1 and 6 Variable distribution for layers 2-5	Layer 1 (Knox) = 0.044 Layer 2 (Eau Claire) = based on geocellular model Layer 3-5 (Mt. Simon) = based on geocellular model Layer 6 (Precambrian) = 0.018
Bulk Compressibility	Constant value for layers 1-6	2E-6 1/m
Boundaries	Constant head, no flow	Constant head nodes specified at E, N, and W edges No flow boundary specified at southern boundary Constant head specified in central portion of Knox
Solution Parameters	WHS, head change criterion = 0.001	<0.01% volumetric budget error
Transport model	SEAWAT	Salinity proxy for CO ₂
Reference Fluid Density	1,100 kg/m ³	Constant distribution
Reservoir Temperature	Not applicable	Not an input parameter in SEAWAT
Source Term	Constant Concentration Source	Low density salinity proxy for CO ₂

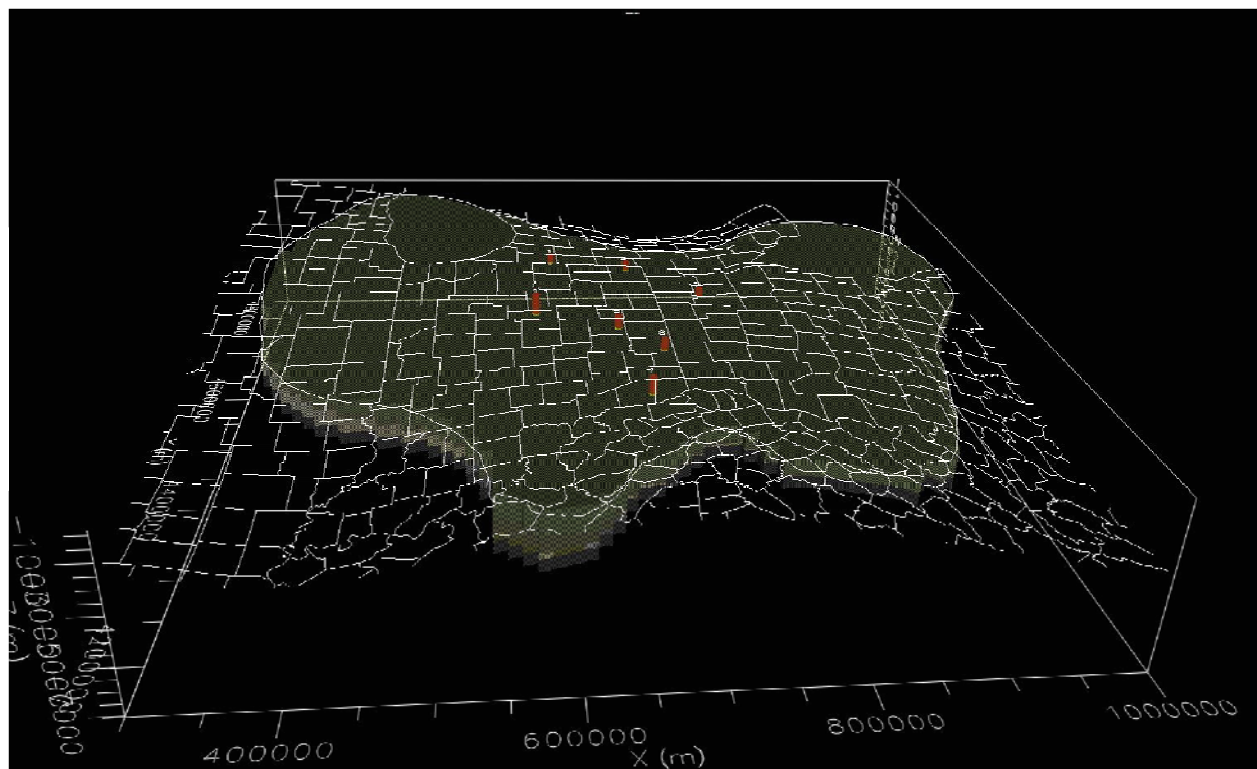


Figure 2-1. 3D Image of SEAWAT Model Setup

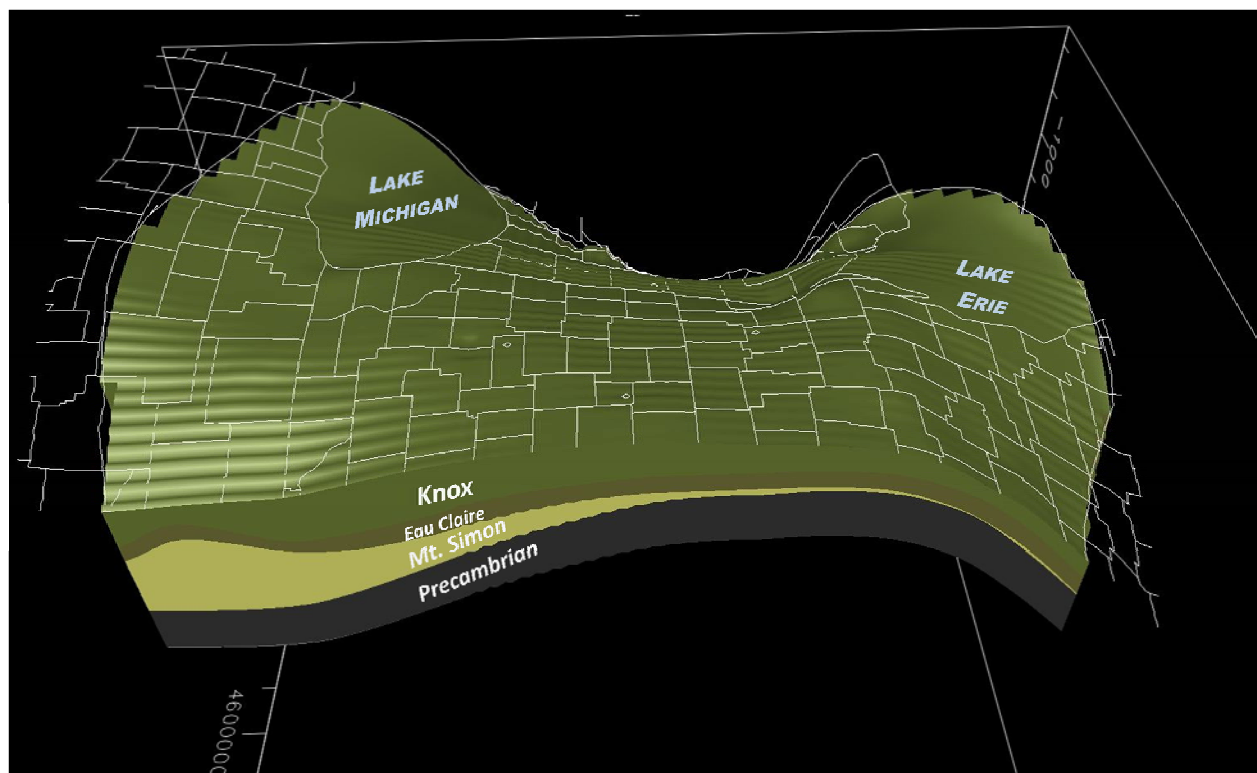


Figure 2-2. SEAWAT Layers

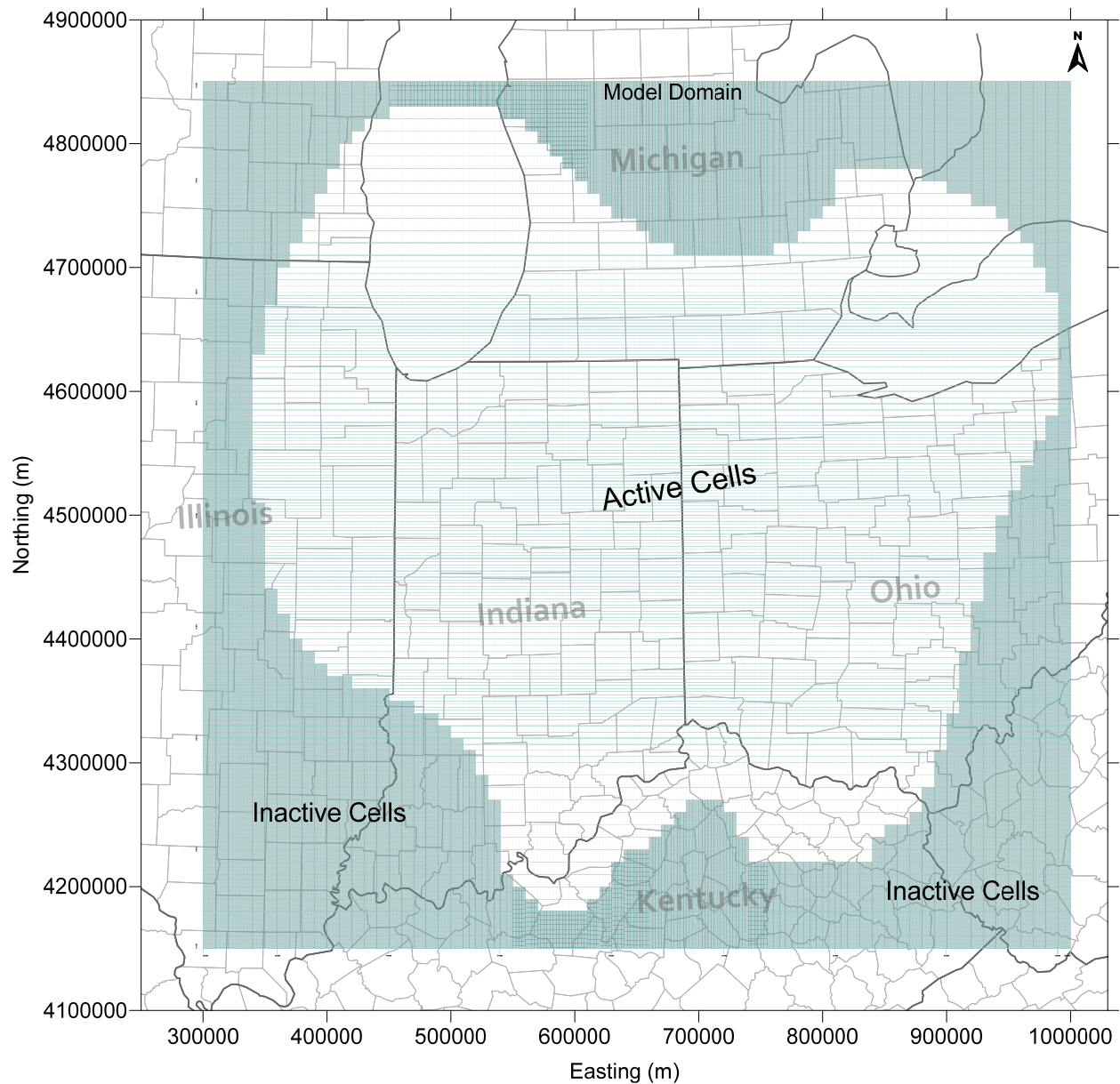


Figure 2-3. SEAWAT Model Domain and Grid

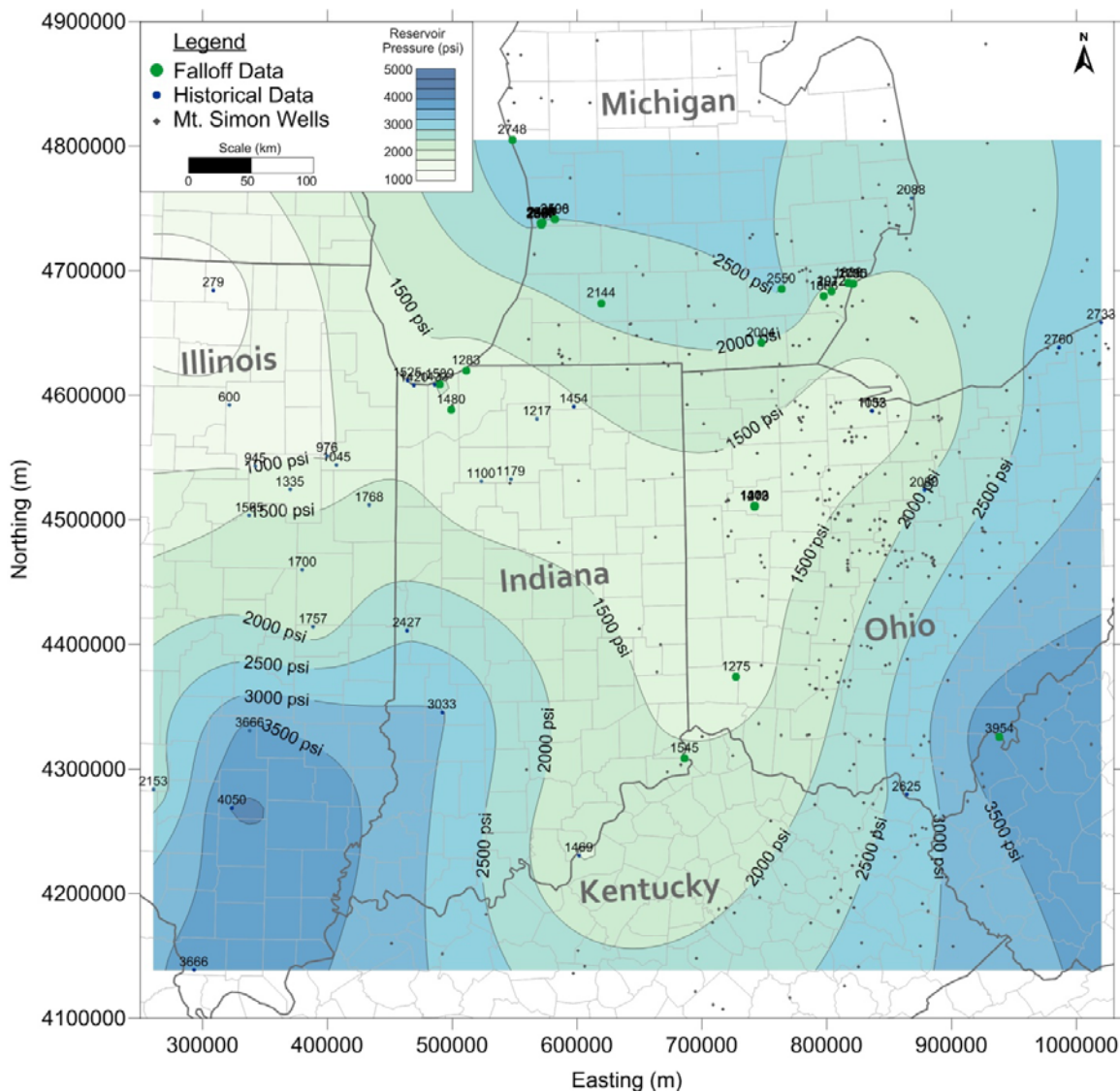


Figure 2-4. Observed Reservoir Pressure Map for Mt. Simon Formation

2.3 Simulation Scenarios

Three main scenarios were simulated with the SEAWAT model (Figure 2-5):

- 1) no injection baseline,
- 2) regional injection fields, and
- 3) on-site injection (Figure 2-5).

As described in the *Conceptual Model Topical Report* (Battelle 2011), there are approximately 131 point sources in the area with emissions greater than 100,000 metric tons CO₂ per year. There are 53 point sources with emissions over 1 million metric tons per year, which have total emissions of 262 million metric tons CO₂ per year. To reduce greenhouse gas emissions in the Arches Province by 25 to 50%, CO₂ storage projects with total storage rates of 70 to 140 million metric tons CO₂ per year would be necessary.

The regional storage field scenario was based on the pipeline routing study completed in earlier portions of the project. The scenario assumes that a pipeline distribution system will be constructed to transport CO₂ from sources to seven regional CO₂ storage fields. The pipeline routing study was conducted using the CO₂ pipeline transport cost estimation model developed by MIT's Carbon Capture and Sequestration Technologies Program. This program was used in conjunction with CO₂ source and carbon sink location data selected for the study. The MIT model was developed as a tool to be used within the ArcGIS software package to calculate a least cost path between two selected points and produce construction cost outputs associated with that path. These pipeline routes suggest there are some central areas where pipeline routes intersect or blend together. These locations may be practical potential regional storage fields. Seven locations were selected as potential regional storage field locations. These locations are fairly arbitrary. Several other locations may be feasible for regional storage fields. However, the seven locations do represent coverage across the Arches Province. The locations are separated by at least 50 km, which should minimize interference between storage fields.

The on-site injection scenario addresses point sources with emissions greater than 1 million metric tons CO₂ per year. These 53 sources account for 91.6% of point source emissions in the Arches Province. The sources are mostly clustered along the Great Lakes coastline and Ohio River Valley, which generally do not have the most appealing geologic setting for CO₂ storage. Scenarios were run for injection of 25% and 50% of each sites' total emissions. The injection period was set at 20 years.

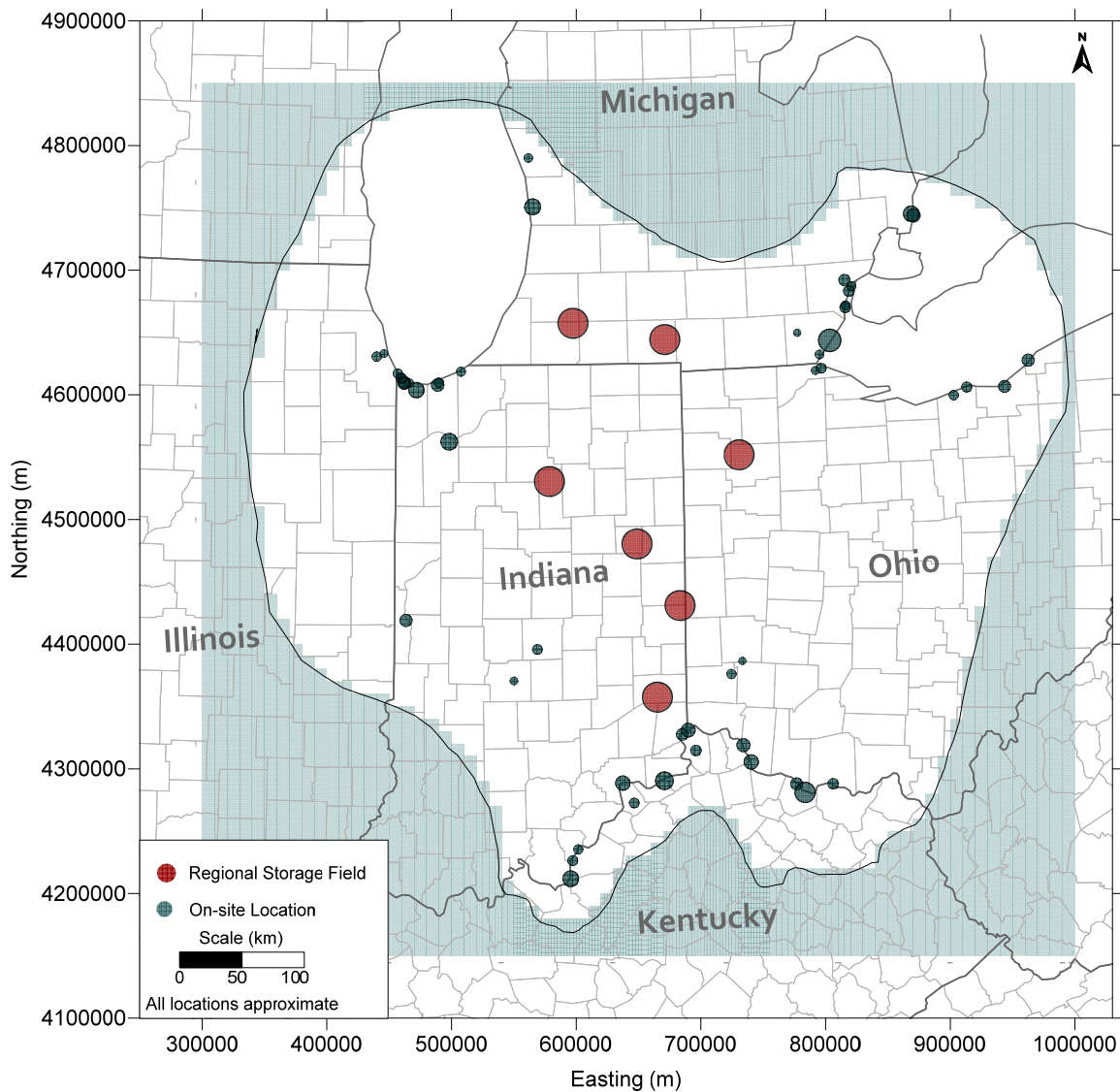


Figure 2-5. On-Site and Regional Injection Field Scenario Location Map

2.4 Results

Three main scenarios were evaluated with the SEAWAT model. The no-injection baseline model was employed for calibration, flow budget analysis, flow vector review, and sensitivity analysis. Regional injection and on-site injection scenarios were analyzed for pressure buildup and fluid migration.

Baseline Scenario- The objective of the baseline simulation was to replicate initial conditions in the Mt. Simon and Eau Claire hydrologic system. The baseline scenario was specified with no injection. Maximum grid spacing in the baseline model was set at 10,000 m by 10,000 m, because higher grid resolution was not necessary near injection wells. The model was calibrated to reservoir pressure in the Mt. Simon as delineated in wells that penetrate the formation. The baseline model was run in transient mode for 36,500 days. The model solution was set to converge at less than 0.001 m head change. Generally the baseline model showed a stable numerical convergence, with less than 0.01% volumetric budget error. Figure 2-6 shows simulated heads for the baseline model. As shown, the model matches

the overall pressure distribution observed in the Mt. Simon sandstone. The model slightly overestimates reservoir pressure in the south-central portion of the model domain.

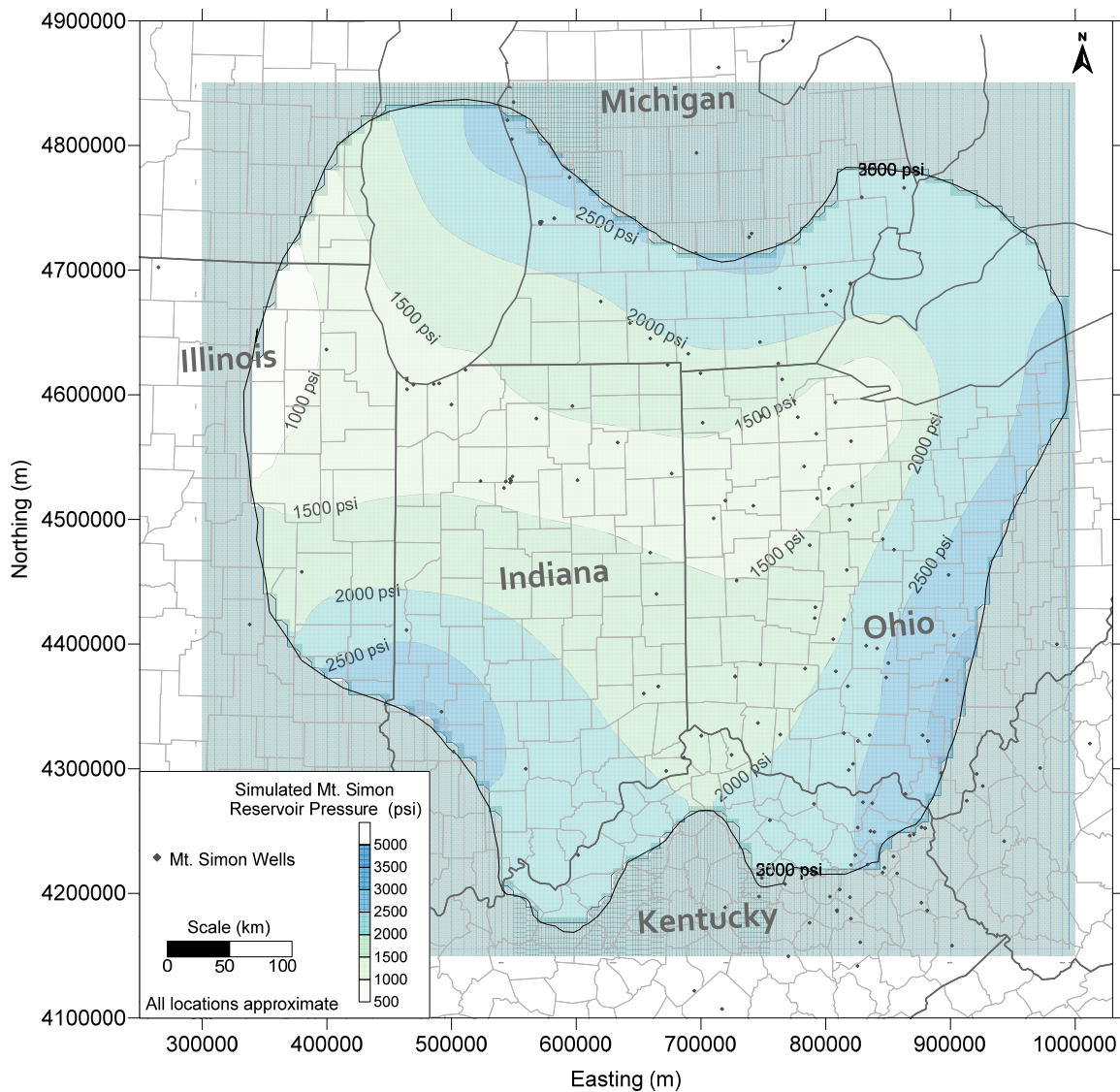


Figure 2-6. SEAWAT Simulated Reservoir Pressure Map for Mt. Simon Formation

Model Calibration- Model calibration statistics were calculated for the baseline run in comparison to observed pressures in 54 wells within the model domain. Figure 2-7 shows a plot of observed versus calculated heads. The plot shows a satisfactory fit with a correlation coefficient of 0.93. The route mean squared error was approximately 354 psi and standard error was 44 psi. This may seem large, but given the pressure range in the simulated area, the normalized route mean square error is only 10.9%.

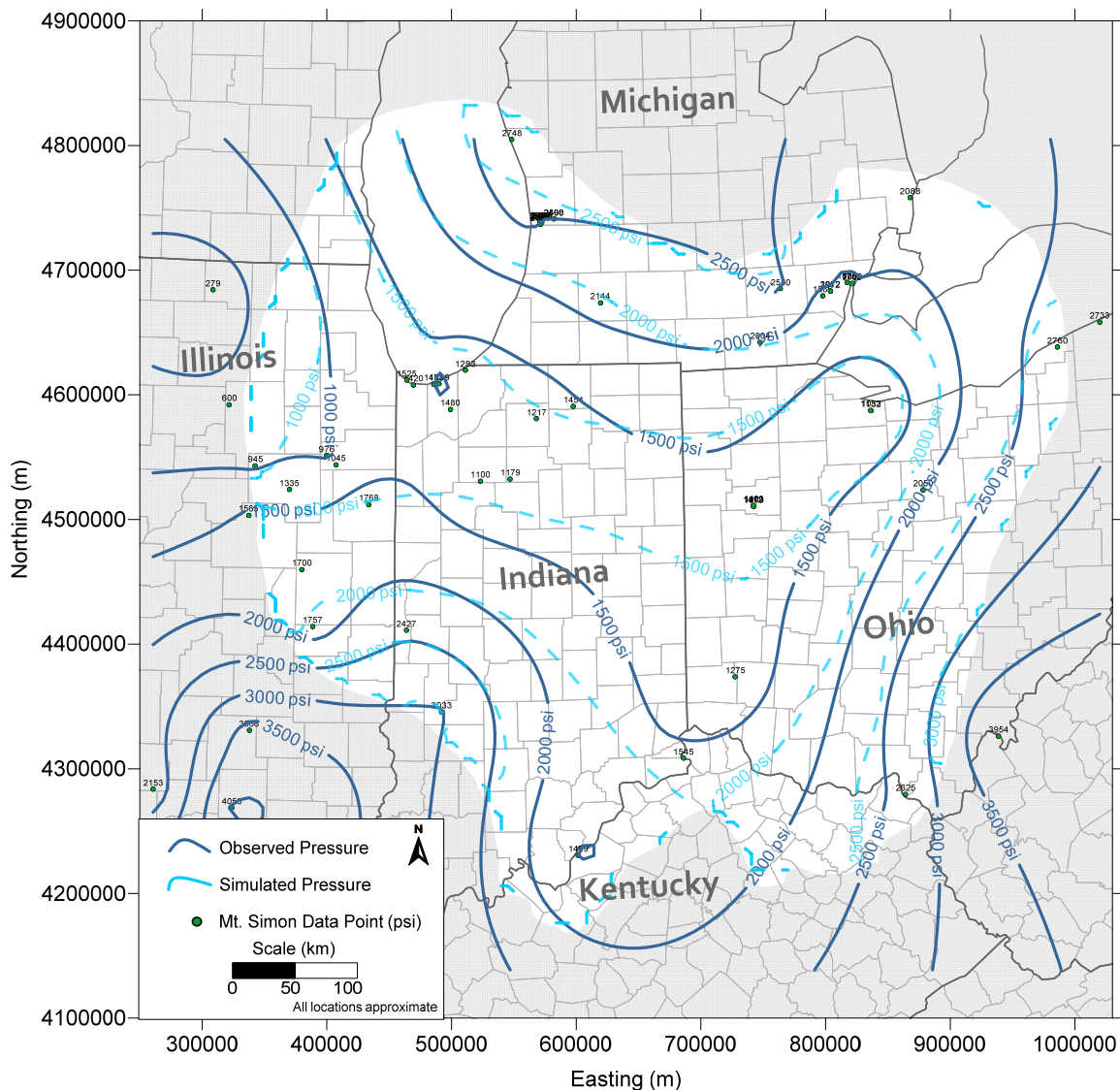


Figure 2-7. Calibration Map for SEAWAT Model Showing Observed vs. Simulated Pressure in the Mt. Simon Formation

Model Flow Budgets- Flow budgets were reviewed to provide additional calibration on model results. Flow budgets were calculated with the ZONEBUDGET module in MODFLOW. The ZONEBUDGET module calculates volumetric flux in and out of a user specified zone based on cell-by-cell flux calculations. The ZONEBUDGET was applied for the entire model domain to estimate the total amount of fluid flux through the system. Results of the ZONEBUDGET calculations were compared with work by Eberts and George analysis of *Regional Ground-Water Flow and Geochemistry in the Midwestern Basins and Arches Aquifer System in Parts of Indiana, Ohio, Michigan, and Illinois* (2000). Eberts and George present a hydraulic budget analysis based on groundwater flow modeling for an area similar to the Arches Province. Their study included surficial aquifer, surface water bodies, and the carbonate-rock aquifer. The carbonate-rock aquifer includes Mississippian-Silurian age rocks.

While it is not directly equivalent to the layers simulated in the Arches Province model, the Eberts and George analysis does provide a measure for comparison on flow budgets. In general, the models should have somewhat comparable flow budgets. The Arches Province model covers a larger domain, so it may

have more flow in the system. However, there is more flow across the carbonate-bedrock units because they are shallow and directly connected to surface water bodies in some areas. Table 2-2 summarizes the simulated flow budgets from the Arches Province baseline simulation (with no pumping) and the carbonate-rock aquifer regional flow system from the Eberts and George study. The Arches Province baseline SEAWAT simulation indicates total flow in and out of the system of 372 million gallons per day, which compares to Eberts and George's budget of 386 million gallons per day for the bedrock-carbonate aquifer. Given the uncertainty on fluid flow in these deep environments, the flow budget analysis provides additional confidence in model setup.

Table 2-2. Comparison of Flow Budgets for Arches Province Simulation and Eberts and George Regional Aquifer System Analysis for Midwestern Basins and Arches

Simulation	Interval	Model Domain	Total Flow (Mgal/d)
Arches Simulations (no injection)	Knox-Precambrian	700 x 700 km	372
Regional Groundwater Flow in the Basins and Arches Aquifer System (Eberts and George, 2000)	Bedrock-Carbonate Aquifer (Mississippian-Silurian)	400 x 440 km	386

Mgal/d = million gallons per day

Model Flow Vectors- Flow vectors were also used to examine simulation results. Flow vectors represent the simulated direction and magnitude of flow within model cells. Figure 2-8 shows simulated flow vectors in the Mt. Simon. Overall, flow rates are fairly low within the study area. There are some higher flow rates near model boundaries, but these areas are separated from the study area by large distances. There is also a zone in central Ohio that has higher flow velocities, which may be related to permeability distribution. Flow vector directions suggest flow from the basins into the center of the Arches Province. The model generally suggests very minor flow in the Eau Claire and the Precambrian layers.

Model results show the average simulated flow velocity in the Mt. Simon is 67 cm/yr. In general, this flow rate agrees with previous studies on the Mt. Simon (Gupta and Bair, 1997), which suggest flow rates in the formation are on the order of 1 meter per year. The model suggests the flow rate in the Eau Claire and Precambrian layers is less than 1 cm/yr.

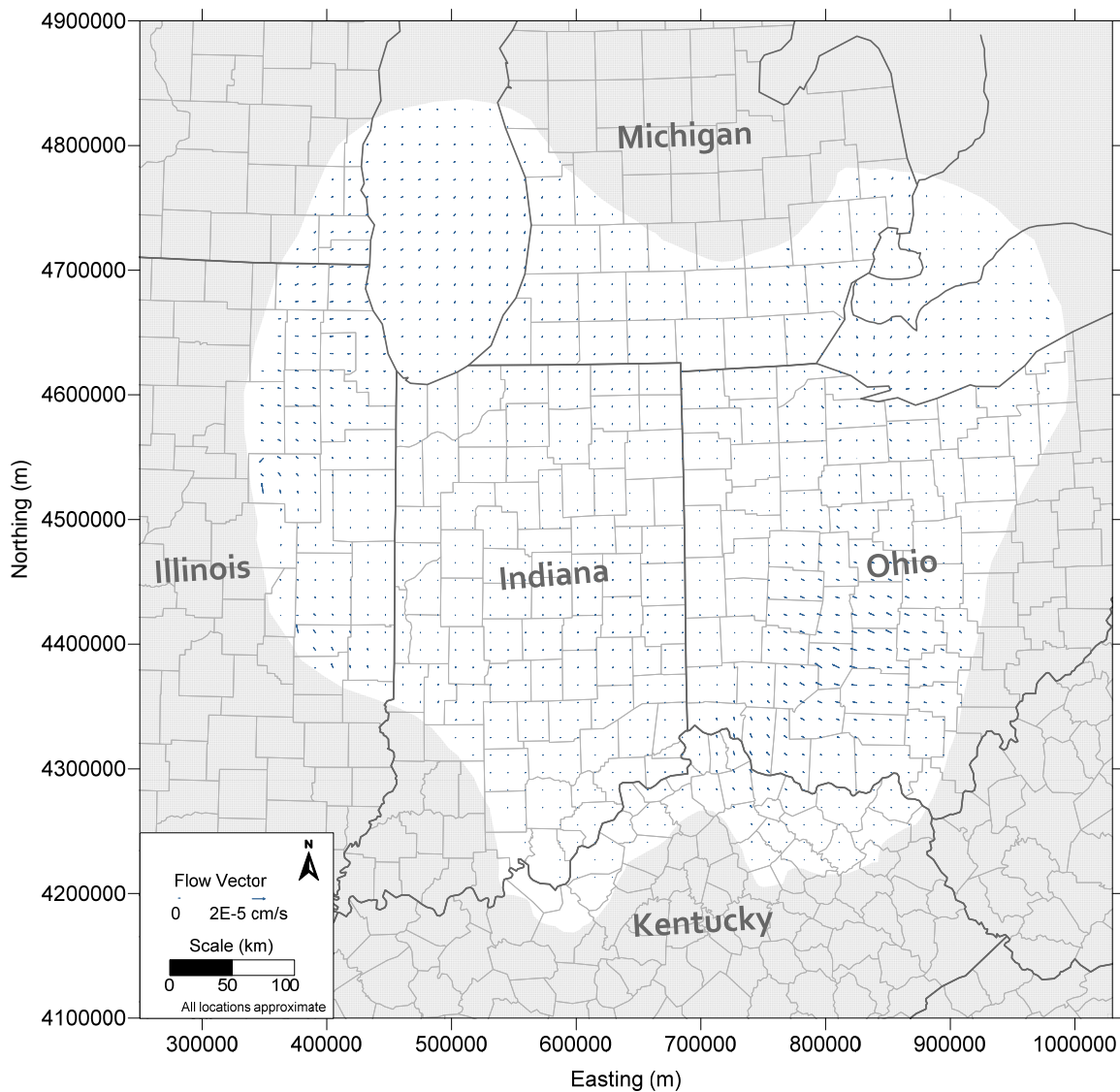


Figure 2-8. Simulated Flow Vector Map for Mt. Simon Sandstone (Model Layer 4)

Sensitivity Analysis- A sensitivity analysis was completed to examine model stability. The sensitivity analysis focused on the permeability of the Mt. Simon, because this input parameter has the greatest impact on simulation results. The permeability distribution in the Mt. Simon was scaled by a factor of 0.2X, 0.5X, 2X, and 5X. Calibration statistics were produced for each simulation run. Figure 2-9 shows a plot of sensitivity factor versus calibration statistics for the sensitivity runs. As shown, error increases away from the baseline input. There is less sensitivity to the lower permeability scaling factor. Overall, the sensitivity analysis suggests the model has a stable solution and suitable permeability distribution.

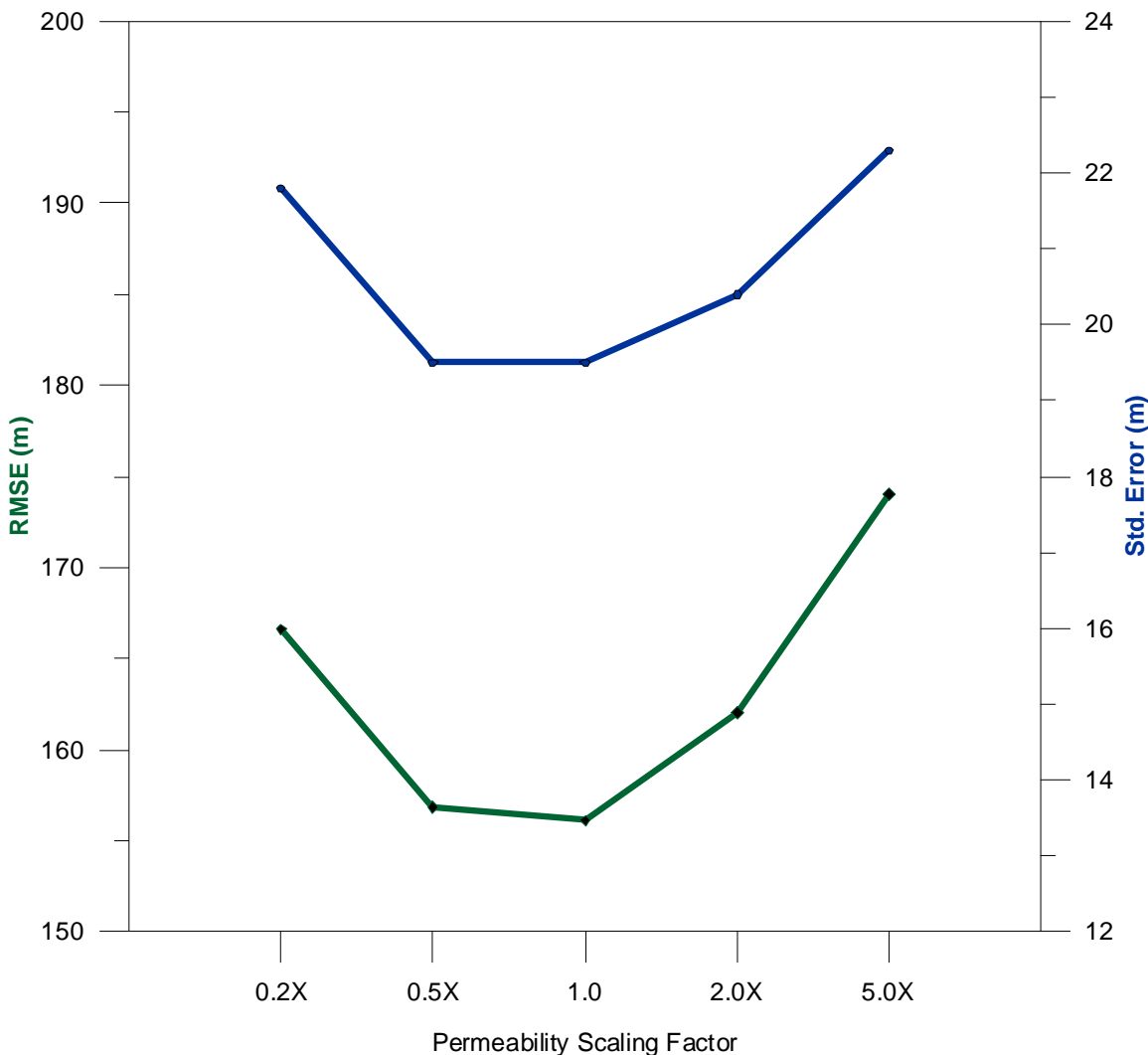


Figure 2-9. Sensitivity Plot for 0.2X to 5.0X Permeability Scaling Factors

Regional Storage Field Scenario- Regional storage scenarios were run with the SEAWAT model to assess pressure buildup and fluid migration due to large injection volumes. The SEAWAT simulations do not simulate super-critical CO₂ fluid. The models can only simulate low density water as a proxy for CO₂. In addition, the SEAWAT model has simplified grid spacing, layering, and injection well depiction. However, the simulations do provide guidance on basin-scale pressure buildup due to large scale injection in the Mt. Simon sandstone.

The regional storage field scenarios were run in transient mode in SEAWAT. Table 2-3 summarizes the regional storage scenarios. Single injection wells were specified at the seven regional storage field locations. Injection rates of 1.0 million metric tons per year to 10 million metric tons per year were simulated. Wells were screened across the entire Mt. Simon thickness. Injection rate was converted from CO₂ to water on a volumetric basis assuming CO₂ density of 0.7 kg/l. Based on this conversion, an injection rate of 1.0 million metric tons CO₂ per year equates to 700 gallons per minute or 3,816 m³/day. Injection was run for 20 years, followed by an 80-year post-injection period. In examining the model results, it was determined that increased grid spacing was necessary to obtain suitable numerical solutions. Grid spacing was increased to 500 m by 500 m near the injection wells.

Table 2-3. SEAWAT Regional Storage Field Scenarios

# Injection Wells	Injection Rate Per Well (million metric tons CO ₂ /yr)	Injection Rate Per Well (m ³ /day water)	Total Injection (million metric tons CO ₂ /yr)
7	1.0	3,800	7.0
7	2.0	7,600	14.0
7	3.0	11,400	21.0
7	5.0	19,000	35.0
7	10.0	38,000	70.0

Figures 2-10 through 2-14 show simulated pressure buildup for the region. The pressure buildup was calculated by subtracting the simulated pressure field under no-injection conditions from the simulated pressure field with injection. Pressure buildup is based on model layer 4 at the end of the 20 year injection period (middle Mt. Simon). As shown, pressure buildup increases with increasing injection. There is some indication of well interference for the southern three injection wells. The radius of pressure buildup is on the order of 10 to 50 km for lower injection scenarios and 50 to 200 km for the larger injection scenarios. In general, these results are very similar to other modeling studies on the Mt. Simon in the Illinois basin (Zou et al., 2010), which suggest that operation of many large scale injection fields would produce an area of pressure buildup covering several thousand square kilometers. The single well scenario for injection rates of 5 to 10 million metric tons CO₂ per year indicate pressure buildup in the injection wells would exceed 1000 psi, which would likely exceed rock fracture pressure limits imposed by underground injection control regulations. Furthermore, injection rates over 5 million metric tons per year in a single well would be difficult to implement due to flow limitations for injection tubing and well sizes. Therefore, it appears that multiple injection wells would be required to facilitate higher injection volumes.

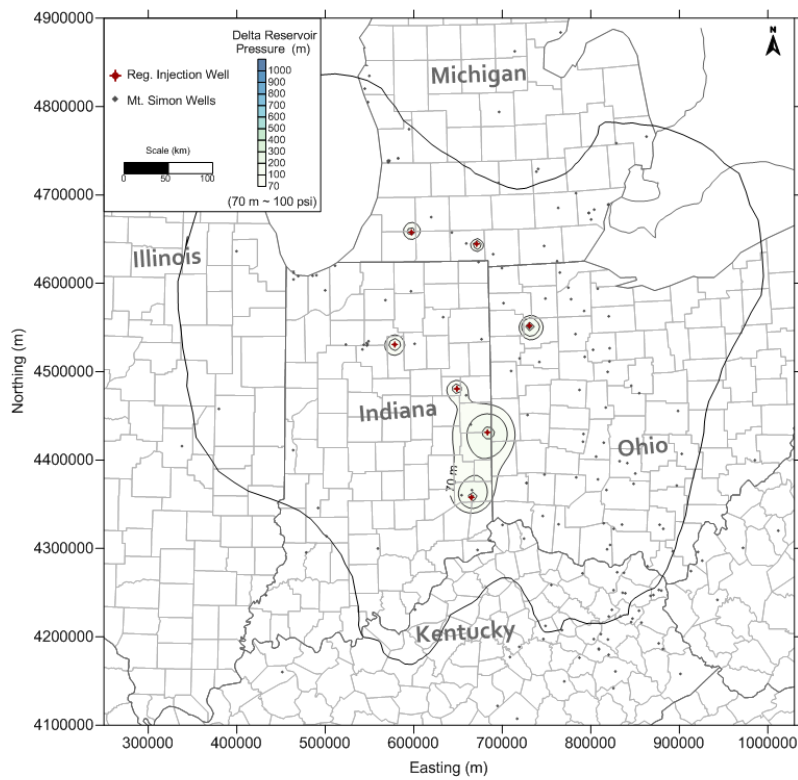


Figure 2-10. SEAWAT Simulated Delta Pressure 1×10 million metric tons/y per well [7 Mt/yr total injection]

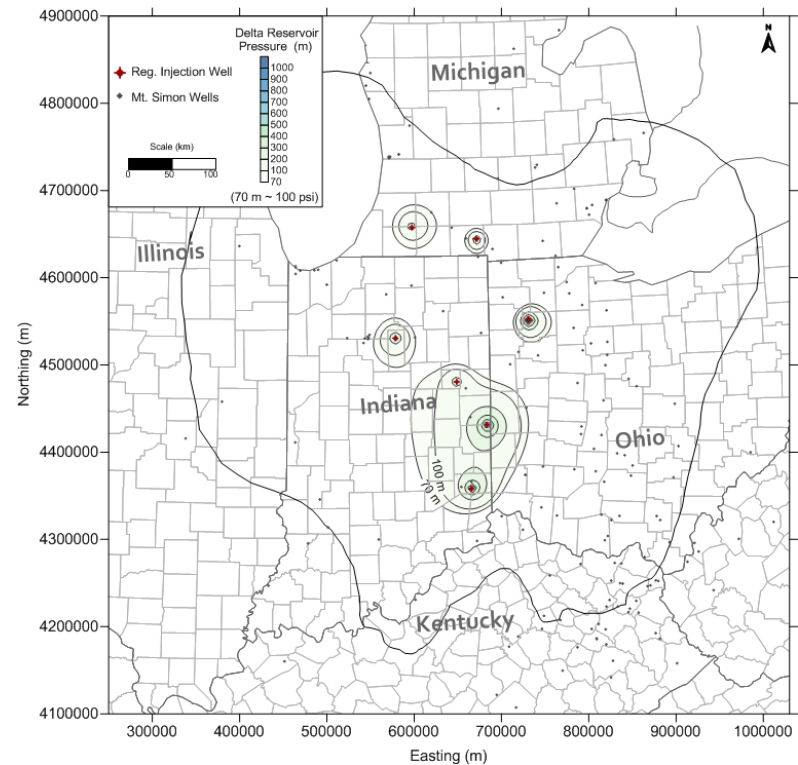


Figure 2-11. SEAWAT Simulated Delta Pressure 7×2 million metric tons/yr per well [14 Mt/yr total injection]

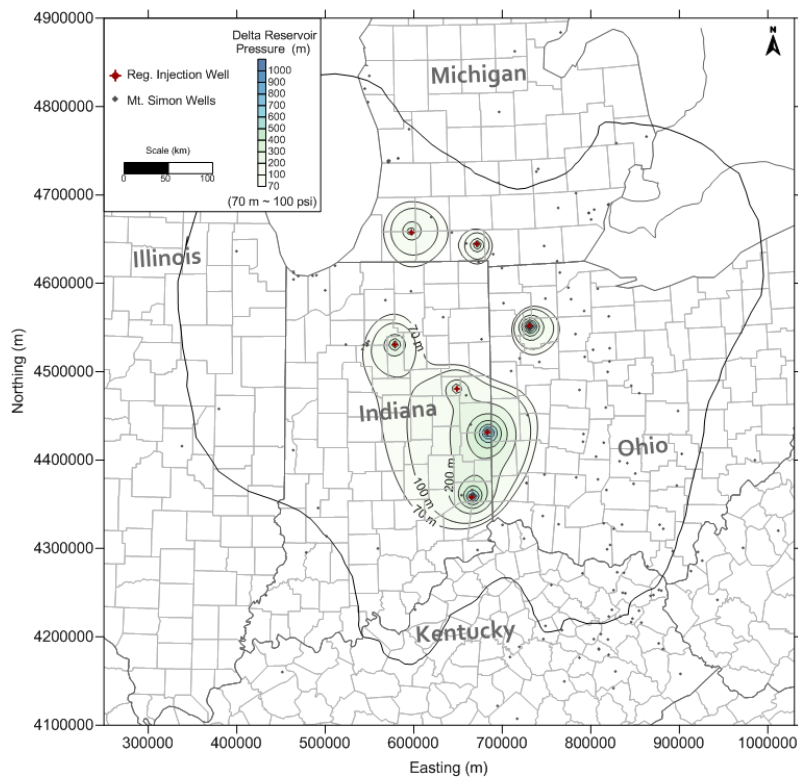


Figure 2-12. SEAWAT Simulated Delta Pressure 7×3 million metric tons/y per well (21 Mt/yr total injection)

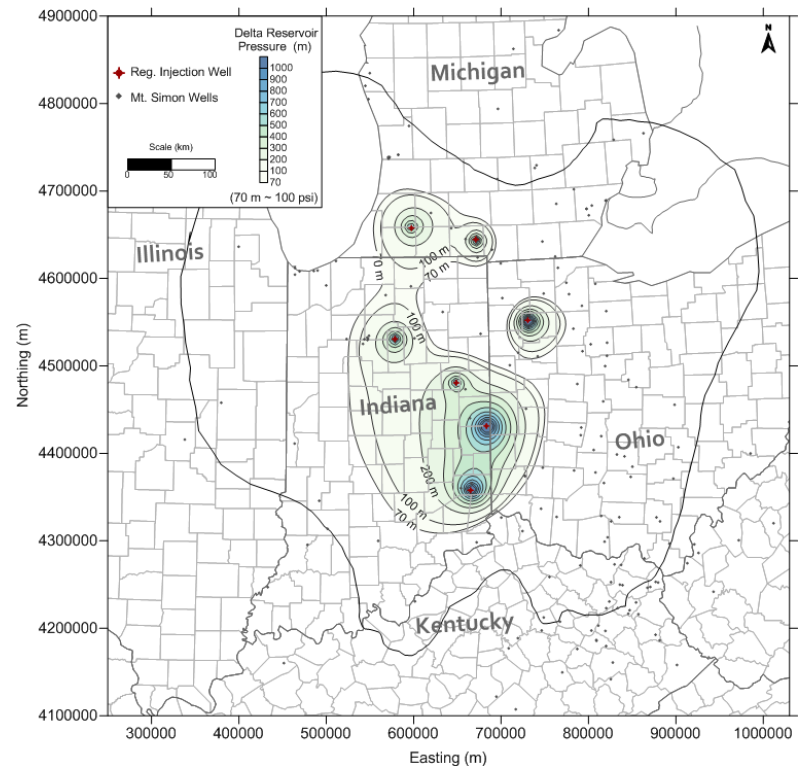


Figure 2-13. SEAWAT Simulated Delta Pressure 7×5 million metric tons/yr per well [35 Mt/yr total injection]

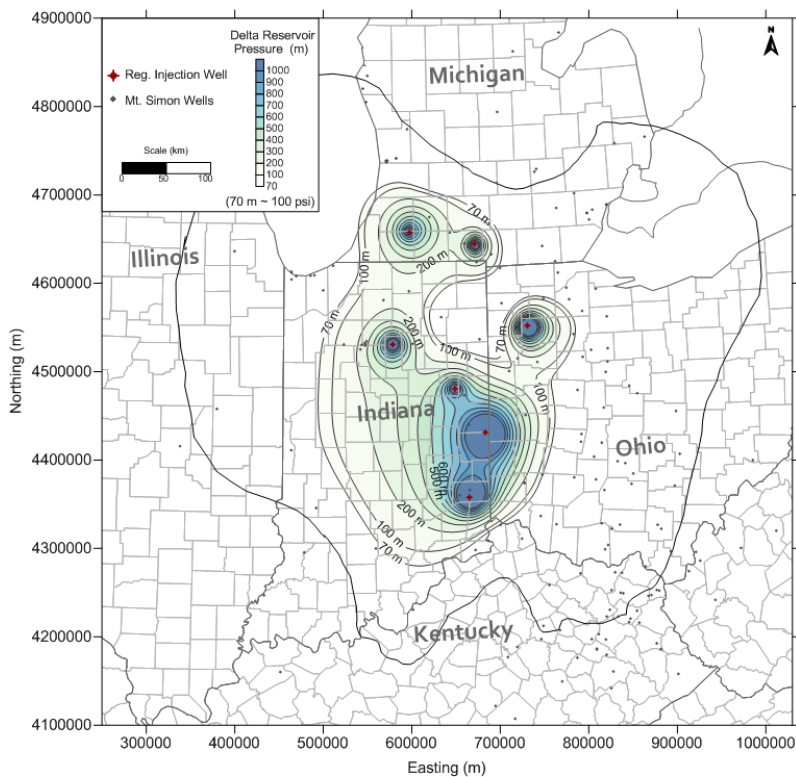


Figure 2-14. SEAWAT Simulated Delta Pressure 7×10 million metric tons/y per well [70 Mt/yr total injection]

The SEAWAT simulations were used as a proxy to examine the extent of potential CO₂ storage zone. These results were evaluated mainly to provide guidance on input parameters for the multiple-phase model. As mentioned earlier, the SEAWAT code cannot simulate supercritical CO₂ fluid, in terms of phase transitions, miscibility, or mobility. Still, a low-density brine fluid can be used as a generalized proxy to examine fluid displacement caused by injection. The low-density brine fluid will demonstrate upward migration and spreading due to injection. Figure 2-15 shows a cross section through a regional injection. The SEAWAT simulation suggests that higher X-Y grid resolution is necessary to portray the CO₂ storage zone. In addition, greater vertical resolution is necessary to track upward migration of the injected fluid. Since the Mt. Simon was represented with only three model layers, it is difficult to simulate upward migration. Results are averaged across thick zones within the Mt. Simon. Similarly, results are averaged in the Eau Claire, because it is portrayed by one layer in the model. Overall, the SEAWAT simulations suggest that relatively high lateral and vertical grid spacing is required around the injection zone to accurately simulate CO₂ plume development. Given the limitations of depicting CO₂ migration, no additional SEAWAT simulations were performed to examine the CO₂ plume.

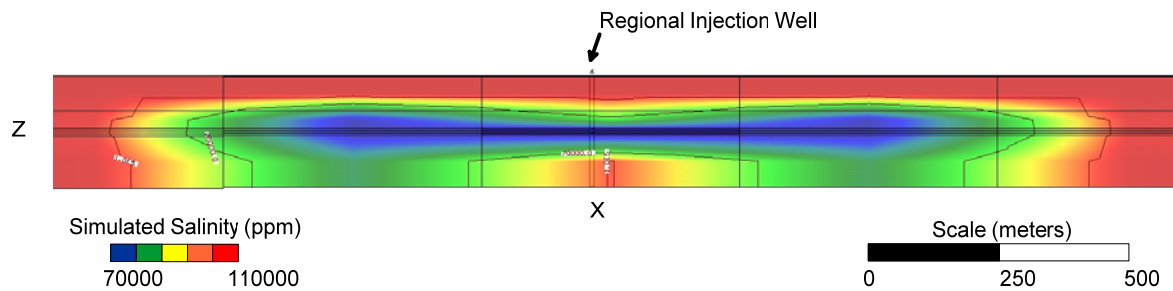


Figure 2-15. SEAWAT Simulation Showing Upward Migration of Low-Density Brine Fluid in Vertical Cross Section Through a Regional Injection Well Injecting at 1 Million Metric Tons CO₂ Per Year after 20 Years of Injection

On-Site Injection Scenario- On-site injection simulations were run with the SEAWAT model to assess pressure buildup and fluid migration due to injection at the source locations in the Arches Province. The SEAWAT simulations have the same limitations discussed in the regional storage field scenarios. Table 2-4 summarizes the on-site simulations. For the on-site scenarios, injection wells were specified at the location of 50 sources located in the active model area (note: two sources considered in an earlier source assessment were not located in the active model area). These sources have annual CO₂ emissions greater than 1 million metric tons CO₂ per year. Scenarios of 10%, 25%, 50%, and 100% of each source's total emissions were run with the SEAWAT model.

Table 2-4. SEAWAT On-Site Injection Scenarios

Injection Scenario	# Sources	Total Injection (million metric tons CO ₂ /yr)	Average Injection Rate per Well (million metric tons CO ₂ /yr)
10%	50	25.6	0.51
25%	50	64	1.28
50%	50	128	2.56
100%	50	256	5.13

Figures 2-16 through 2-18 show maps of simulated pressure buildup for SEAWAT simulations for 10%, 25%, and 50% on-site injection. Since injection is distributed across 50 sources, the pressure buildup does not cover as large an area as in the regional storage scenarios. However, there is a zone of high pressure buildup in the southwest corner of the model where several large sources are located along the Ohio River. Model results are not reliable in this area because the pressure buildup extends to the model boundary, which can lead to model errors.

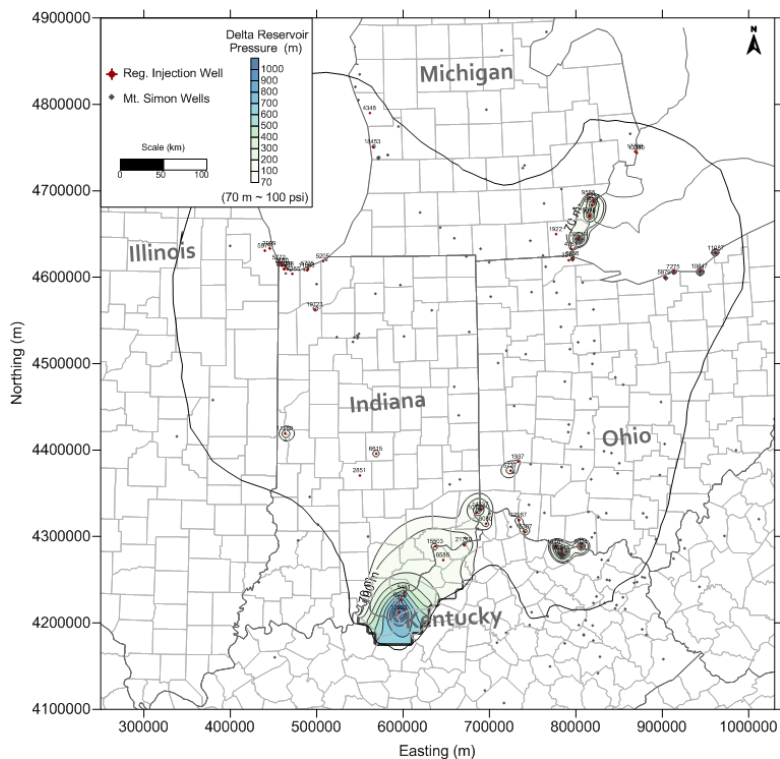


Figure 2-16. SEAWAT Simulated Delta Pressure- 10% On-Site Injection (25.6 Mt/yr total injection)

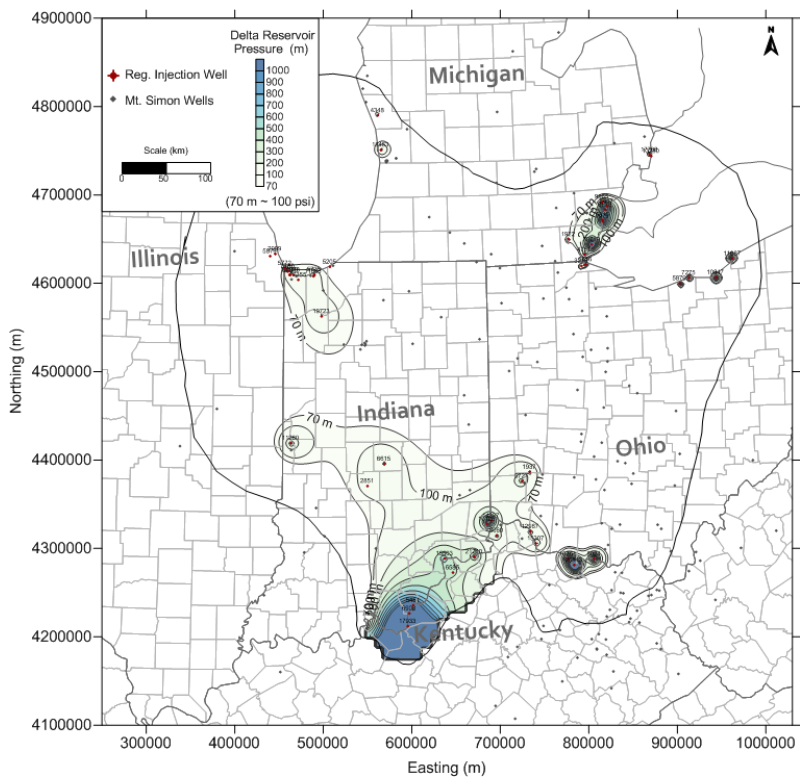


Figure 2-17. SEAWAT Simulated Delta Pressure- 25% On-Site Injection (64 Mt/yr total injection)

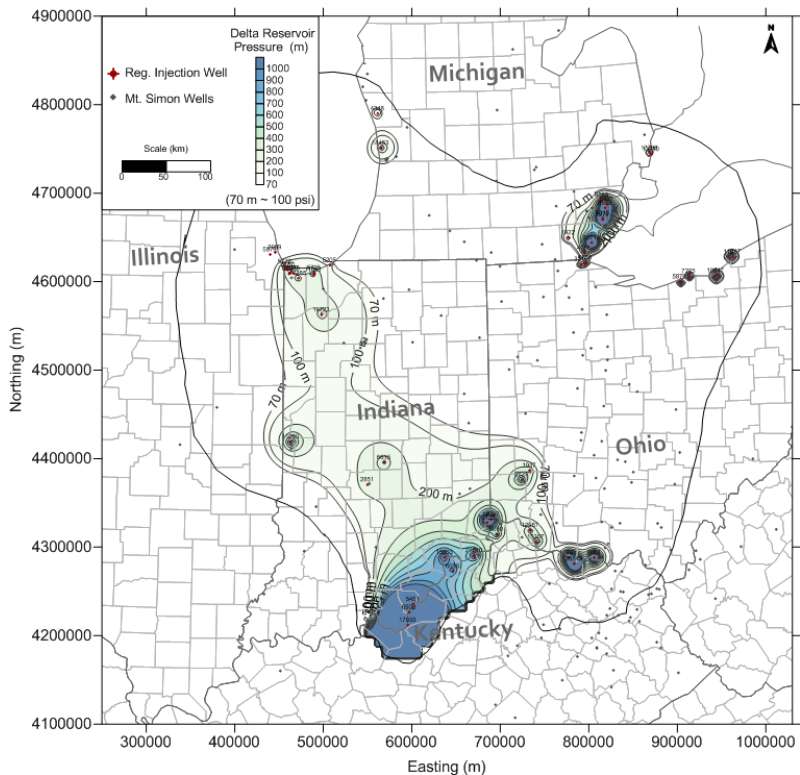


Figure 2-18. SEAWAT Simulated Delta Pressure- 50% On-Site Injection (128 Mt/yr total injection)

Section 3.0: SCOPING SIMULATIONS

To better understand regional storage field applications in the Arches Province, a series of scoping simulations were performed. These preliminary simulations were focused on assessing storage field arrangement in terms of distance between storage fields, number of injection wells in the fields, pressure interference from multiple wells, and injection schedules. The scoping level work included capacity analysis using analytical equations and more multi-phase CO₂ injection simulations with the numerical simulation code STOMPCO2.

3.1 Scoping Simulations Overview

The first set of simulations was based on generic conditions in the model domain. Simulations were designed to represent a cluster of injection wells at a regional storage site. In this arrangement, a well in the middle of each regional storage site would essentially inject into a cylinder of finite lateral extent due to well interference, and could be taken as the conservative case. Using this description of a well in a closed volume as a representative case, simple two-dimensional (2D) r-z simulations were carried out to examine the interplay between well spacing and pressure buildup. The model domain consists of the Eau Claire sealing unit and the Mt. Simon sandstone where CO₂ is injected.

The second set of simulations was based on site-specific conditions in the model domain. Seven potential regional storage field locations were identified using a geographic information system (GIS) study that takes into consideration the location of stationary CO₂ sources and least cost CO₂ pipeline distribution networks. Each regional site has a storage area of approximately 50 miles, and each site is expected to inject 10 to 20 million metric tons CO₂ per year. Two representative well configurations were selected to mimic flow geometries in the middle and the edge of the injection well cluster. As before, 2D r-z simulations were designed to evaluate the range of conditions to be expected with respect to pressure buildup and plume movement. In these simulations, the model domain also consists of the Eau Claire sealing unit and the Mt. Simon sandstone where CO₂ is injected.

The simulations were carried out using Subsurface Transport Over Multiple Phases (STOMP). The STOMP simulator was developed by the Pacific Northwest National Laboratory for modeling subsurface flow and transport systems and remediation technologies. The simulator's fundamental purpose is to produce numerical predictions of thermal and hydrogeologic flow and transport phenomena in variably saturated subsurface environments, which are contaminated with volatile or nonvolatile organic compounds. The governing coupled flow equations are partial differential equations for the conservation of water mass, air mass, (dissolved) organic compound mass and thermal energy. Quantitative predictions from the STOMP simulator are generated from the numerical solution of these partial differential equations that describe subsurface environment transport phenomena. Solution of the governing partial differential equations occurs by the integral volume finite difference method. The governing equations that describe thermal and hydrogeological flow processes are solved simultaneously using Newton-Raphson iteration to resolve the nonlinearities in the governing equations. Governing transport equations are partial differential equations for the conservation of solute mass. Solute mass conservation governing equations are solved sequentially, following the solution of the coupled flow equations, by a direct application of the integral volume finite difference method. The STOMP simulator is written in the FORTRAN 77 language, following American National Standards Institute (ANSI) standards (White and Oostrom, 2000).

3.2 Model Setup – Generic Case

Figure 3-1 shows the model geometry used for the generic case simulations. The model consists of 20 vertical rows that extend from the top of the Eau Claire to the base of the Mt. Simon, and 100 radial columns that extend from the center of the injection well to the closed (symmetry) outer boundary. Vertically, the model is 357 m thick (from a depth of 1000 m to 1357 m), and radially, the model has variable radial extent depending on the assumed site radius and the number of wells in the injection cluster (as described in the next section). At the bottom of the model, the reference pressure and temperature are assumed to be 2000 psi and 100 °F, respectively. These parameters represent fairly typical conditions in the Arches Province.

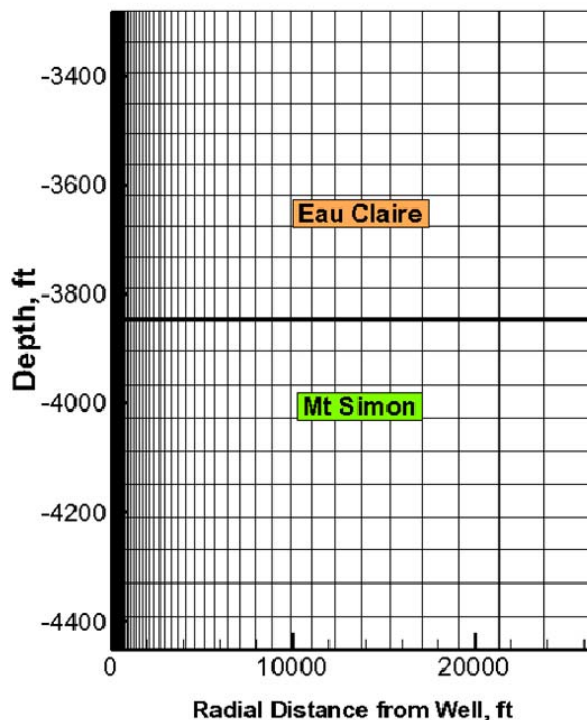


Figure 3.1 Model Geometry, Generic Case

Porosity and permeability for the Eau Claire and the Mt. Simon are based on average conditions within the model domain. Capillary pressure and relative permeability data are based on assumed values. These are shown in Table 3-1.

Table 3.1 Model Parameters, Generic Case

Unit	Thickness (m)	Porosity (%)	Permeability (mD)	Capillary Pressure and Relative Permeability Parameters
EC	172	7	0.02	Brooks-Corey saturation function card with the Mualem porosity distribution model (capillary entry head = 34.9 cm, lambda parameter = 1.36, minimum water saturation = 0.0767);
MS	185	11	53	

3.3 Scenarios – Generic Case

The generic case considers three site radii (25 miles, 32 miles, 40 miles) and three well arrays (7×7, 6×6, 5×5). Constant rate CO₂ injection is assumed at a rate of ~100 MMT/yr (for all three sites) for 30 years into MS. This leads to the following combinations with respect to model dimensions and per-well injection rate, as shown in Table 3-2.

Table 3.2. Model Dimensions and Injection Rate, Generic Case

Site radius →		25 miles	32 miles	40 miles	Injection Rate (MMT/yr)
Well array	# of wells	Storage radius (m)			
7×7	49	5782	7401	9251	0.68
6×6	36	6746	8635	10793	0.93
5×5	25	8095	10362	12952	1.33

Performance metrics for these simulations are taken to be: (a) 2-D pressure and saturation contours at 30 yrs, and (b) pressure buildup at the mid-point of the Mt. Simon.

3.4 Results – Generic Case

Figure 3-2 shows pressure and saturation contours at $t = 30$ years for the 25 mile site radius, 5×5 well array scenario. This set of conditions corresponds to the smallest sized system at the highest injection rate (see Table 3-2). As expected, the pressure contours suggest an upward gradient between the Mt. Simon and the Eau Claire (left panel). The saturation contours also show the development of significant buoyant effects – especially at the Eau Claire-Mt. Simon interface.

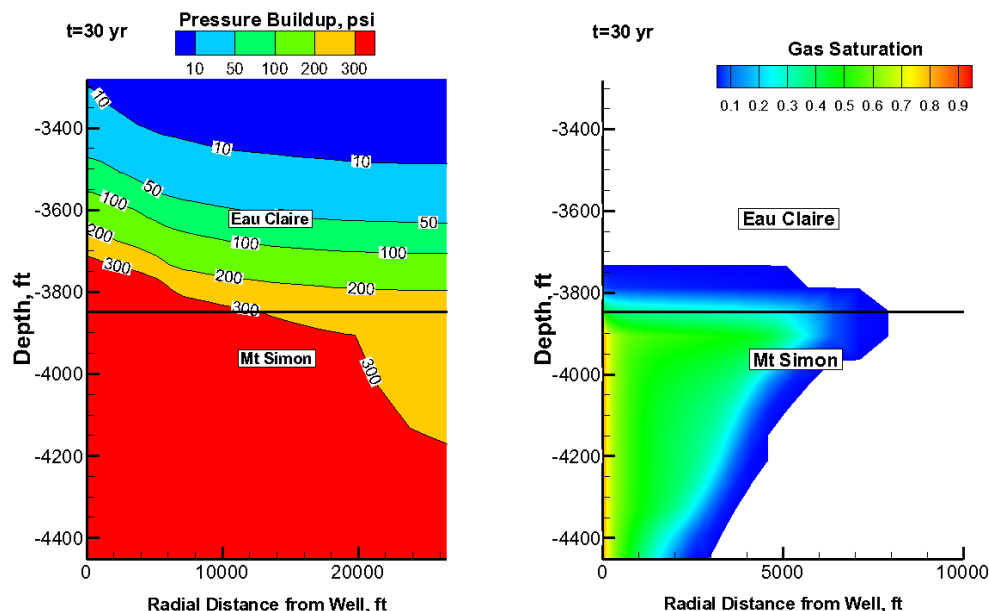


Figure 3-2. Pressure and Saturation Contours (25 mile site radius, 5×5 well array)

Figure 3-3 illustrates the pressure buildup at the mid-point of the Mt. Simon. After an initial transient period, the effect of the closed outer boundary can be clearly seen in the pseudo-steady state type pressure buildup after ~ 2200 days, where pressure tends to increase linearly with time. Also shown for comparison is the fracture pressure, which is not exceeded during the injection period.

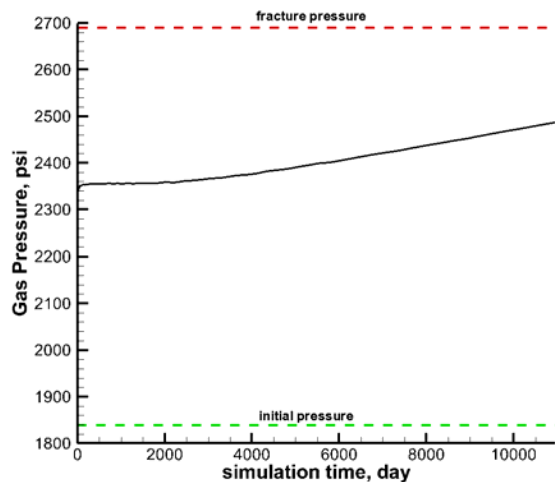


Figure 3-3. Pressure Buildup at Mid-point of Mt. Simon (25 mile site radius, 5 \times 5 well array)

Figure 3-4 shows pressure and saturation contours at $t = 30$ years for the 32 mile site radius, 6 \times 6 well array scenario. This set of conditions corresponds to the mid-sized system at the medium injection rate (see Table 3-2). The pressure contours suggest less upward gradient between the Mt. Simon and the Eau Claire (left panel) than that seen earlier in Figure 3-2. Similarly, the saturation contours (right panel) show the development of less significant buoyant effects at the Eau Claire-Mt. Simon interface than seen in Figure 3-2.

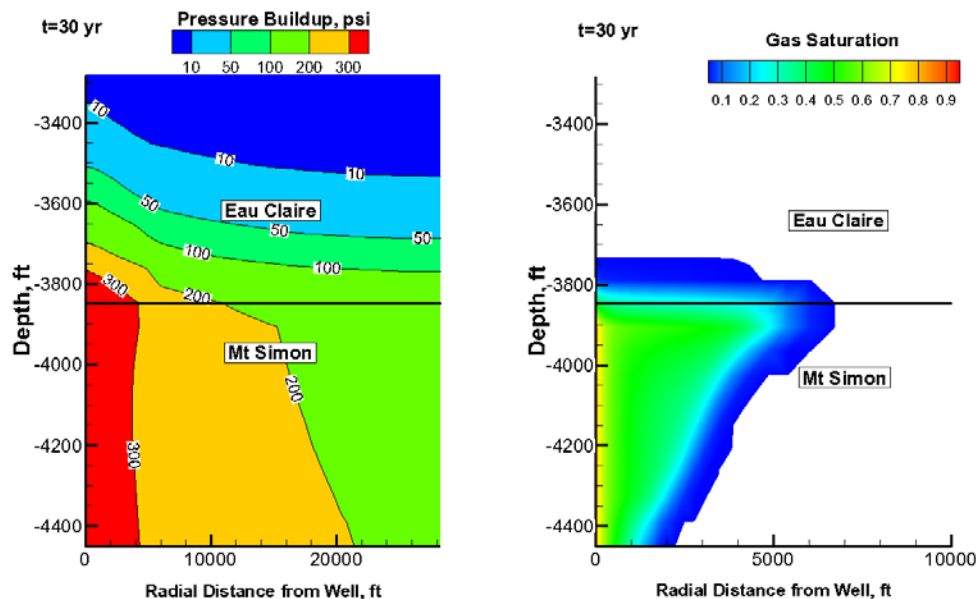


Figure 3-4. Pressure and Saturation Contours (32 mile site radius, 6×6 well array)

Figure 3-5 shows the simulated pressure buildup for this scenario at the mid-point of the Mt. Simon. After an initial transient period, the effect of the closed outer boundary can be clearly seen in the pseudo-steady state type pressure buildup after ~3000 days, where pressure tends to increase linearly with time. Also shown for comparison is the fracture pressure, which is not exceeded during the injection period.

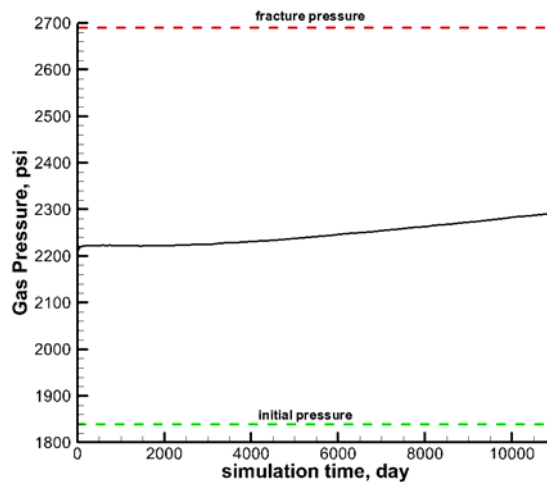


Figure 3-5. Pressure Buildup at Mid-point of the Mt. Simon (32 mile site radius, 6×6 well array)

Figure 3-6 shows pressure and saturation contours at $t = 30$ years for the 40-mile site radius, 7×7 well array scenario. This set of conditions corresponds to the largest system at the smallest injection rate (see Table 3-2). The pressure contours suggest primarily horizontal flow in the near-wellbore region, with some cross-flow between the Mt. Simon and the Eau Claire (left panel) at the right-edge of the model. Similarly, the saturation contours (right panel) show the development of moderate buoyant effects at the Eau Claire-Mt. Simon interface.

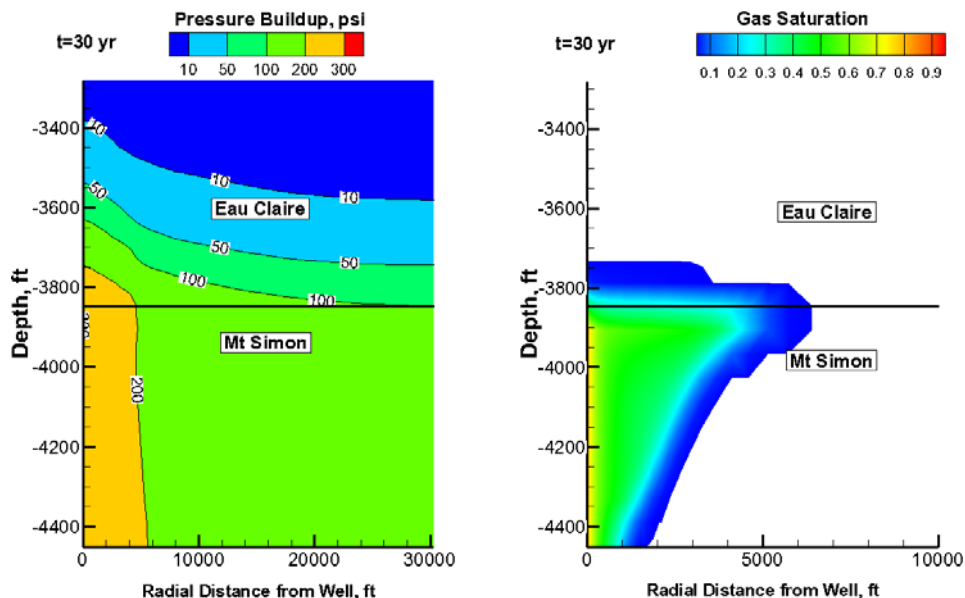


Figure 3-6. Pressure and Saturation Contours (40 mile site radius, 7×7 well array)

Figure 3-7 shows the pressure buildup for the 7×7 well array scenario at the mid-point of the Mt. Simon. After an initial transient period, the effect of the closed outer boundary can be clearly seen in the pseudo-steady state type pressure buildup after ~ 4000 days, where pressure tends to increase linearly with time. Also shown for comparison is the fracture pressure, which is not exceeded during the injection period.

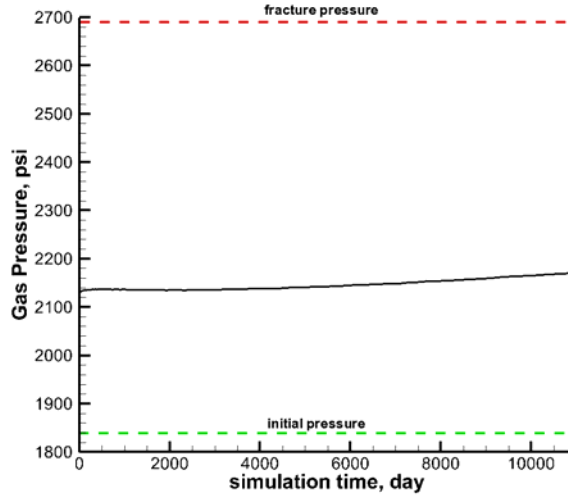


Figure 3-7. Pressure Buildup at Mid-point of the Mt. Simon (40 mile site radius, 7×7 well array)

Figure 3-8 shows the pressure buildup at 30 years as a function of site radius and well array from all of the scenarios detailed in Table 3-2. This figure provides information on the interplay between well spacing and pressure buildup that can be useful for system design when used in conjunction with site-specific information.

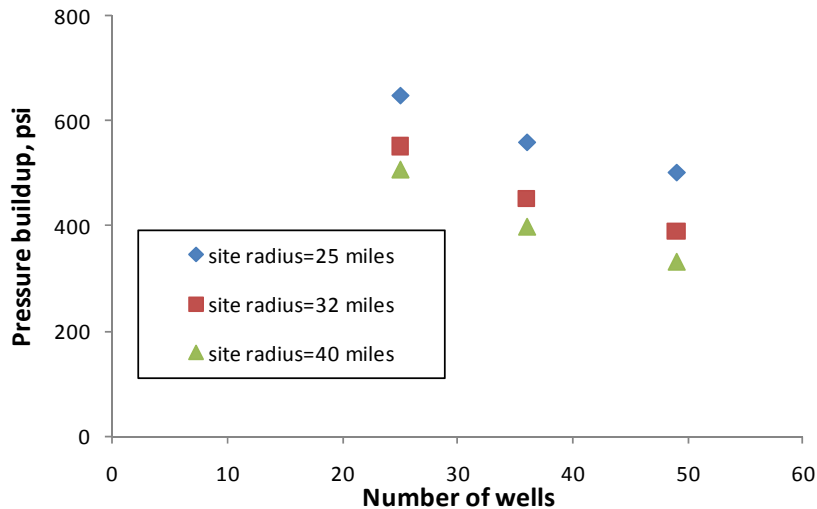


Figure 3-8. Pressure Buildup as a Function of Site Radius and Well Array

3.5 Summary – Generic Case

Thus far, simple scoping simulations have been presented to examine the relationship between well spacing versus pressure buildup. These preliminary calculations have been carried out with “average” porosity/permeability values and generic assumptions regarding storage site location and dimension. The next set of simulations address site-specific cases, including stratigraphic column variability, vertical heterogeneity in porosity and permeability, and relative permeability model choice.

3.6 Model Setup – Site-specific Case

The site-specific simulations follow the strategy adopted in the generic case simulations, i.e., the aim is not to conduct a full basin-scale simulation, but to simplify the problem by studying the effect of equivalent single well systems. As before, simple 2D r-z simulations were carried out to examine plume migration, pressure propagation, and CO₂ flux across the Mt. Simon-Eau Claire interface.

The starting point of these simulations is the map of seven potential regional storage site locations shown in Figure 3-9. These locations were selected on the basis of GIS analyses that balanced the location of stationary CO₂ sources with existing pipeline networks.

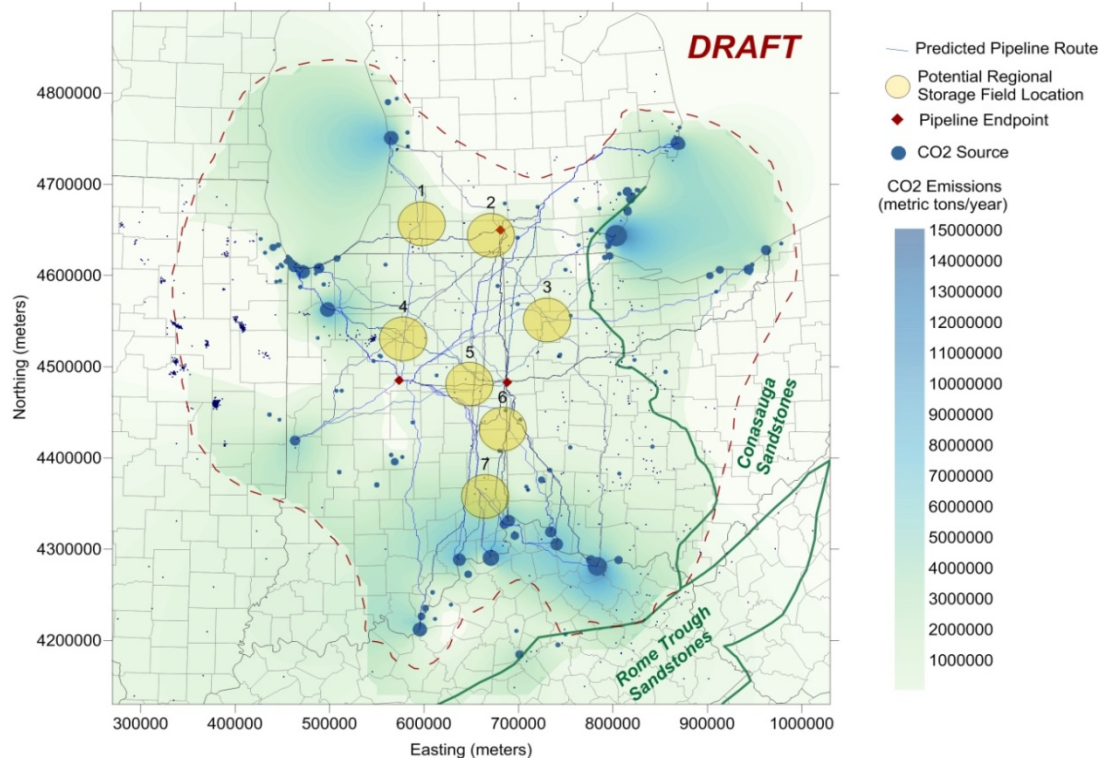


Figure 3-9. Potential Regional Storage Field Locations

A vertical stratigraphic column was extracted at the mid-point of each of the seven sites shown in Figure 3-9. These columns are depicted in Figure 3-10, illustrating the spatial variability in layer thicknesses across the entire Arches Province study area. These represent a broad range of conditions with respect to the depth of the Mt. Simon, relative thickness of the Eau Claire and the Mt. Simon, and the amount of buffer available above the Eau Claire. For example, Site 3 has the lowest Mt. Simon thickness, combined with a much thicker Eau Claire, and the smallest column of overlying formations. Site 1 has the thickest

column of the Mt. Simon beneath a much thinner Eau Claire, but the thickest column of overlying formations. Site 7 represents more or less average conditions across the seven sites.

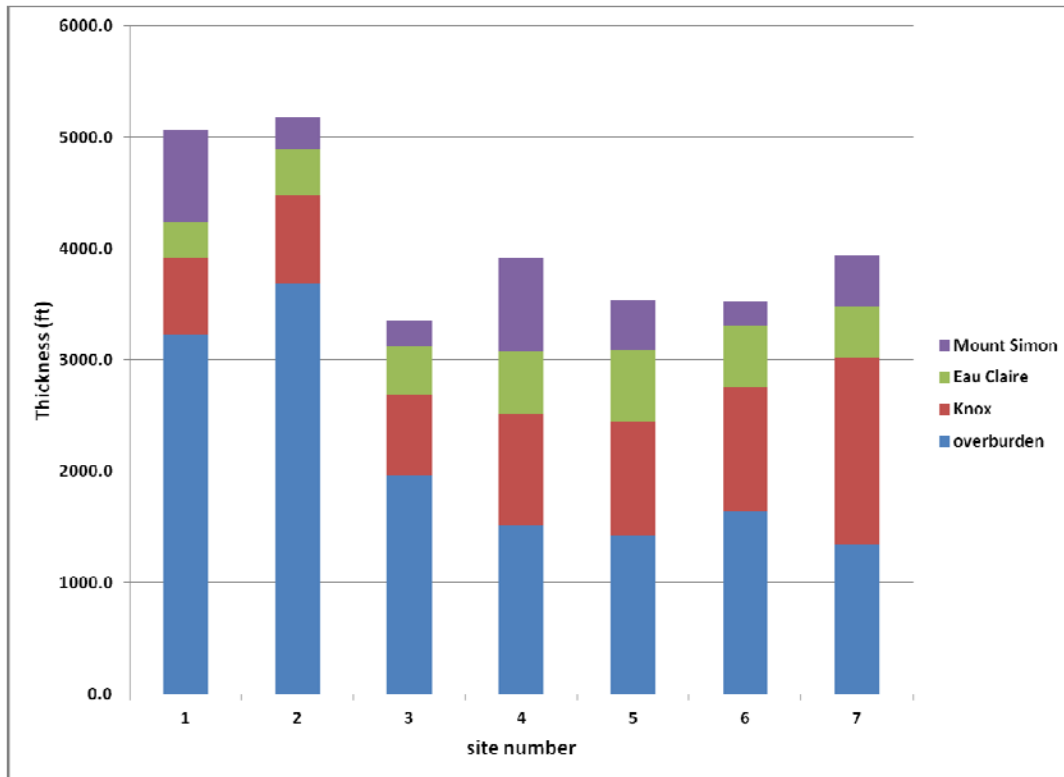


Figure 3-10. Stratigraphic Columns at Each Regional Site

Each site is assumed to have a 4×4 array of injection wells – such that the nominal injection rate is ~ 1 MMT/yr/well. Within this array, two end member scenarios were identified. The first one corresponds to a well in the middle of the model domain, where symmetry conditions create a no-flow boundary on all sides. This is designated as Model A in Figure 3-11. The second corresponds to a well at the edge of the well network, which can be represented as an equivalent semi-infinite system. This is designated as Model B in Figure 3-11. Model A can be seen as the conservative case, as it will result in the maximum amount of pressure buildup. Model B is the other end-member case, as it will result in the minimum amount of pressure buildup.

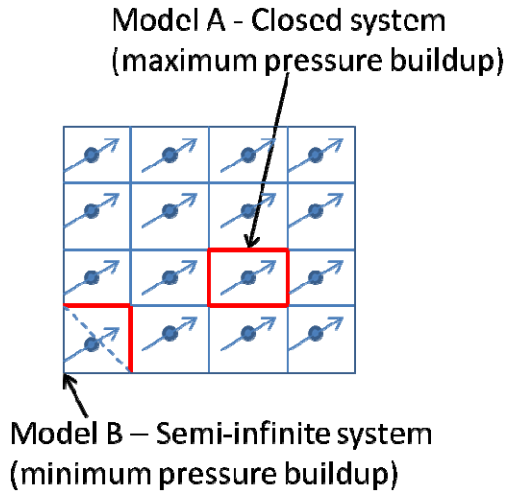


Figure 3-11. Model Domain Simplification

The first set of simulations described here correspond to Site 7, Model A. Figure 3-12 shows the model geometry used for this case. The model consists of 28 vertical layers that extend from the top of the Eau Claire to the base of the Mt. Simon, and 200 radial columns that extend from the center of the injection well to the closed (symmetry) outer boundary. Vertically, the model is 280 m thick (from a depth of 644 m to 924 m), and radially, the model has variable radial extent depending on the assumed site radius and the number of wells in the injection cluster (as described in the next section). At the bottom of the model, the reference pressure and temperature are assumed to be 1870 psi and 92 °F, respectively.

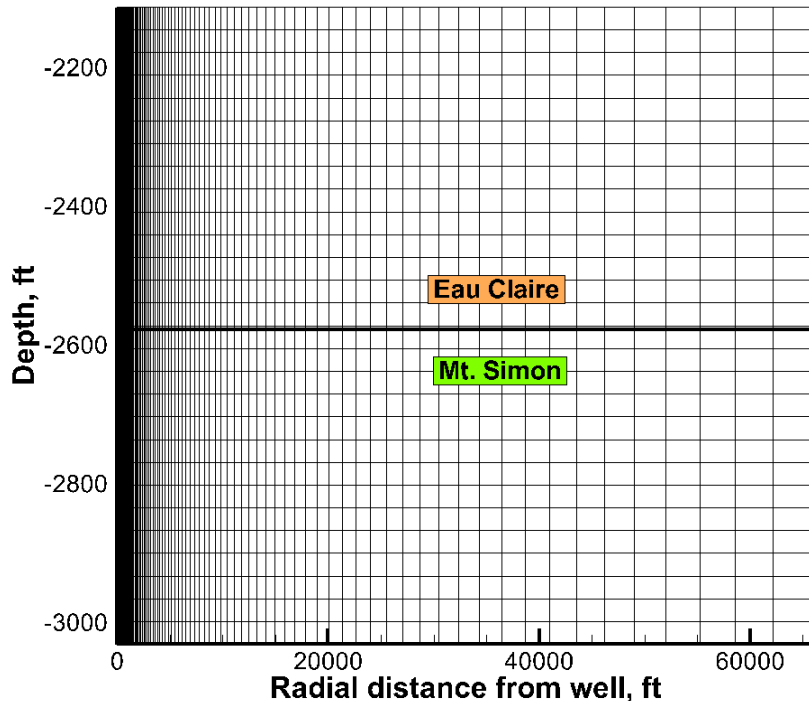


Figure 3-12. Model Geometry (Site 7, Model A)

The averaged porosity profile is shown in Figure 3-13 (left panel). Here, the Eau Claire has been subdivided into three primary flow units, and the Mt. Simon has been divided into six primary flow units. The primary flow units have also been subdivided into additional computational model layers. Note that EC2 and MS2 are low porosity layers sandwiched between two higher-porosity layers. Note also that MS4, MS5 and MS6, in combination, have characteristics similar to that of MS2. The averaged permeability profile, also shown in Figure 3-13 (right panel), mirrors the porosity layering since it is estimated from porosity using a simple exponential transform:

$$k = 0.000226 \exp\left(\frac{37.27\varphi}{100}\right)$$

where

k = permeability (mD),

Φ = porosity (%).

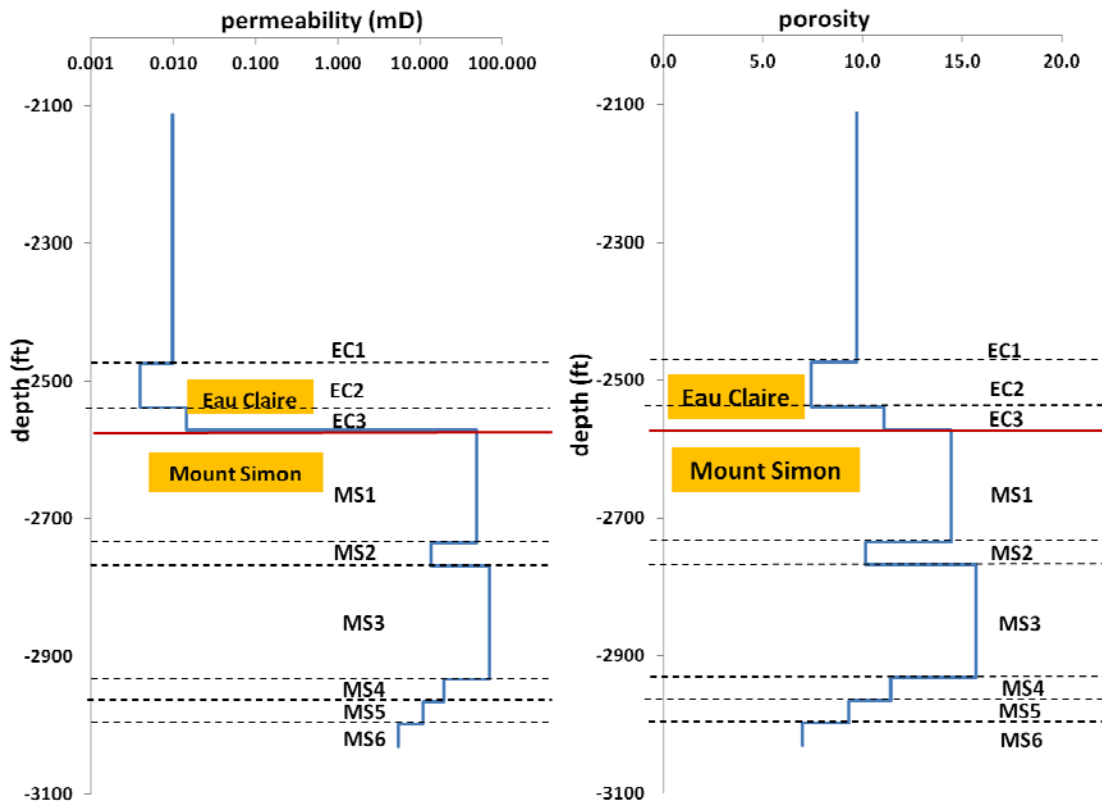


Figure 3-13. Averaged Permeability Profile (left panel) and Porosity Profile (right panel) at Site 7

Two variants were created to characterize the relative permeability – capillary pressure relationship.

Case 1 (VG Mualem) – For the Mt. Simon, the capillary entry pressure value, corresponding to the porosity and permeability of the reference layer, is taken from a preliminary FutureGen modeling study (White and Zang, 2011). Leverett-J function scaling was used to evaluate the value of the capillary entry pressure for each of the layers of the Mt. Simon in this current model, depending on the layer's porosity and permeability. The procedure is similar for the Eau Claire, with the only difference being that the

capillary entry pressure value, and the corresponding porosity and permeability of the reference layer, are taken from Zhou et al. (2010). The Leverett J-scaling is expressed as (Leverett, 1941):

$$\frac{P_c \sqrt{k/\phi}}{\sigma \cos \theta} = J(S_w, \Gamma)$$

where

P_c = capillary pressure
 J = Leverett J-function
 k = absolute permeability
 Φ = porosity
 σ = interfacial tension
 θ = contact angle
 S_w = water saturation
 τ = tortuosity.

Case 2 (VG Mualem fit) – Mercury injection capillary pressure (MICP) tests were performed on 14 samples from the Mt. Simon, and two samples from the Eau Claire. The sample Leverett J function data for each of the two units was plotted as a function of S_w , and a curve is fit through the 14 samples, and 2 samples, respectively, to obtain $J_{MS}(S_w, \tau)$ and $J_{EC}(S_w, \tau)$. Using the Leverett J -function scaling, it is possible to calculate $P_c = f(S_w)$, for a given layer, of porosity Φ , permeability k , interfacial tension σ and contact angle θ .

A non-linear least squares optimization procedure is then employed to fit this capillary pressure data to the van-Genuchten saturation function (van Genuchten, 1980). From this procedure, the van-Genuchten model parameters are obtained, which are used as input in the STOMP saturation function card.

$$\log h = \frac{\left(\left(\frac{S_w - S_{wr}}{1 - S_{wr}} \right)^{\frac{1}{m}} - 1 \right)^{\frac{1}{n}}}{\alpha}$$

where

h = capillary pressure head
 S_w = water saturation
 S_{wr} = irreducible water saturation
 and m , n , α = van-Genuchten model parameters.

The corresponding relative permeability curves are shown in Figure 3-14. Capillary pressure related parameters are given in Table 3-3. The van-Genuchten saturation function, and the Mualem porosity distribution models are used in the saturation function and relative permeability cards, respectively.

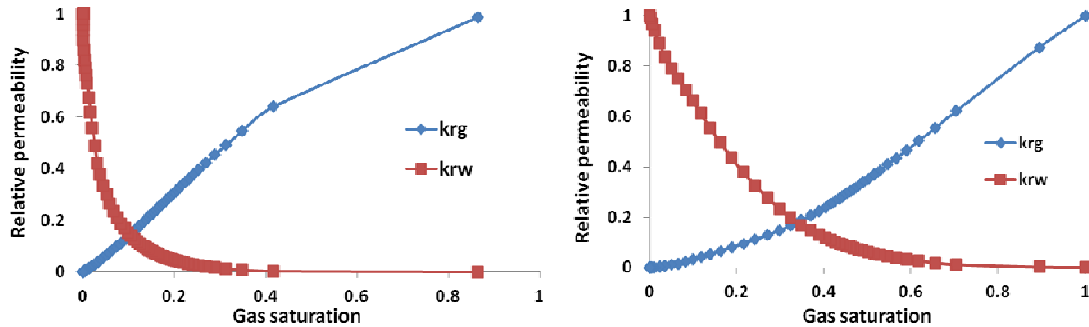


Figure 3-14. Relative Permeability Curves (Case 1 [VG_Mualem] – left panel, and Case 2 [VG_Mualem_fit] – right panel)

Table 3-3. Capillary Pressure Curve Parameters, Case 1 and Case 2

Rock Type	van-Genuchten α Parameter (1/ft)	van-Genuchten n Parameter	Irreducible Water Saturation ($S_{w,irr}$)	van-Genuchten m Parameter
Case 1				
EC	0.000643	1.695	0.4	0.41
MS	0.0461	1.695	0.3	0.41
Case 2				
EC1, EC3	0.3902	5.61	0.0021	0.822
EC2	0.365	5.904	0.0028	0.8306
MS1, MS3	0.829	3.623	9.87E-05	0.724
MS2, MS4, MS5	0.7006	3.96	0.00014	0.747
MS6	0.643	4.15	0.00017	0.759

3.7 Scenarios – Site-Specific Case

As has been described earlier, seven stratigraphic columns were extracted to form representative models covering the entire Arches study area (Figure 3-10). For each of these sites, two model configurations were identified. Model A represents the conservative closed outer boundary case, and Model B represents the semi-infinite outer boundary case (Figure 3-11). Finally, there are two sets of relative permeability curves, viz: Case 1 (VG_Mualem), and Case 2 (VG_Mualem_fit). This leads to a total of 28 scenarios. In each of these cases, CO_2 injection is simulated for 30 years at the rate of 0.93 MMT/yr. In the next section, the results for two of these 28 scenarios - Site 7, Model A, and Cases 1 and 2 are described.

3.8 Results – Site-Specific Case

Figure 3-15 shows pressure and saturation contours at $t = 30$ years for Site 7, Model A, Case 1. The pressure contours (left panel) suggest primarily horizontal flow in the near-wellbore region, although the saturation contours (right panel) show the development of buoyancy driven effects as indicated by the angled CO_2 -brine interface.

Pressure contours for Case 2 (Figure 3-16, left panel) show similar behavior, i.e., vertical contours within the Mt. Simon indicating near-horizontal flow. However, saturation contours for Case 2 (right panel) show an attenuated front, possibly because of the lower relative permeability to CO₂ in Case 2 compared to Case 1 (Figure 3.15).

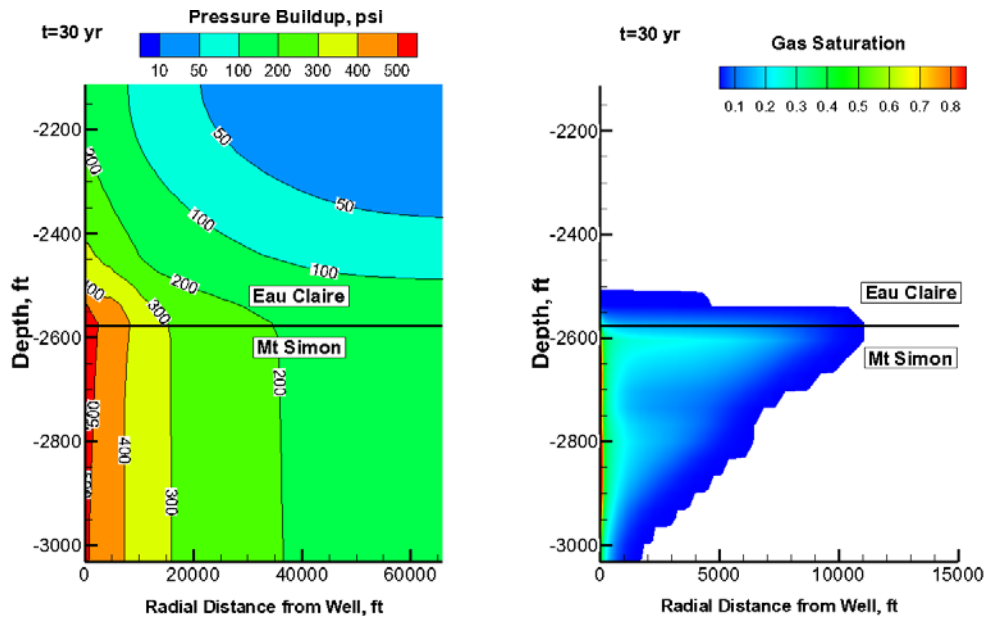


Figure 3-15. Pressure and Saturation Contours (Site 7, Model A, Case 1)

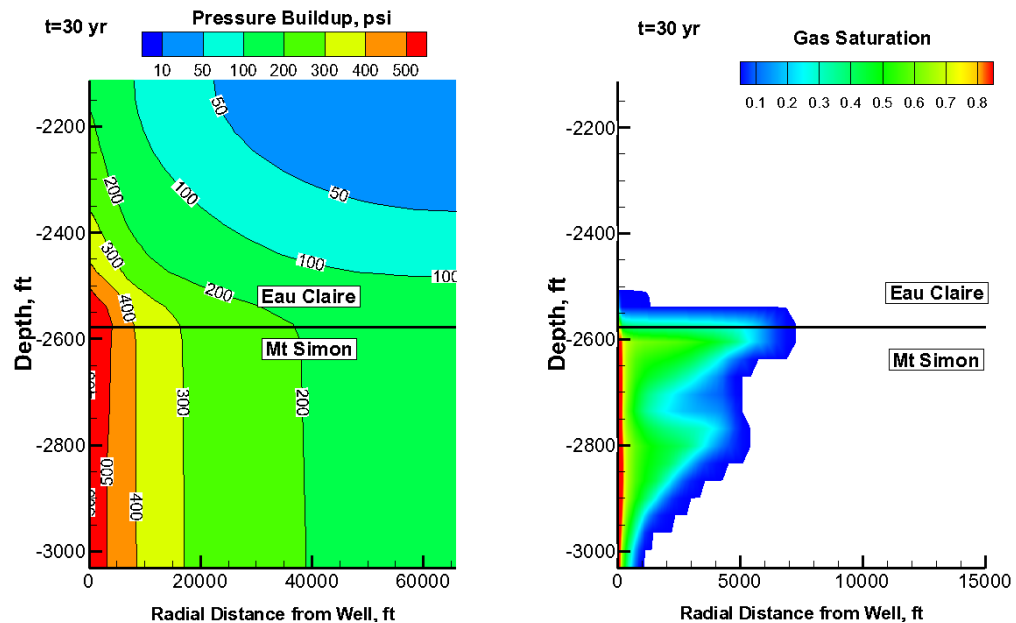


Figure 3-16. Pressure and Saturation Contours (Site 7, Model A, Case 2)

Figure 3-17 shows the pressure buildup history at the mid-points of the Eau Claire for the two relative permeability variants (Case 1 and Case 2). At late times, both sets of pressure curves tend to converge, suggesting that the pressure front is essentially responding to the properties of the brine-filled region beyond the CO₂ front, and is therefore relatively insensitive to relative permeability differences.

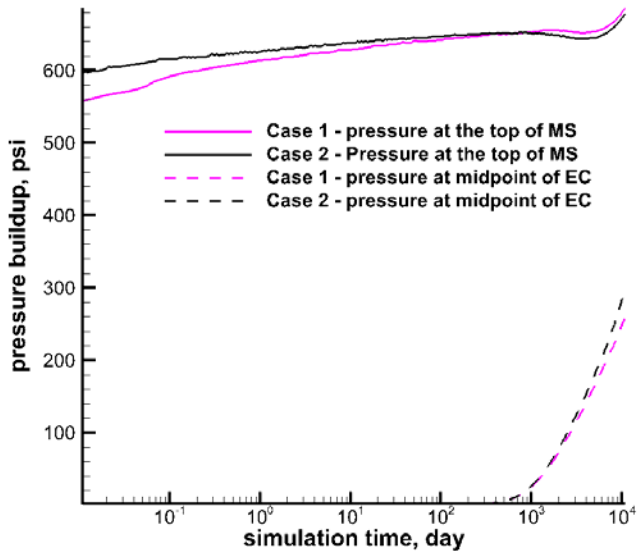


Figure 3-17. Injection Well Pressure Buildup (Site 7, Model A Case 1, Case 2)

The cumulative mass flux across the Mt. Simon-Eau Claire interface is shown in Figure 3-18. Here, the impact of relative permeability effects is shown. Case 1 has a much higher relative permeability to CO₂ than Case 2 (Figure 3-15), which leads to a higher mobility for CO₂ and, hence, greater movement of CO₂ mass across the Eau Claire-Mt. Simon interface.

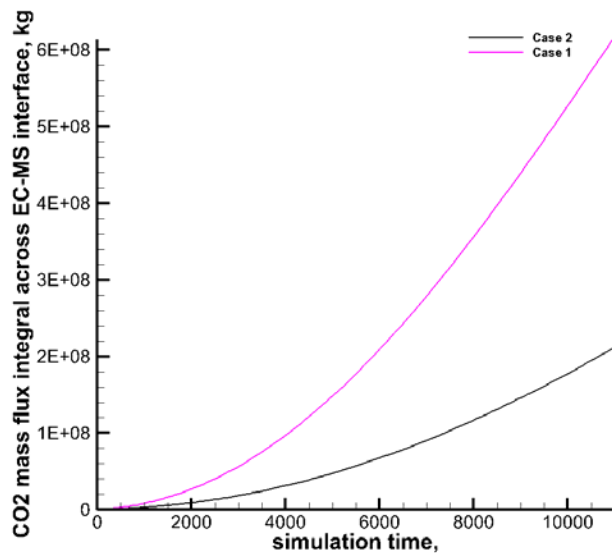


Figure 3-18. CO₂ Mass Flux Integral across EC-MS Interface (Site 7, Model A, Case 1, Case 2)

3.9 Summary – Site-specific Case

Scoping level simulations were completed for one of the sites (Site 7), which represents average conditions for layer thicknesses in the Arches study area. Also, the simulations use the configuration for Model A, which has a closed outer boundary and thus produces the highest pressure buildup. Both relative permeability variants (Case 1 and Case 2) have been utilized, and show different system response for saturation contours and CO₂ mass flux integral across the Mt. Simon-Eau Claire interface. Pressure response is relatively unaffected by relative permeability effects.

3.10 CO₂ Storage Capacity Analysis

In association with the scoping level simulations, estimations of injected CO₂ plume radii were calculated for various storage site scenarios (i.e., storage efficiency factors) and locations. These estimates were developed to provide another measure to validate simulation results against. The results also provide some general guidance for CO₂ storage infrastructure analysis. For all calculations it was assumed that injection of CO₂ takes place for 20 years at a given, constant rate. Site-specific characteristics were extracted from the geocellular model for use in the final calculation of plume size. These estimated attributes included reservoir thickness, average porosity, and fluid density of CO₂ (based on local estimated pressure and temperature conditions). The plume radius calculation was calculated based on a variation of the U.S.DOE Carbon Atlas capacity equation (U.S.DOE, 2008):

$$r = \sqrt{\frac{\text{Total Mass Injected}}{\pi h \Phi E_f}}$$

where

r = plume radius estimate
h = reservoir thickness
Φ = average reservoir porosity
E_f = storage efficiency factor.

In the first scenario, it was assumed that seven regional storage sites, or fields, were implemented wherein CO₂ is transmitted via pipeline for injection into the Mt. Simon. Two separate injection rates were used to determine two plume radii for each of the seven regional sites: 10 and 20 MMT/yr (million metric tonnes per year). Injection was assumed to take place for 20 years. The storage efficiency factors used were 0.01, or 1%, and 0.04, or 4%. Figure 3-19 shows the calculated plume radii for the seven regional sites.

In the second scenario, it was assumed that 50 source-located storage sites, or fields, were implemented wherein CO₂ was injected into the Mt. Simon at, or near, the source itself. Injection rates used in the plume radii calculations were assumed to be 25% and 50% at each source, per year. Injection was assumed to take place over 20 years. The storage efficiency factors used were 1% and 4%. Figure 3-20 shows the calculated plume radii for the 50 site-source locations. It should be noted that Mt. Simon thickness, particularly in Ohio, has a significant effect on the calculated plume sizes.

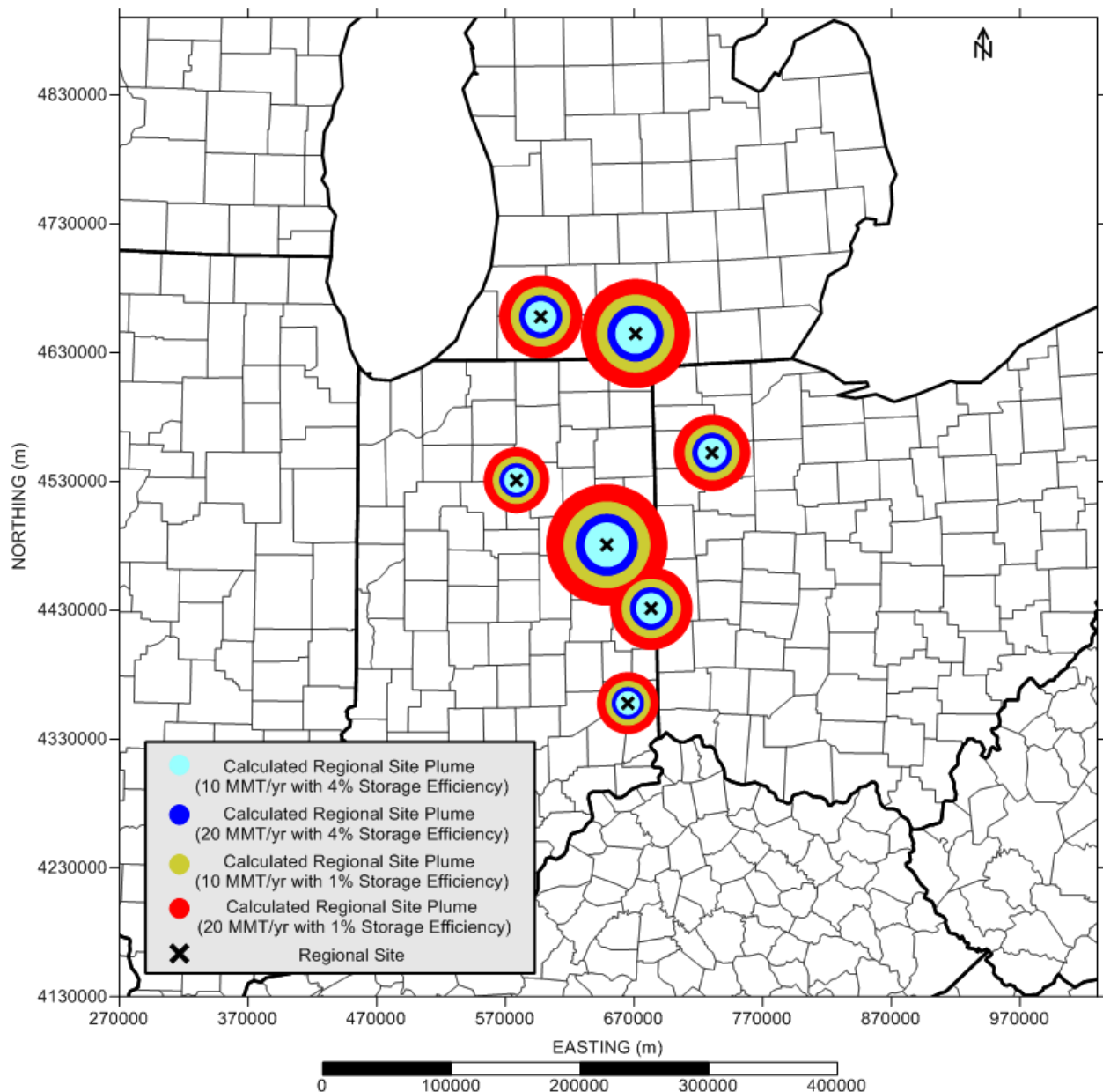


Figure 3-19. Calculated Plume Radii for Seven Regional Storage Sites in the Mt. Simon for 20 Year Injection at 10 and 20 MMT/yr with 1% and 4% Storage Efficiency Factors

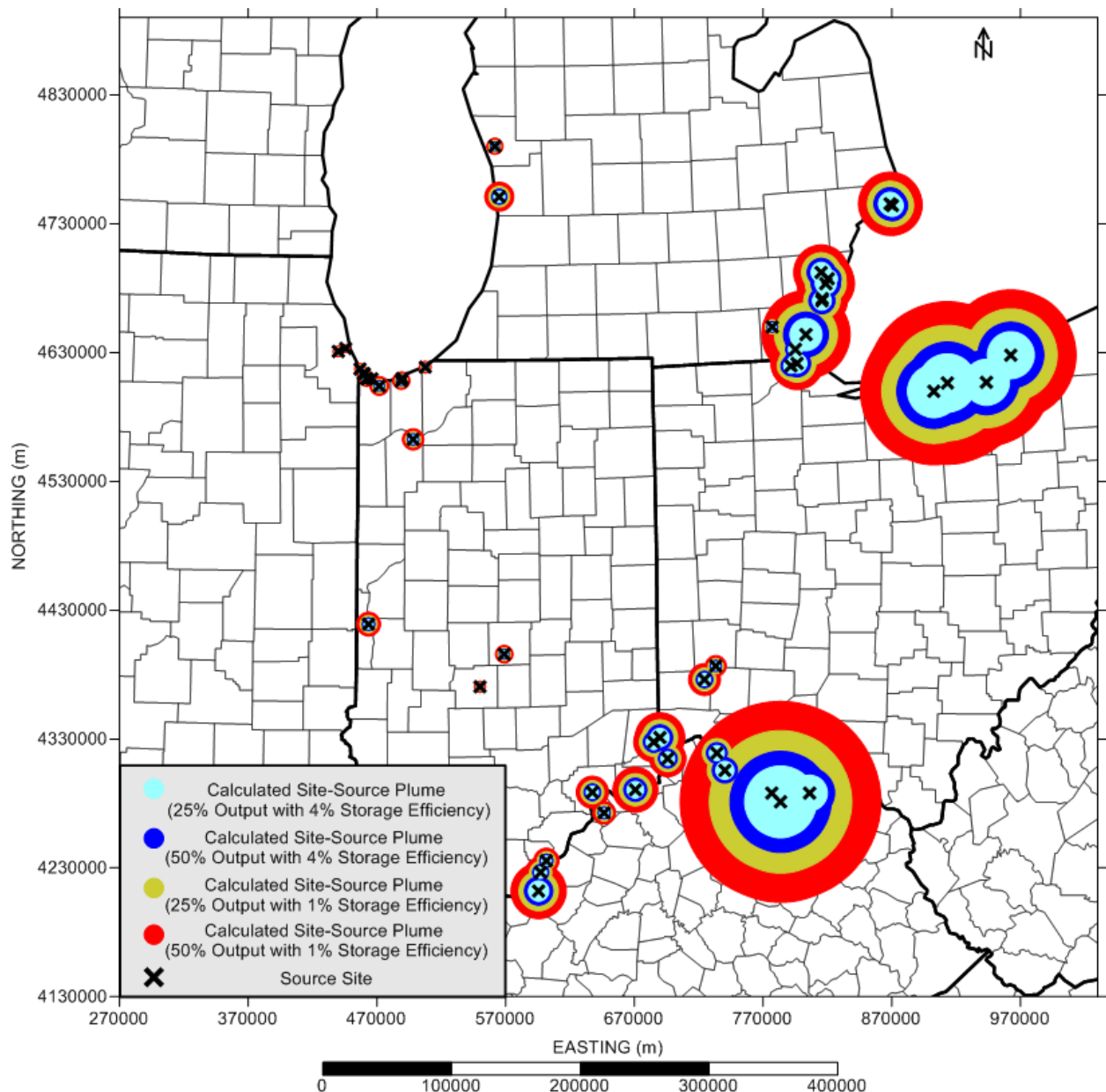


Figure 3-20. Calculated Plume Radii for 50 Source-Located Storage Sites in the Mt. Simon for 20 Year Injection Using 25% and 50% CO₂ Source Output with 1% and 4% Storage Efficiency Factors

Section 4.0: PRELIMINARY BASIN SCALE SIMULATIONS

As part of the variable density modeling effort, preliminary basin scale simulations were completed with multiple-phase simulation code STOMPCO2. These simulations included simplified grid spacing, input parameters, and injection schedule. The objective of the simulations was to examine upscaling issues, numerical solution, and boundary conditions. The preliminary basin scale simulations will form the basis of the more complex simulations. More detail and resolution will be added in these full, basin scale simulations in the final portion of the project.

4.1 Basin Scale Simulation Overview

The preliminary basin-scale multi-phase simulations were executed using the sequential version of the Subsurface Transport Over Multiple Phases (STOMP-CO2) simulator (<http://stomp.pnl.gov>) developed at Pacific Northwest National Laboratory. STOMP-CO2 is an operational mode of the collection of STOMP multi-fluid flow and reactive transport simulators. STOMP-CO2 solves three nonlinear hyperbolic partial differential conservation equations: 1) water mass, 2) CO₂ mass, and 3) salt mass. The governing equations are transformed to algebraic form using integral volume spatial discretization on structured orthogonal grids (e.g., Cartesian, cylindrical, curvilinear boundary fitted) and a backward-Euler temporal discretization (i.e., fully implicit). Details concerning the solved governing equations and numerical solution approaches are reported in the STOMP Theory Guide (White and Oostrom 2000) and details concerning the use of STOMP-CO2, including input formatting details, are reported in the STOMP User's Guide (White and Oostrom, 2006). STOMP-CO2 has reactive transport capabilities through the ECKEChem module (White and McGrail, 2005).

Isothermal conditions were assumed for these preliminary simulations, although the non-isothermal operational mode, STOMP-CO2e, can be applied if the CO₂ being injected is at a temperature that is significantly different from the formation temperature. Salt precipitation can occur near the injection well in higher permeability layers, reducing the reservoir injectivity by completely plugging pore throats making the layer impermeable. The STOMP-CO2 simulator accounts for precipitation of salt.

Injected CO₂ partitions in the reservoir between the free (or mobile) gas, entrapped gas, and aqueous phases. Sequestering CO₂ in deep saline reservoirs occurs through four mechanisms: 1) structural trapping, 2) aqueous dissolution, 3) hydraulic trapping, and 4) mineralization. Structural trapping is the long-term retention of the buoyant supercritical CO₂ phase in the pore space of the reservoir rock held beneath one or more impermeable caprocks. Aqueous dissolution occurs when CO₂ dissolves in the brine resulting in an aqueous phase density greater than the ambient conditions. Hydraulic trapping is the pinch-off trapping of the CO₂ phase in pores as the brine re-enters pore spaces previously occupied by the CO₂ phase. Generally, hydraulic trapping only occurs with the cessation of CO₂ injection. Mineralization is the chemical reaction that transforms formation minerals to carbonate minerals. The processes modeled by STOMP-CO2 include all four mechanisms described above. However, for the preliminary simulations, the mineralization reactions were not considered.

4.2 Model Setup

The three-dimensional (3D) geocellular porosity (Figures 4-1 and 4-2) and permeability (Figures 4-3 and 4-4) grids developed in EarthVision and described in the *Arches Province Conceptual Model Topical Report* (Battelle, 20110) were used as the basis for the material properties for the numerical model. These grids were regularly spaced and consisted of about 50 million cells. For the preliminary simulations, a simplified model was constructed by upscaling the porosity and permeability grids to a mesh of 93,964 cells.

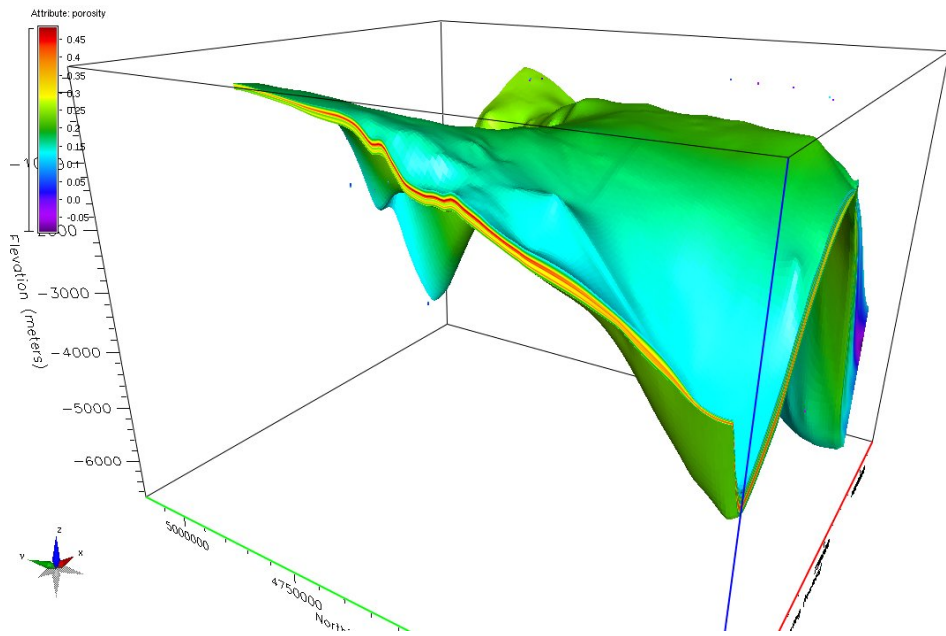


Figure 4-1. Geocellular Model Porosity Distribution for the Eau Claire

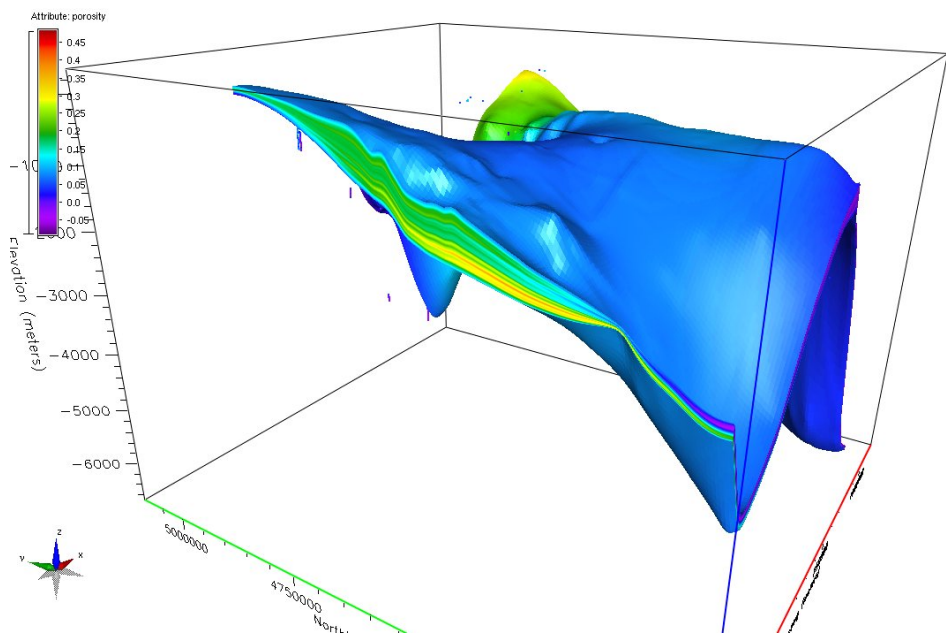


Figure 4-2. Geocellular Porosity Distribution for the Mt. Simon

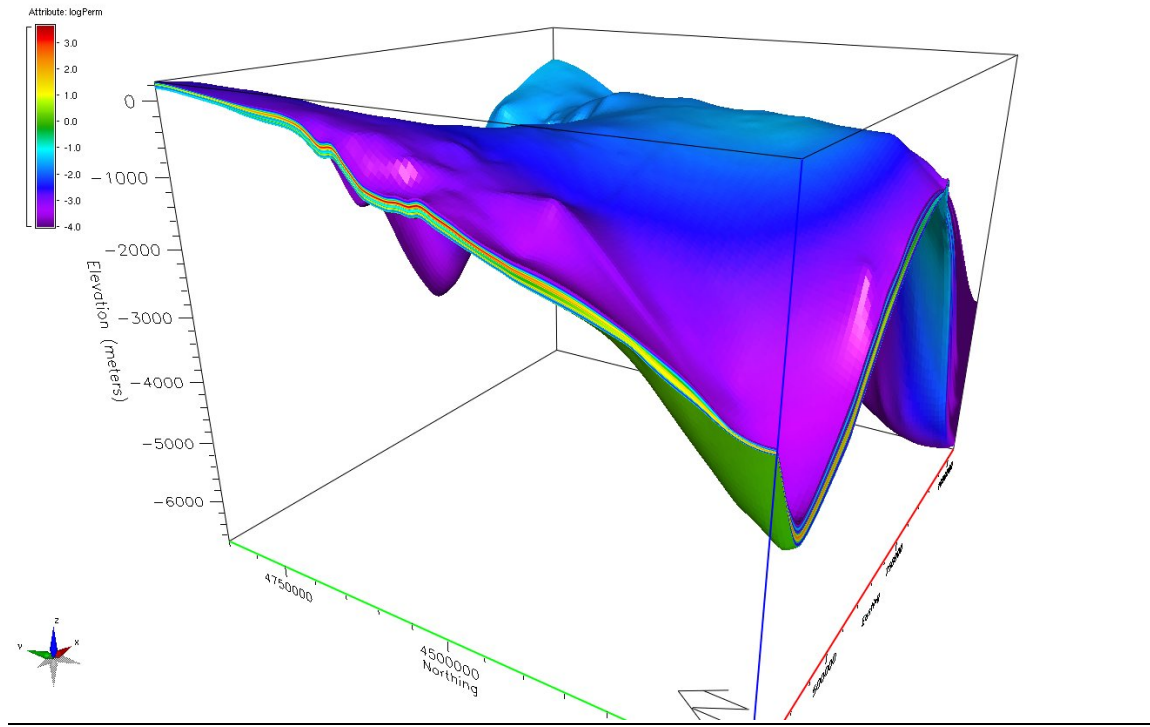


Figure 4-3. Geocellular Model Permeability Distribution for the Eau Claire

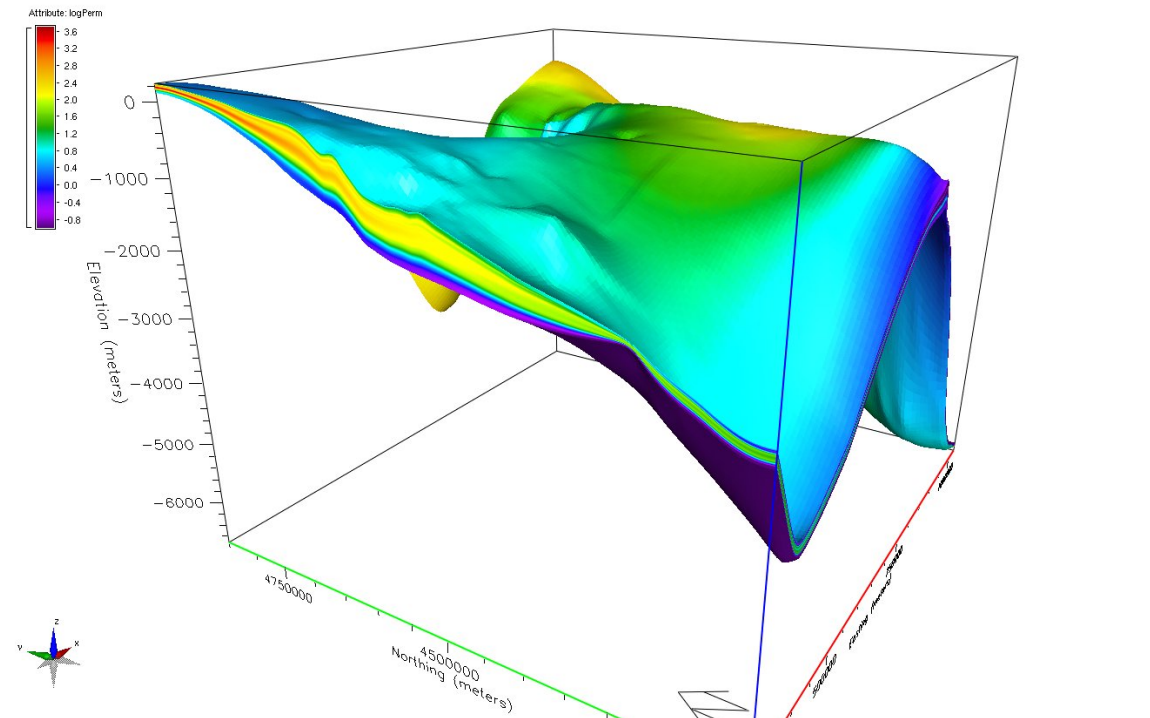


Figure 4-4. Geocellular Model Permeability Distribution for the Mt. Simon

Simulation Domain and Mesh Generation

The simulation domain was based on the same 700 km x 700 km area for which the property grids were generated. Seven sources were located in the region representing the regional injection fields defined by the Arches Province source study described in the *Arches Province Conceptual Model Topical Report* (Battelle, 2011). A boundary fitted mesh with variable grid spacing was generated so that the grid resolution was finer near the injection wells and became increasingly coarser moving away from the wells. This created a tartan type pattern shown in Figure 4-5. The cell size at an injection location was 500 m, the cell size increase factor was 1.3, and the maximum cell size at the edge of the domain was 34 km. The mesh consists of 139 nodes in the X dimension by 169 nodes in Y dimension.

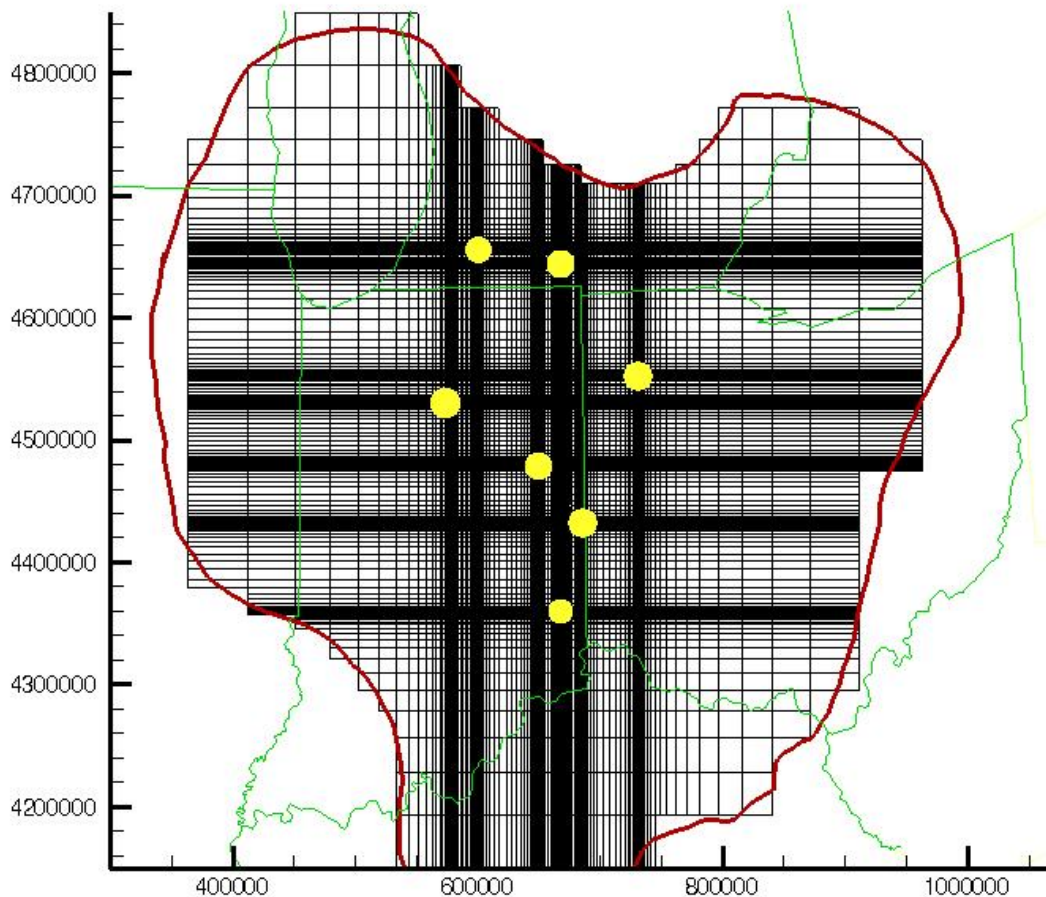


Figure 4-5. Plan View Numerical Model Mesh Showing Injection Well Locations

The domain was vertically discretized into four layers to match the conformal grid of the porosity and permeability distributions and corresponding to the Lower, Middle, and Upper Mt. Simon and the Eau Claire. This resulted in a boundary fitted mesh having a total number of 93,964 simulation cells (Figure 4-6). The active simulation domain was defined by a polygon representing the study area where the Mt. Simon is a viable sequestration target. Using a boundary fitted grid structure preserves the structural surfaces of the geologic layers and variations in the thickness of units. This is particularly important for modeling the pressure distribution in the Arches Province because of the very large structural relief in the area.

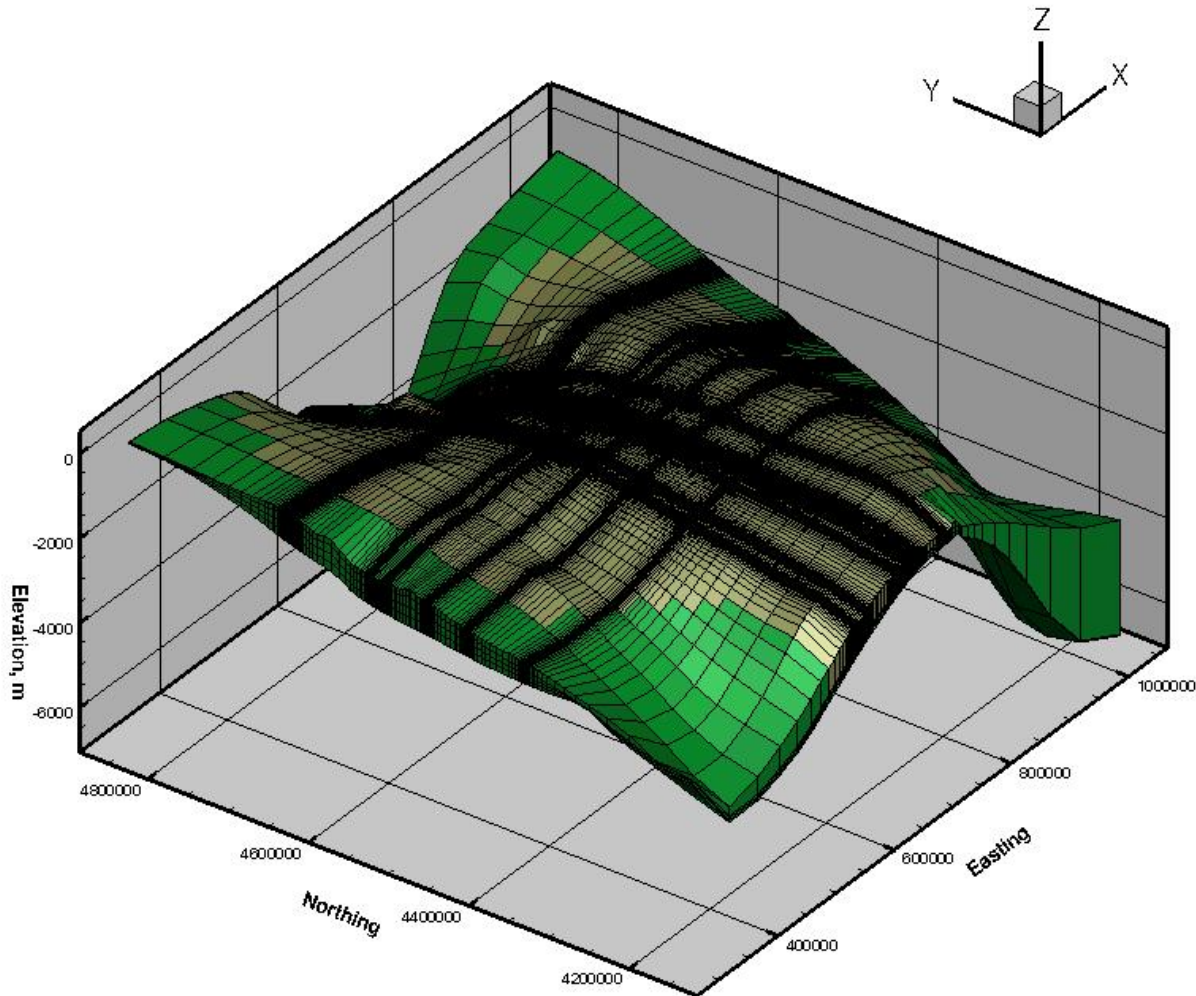


Figure 4-6. Three-Dimensional Boundary Fitted Grid (Inactive Cells are Shown in Green)

Upscaling Hydraulic Properties

Hydraulic properties (i.e., porosity and permeability) were generated for a uniform horizontal resolution of 5x5 km and a very high vertical resolution (about 2 m). This resulted in 2502 values for each property of a vertical profile. In total, data were available for $147 \times 141 \times 2502 = 49,742,262$ cells with a constant lateral size but variable vertical size. These cells are referred to as the data cells. The properties for the data cells were upscaled to the 93,964 boundary-fitted simulation cells, whose sizes vary spatially as described above. In a boundary fitted cell, the x, y coordinates form a rectangle, while the z coordinates at either the top or bottom surface vary spatially and often are not in a plane (Figure 4-6). This makes for a non-trivial translation from a regularly spaced grid to a boundary fitted grid. In addition, the size of a simulation cell in a particular direction may be larger or smaller than that of a data cell, which may completely fall within or partially overlap with the simulation cell (Figure 4-7).

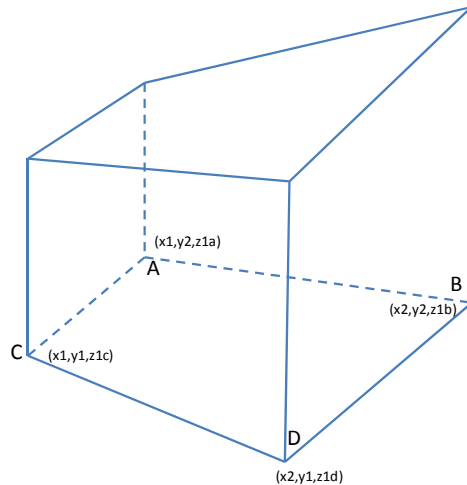


Figure 4-6. Schematic of a Boundary Fitted Cell

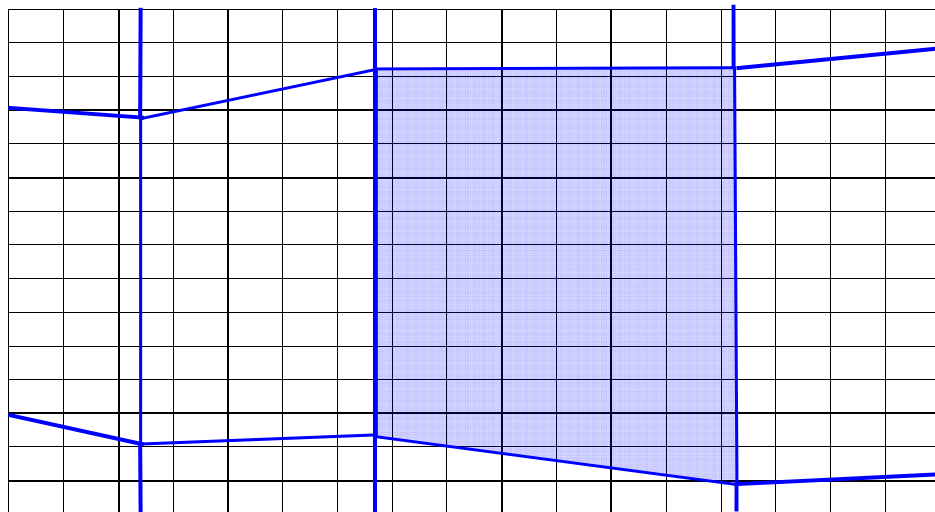


Figure 4-7. Schematic Showing the Data Cells (in black lines) and Simulation Cells (in blue lines)
(The cells or the portion of the cells that fall within the boundary of a simulation cell are contributors for property upscaling.)

Proper upscaling strives to preserve the property distribution as accurately as possible when translating properties from a grid with a fine resolution to a coarser one. The property of a simulation cell is the volume-weighted average of those of the contributing data cells. Porosity data are typically considered to be normally distributed and the arithmetic mean is the best measure of central tendency for a normal distribution. The upscaled porosity is shown in Figure 4-8. Permeability data are typically considered to be log-normally distributed and the geometric mean is the best measure of central tendency for a log-normal distribution. However, for an anisotropic system, the lateral and vertical permeability must be calculated differently. The geometric mean (k_g) was used for the vertical permeability, and the arithmetic mean (k_a) was used for the lateral directions. Hence, the upscaled k for each simulation cell is anisotropic. The upscaled permeability in the lateral and vertical directions is shown in Figures 4-9 and 4-10, respectively.

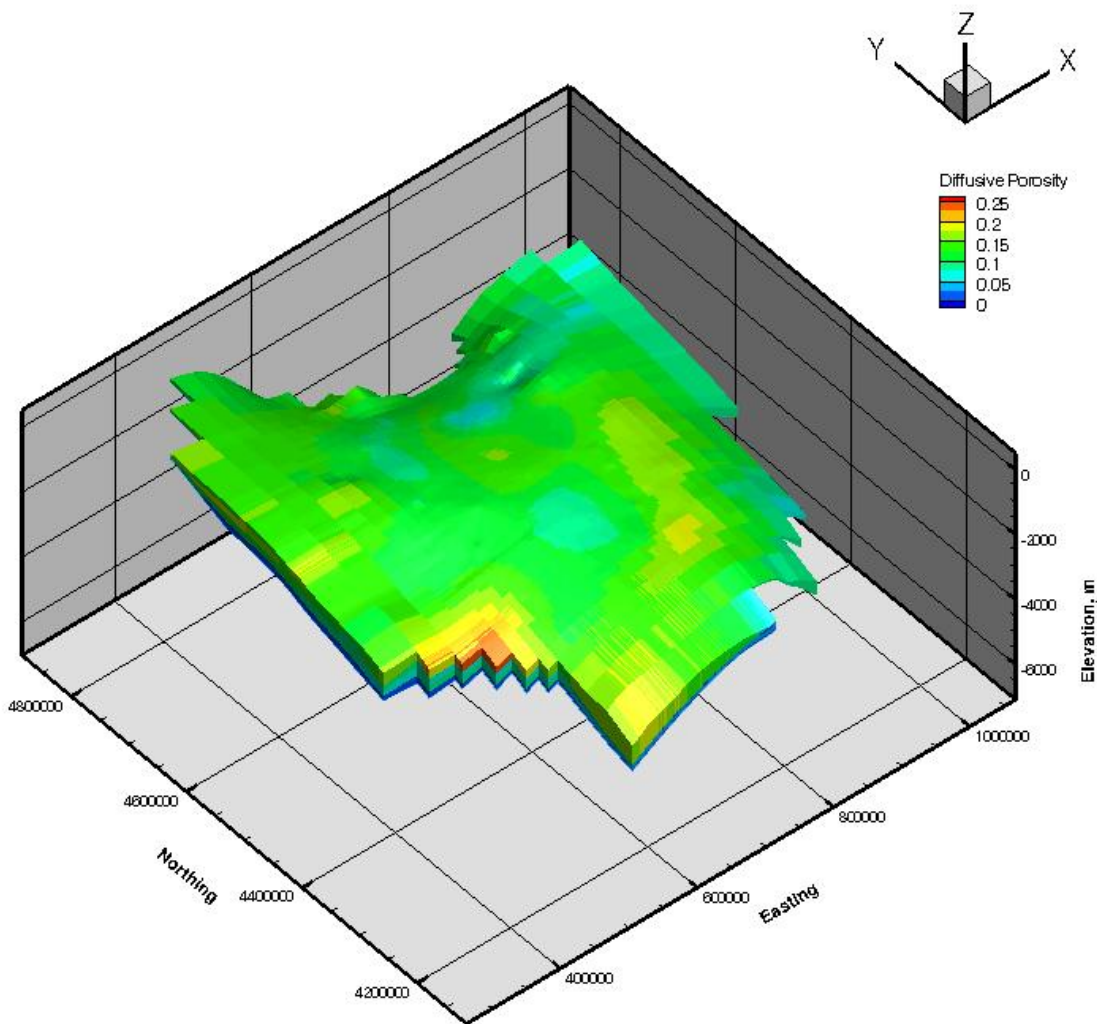


Figure 4-8. Porosity Distribution Upscaled to Boundary Fitted Simulation Mesh

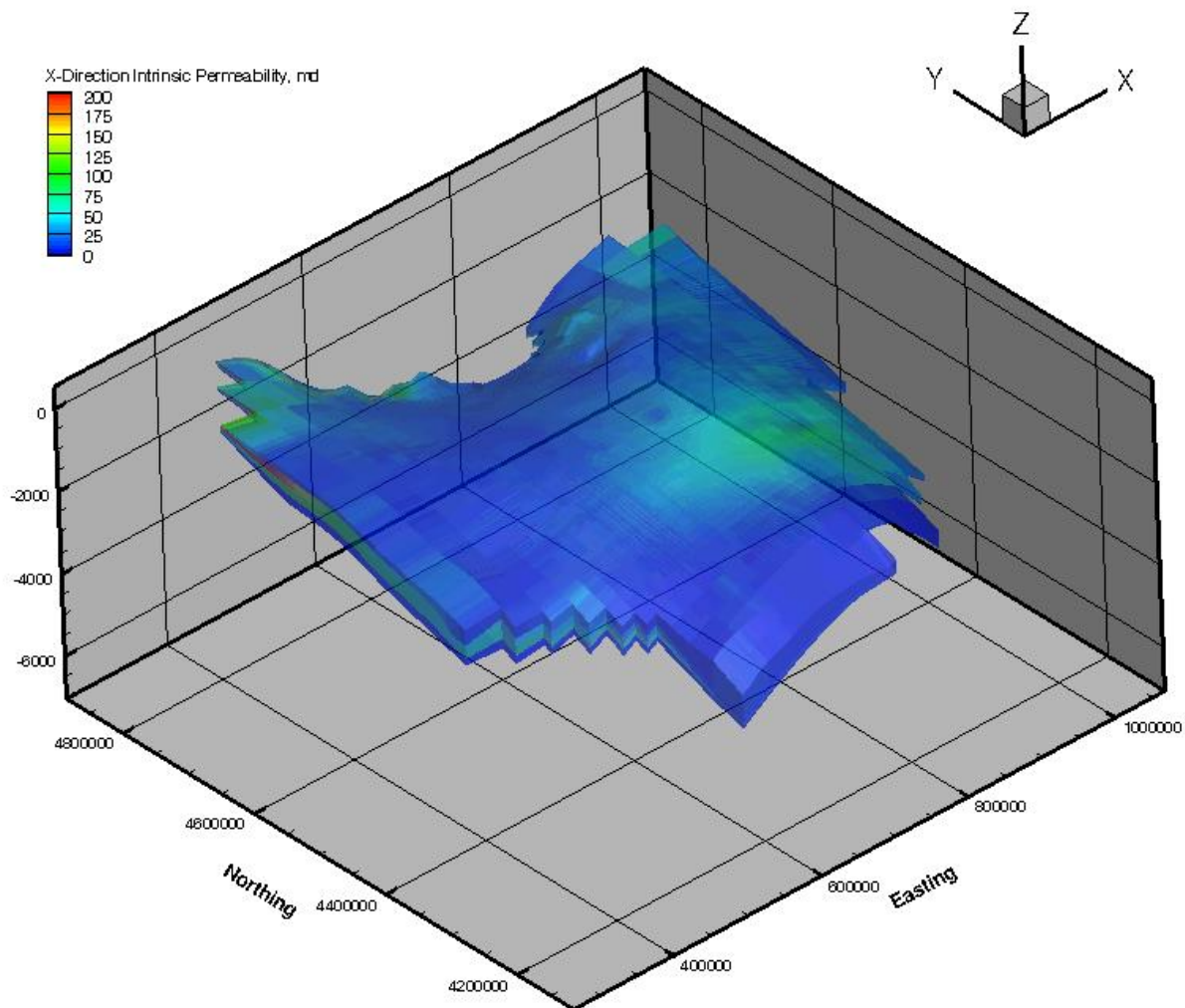


Figure 4-9. Lateral Permeability Distribution Upscaled to Boundary Fitted Simulation Mesh

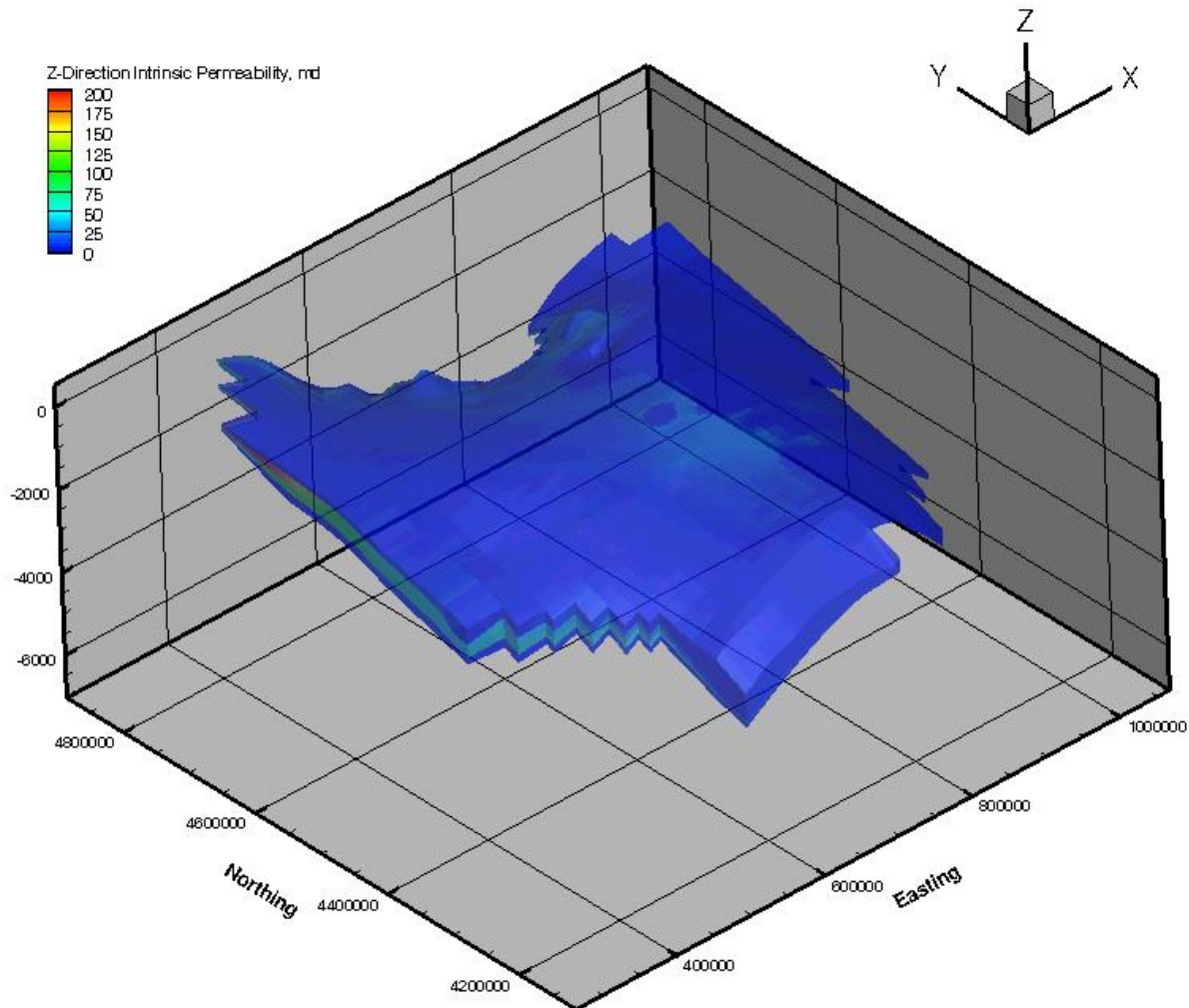


Figure 4-10. Vertical Permeability Distribution Upscaled to Boundary Fitted Simulation Mesh

Initial conditions were determined by executing a steady-state simulation to establish equilibrium conditions for pressure and temperature. Figure 4-11 shows the initial aqueous pressure determined from the steady-state simulation and Figure 4-12 shows the initial temperature.

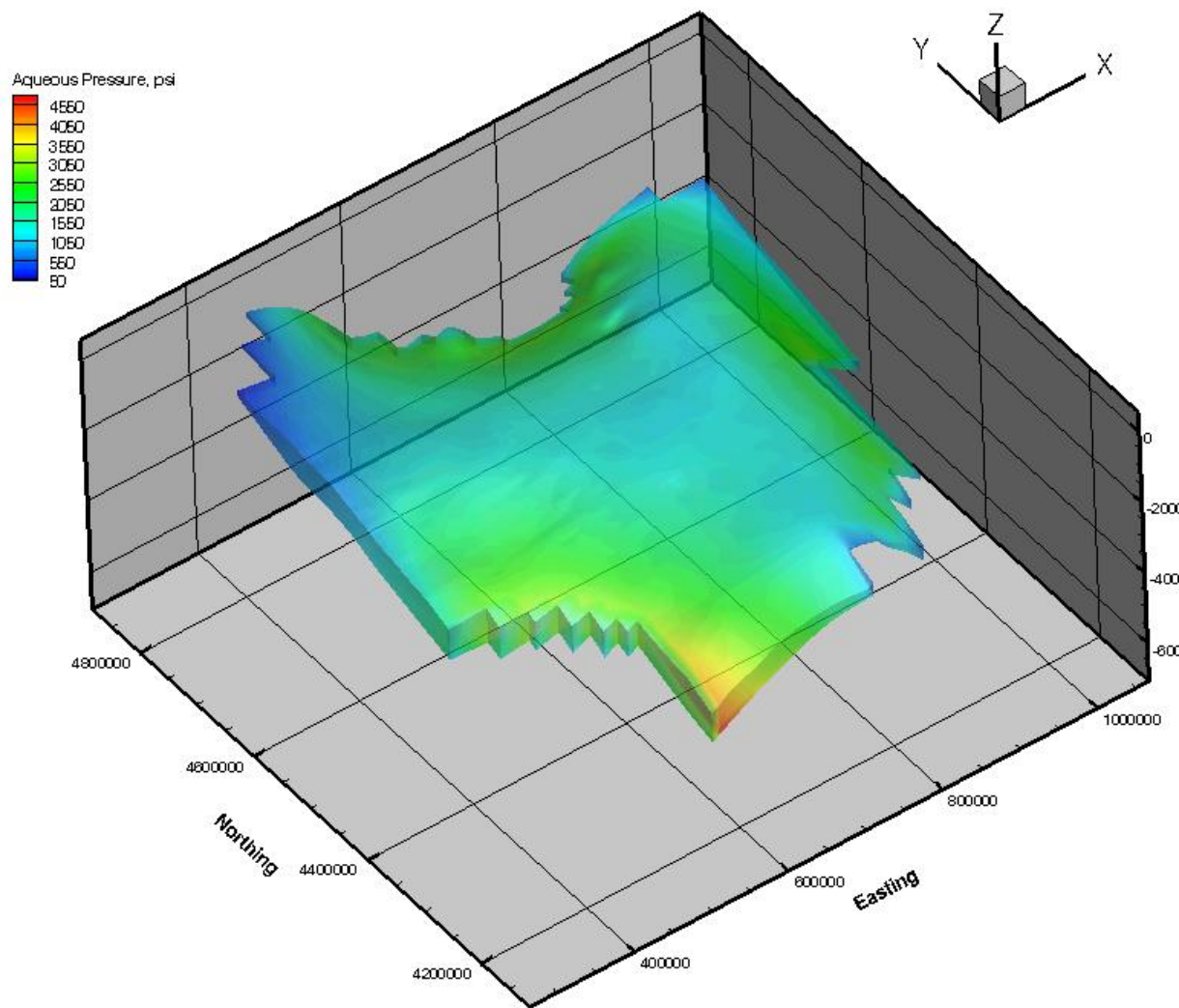


Figure 4-11. Initial Reservoir Pressure Established from Steady-State Simulation

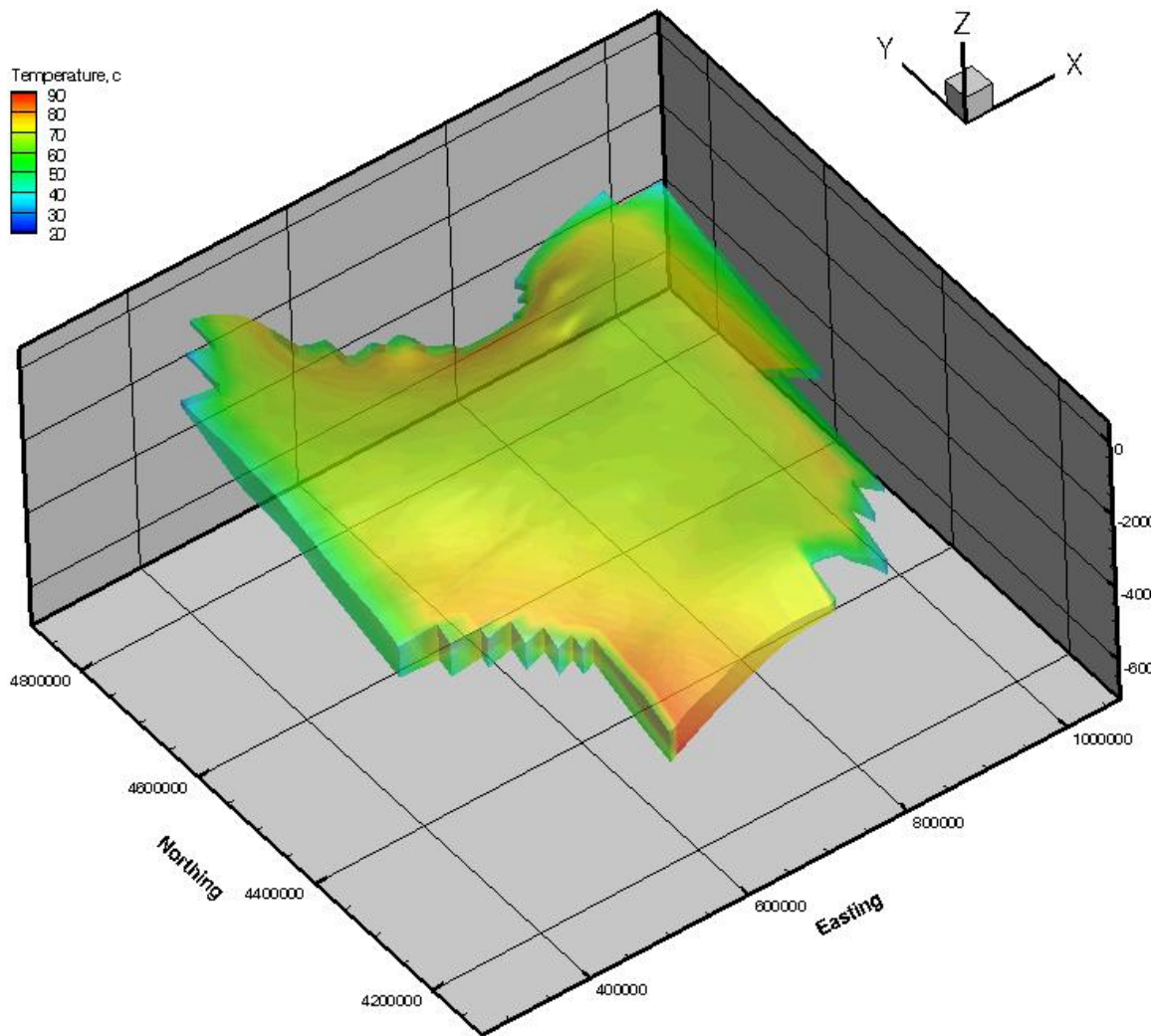


Figure 4-12. Initial Reservoir Temperature Established from Steady-State Simulation

4.4 Simulation Results

The pressure and temperature conditions established in the steady-state simulation were used as initial conditions for the transient simulation of CO₂ injection. The top and bottom boundaries were set as no-flow boundaries for aqueous fluids and for CO₂ gas. The lateral boundary conditions were set to hydrostatic pressure based on the initial pressure distribution. CO₂ was injected at seven locations at a rate of 20 MMT/yr for 15 years. Figure 4-13 shows the gas pressure after 15 years of CO₂ injection. However, the permeabilities near the injection locations are small relative to the injection rate, and therefore the injection quickly becomes pressure limited and not all of the CO₂ mass can be injected. Whereas the total CO₂ mass based on the injection rate and injection duration is 2,100 MMT, only 350 MMT was actually injected into the domain. In addition, in most of the areas of the injection locations, the Mt. Simon is relatively thin and shallow. This results in very slight, localized pressure increases in the areas of the injection locations as seen in Figure 4-14.

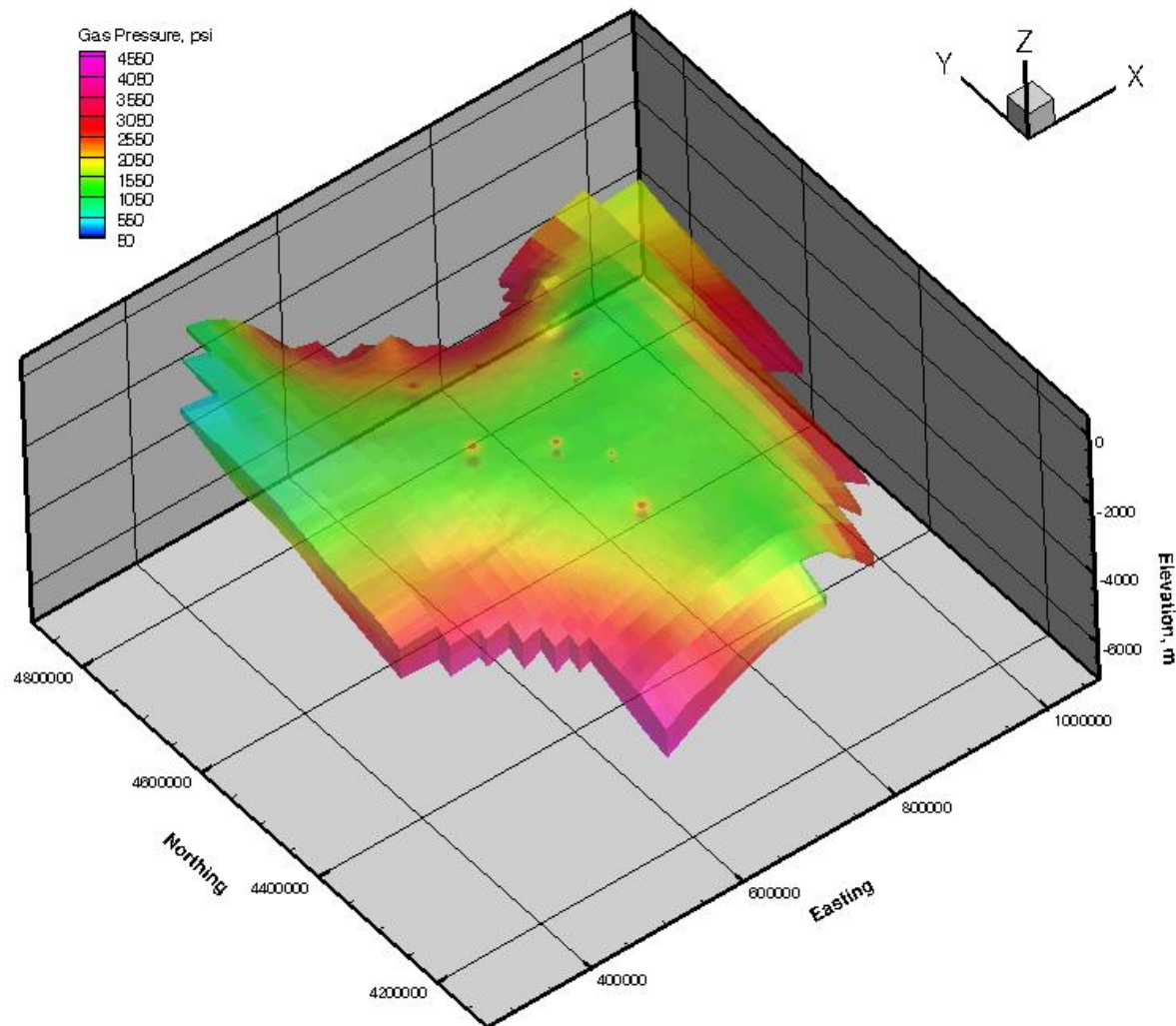


Figure 4-13. Gas Pressure after 15 years of CO₂ Injection

The local CO₂ gas pressure and CO₂ gas saturation for each injection location is shown in Figures 4-14 and 4-15. Permeability in the same areas is shown in Figure 4-16. The thickness of the reservoir and the permeability control the amount of CO₂ that can be injected. For example, Well 7 has the highest permeability in the injection area; however, the reservoir is thin there, limiting the mass that can be injected at that location.

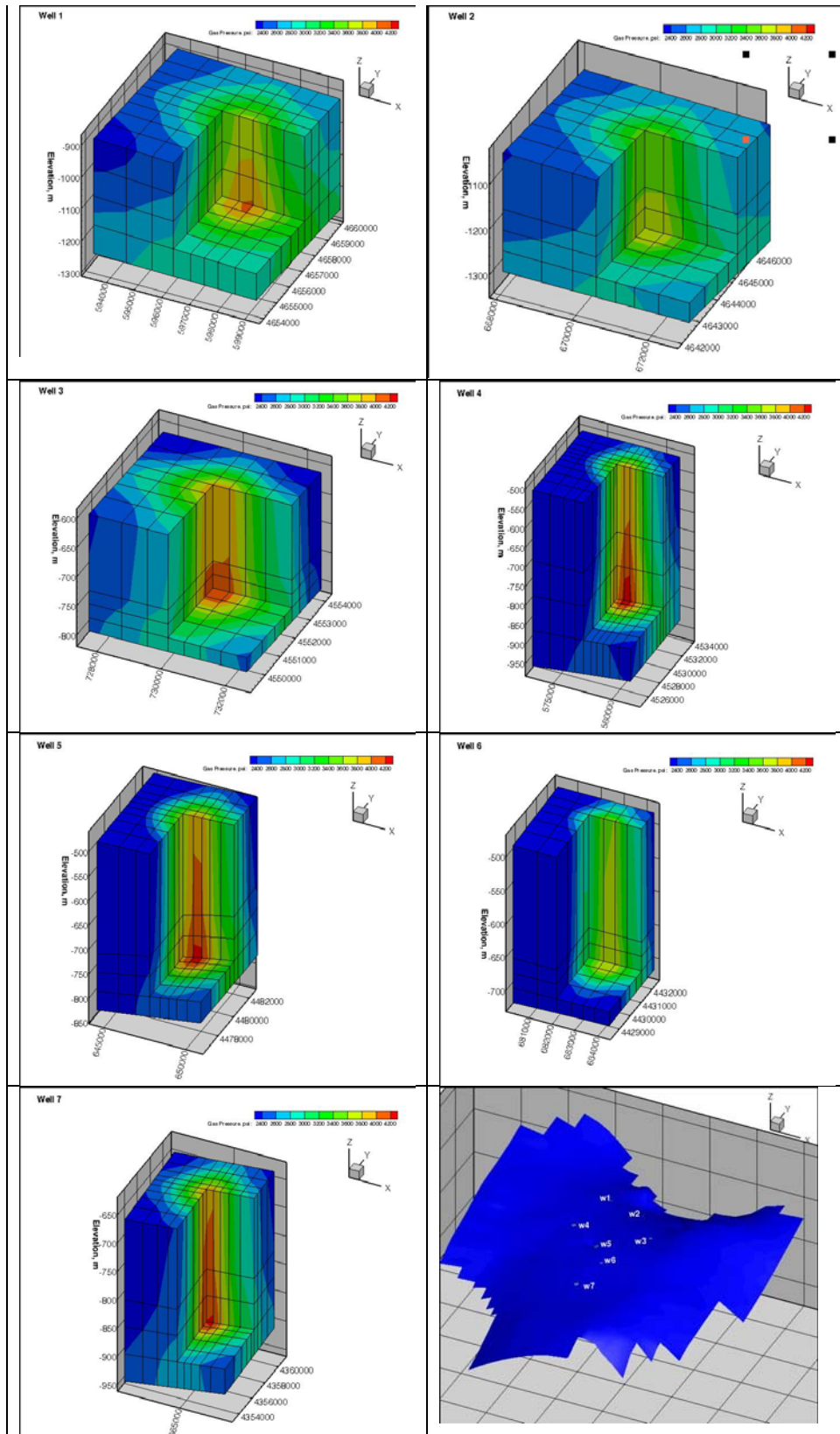


Figure 4-14. Gas Pressure in the Area Near Each Injection Location After 15 Years of CO₂ Injection

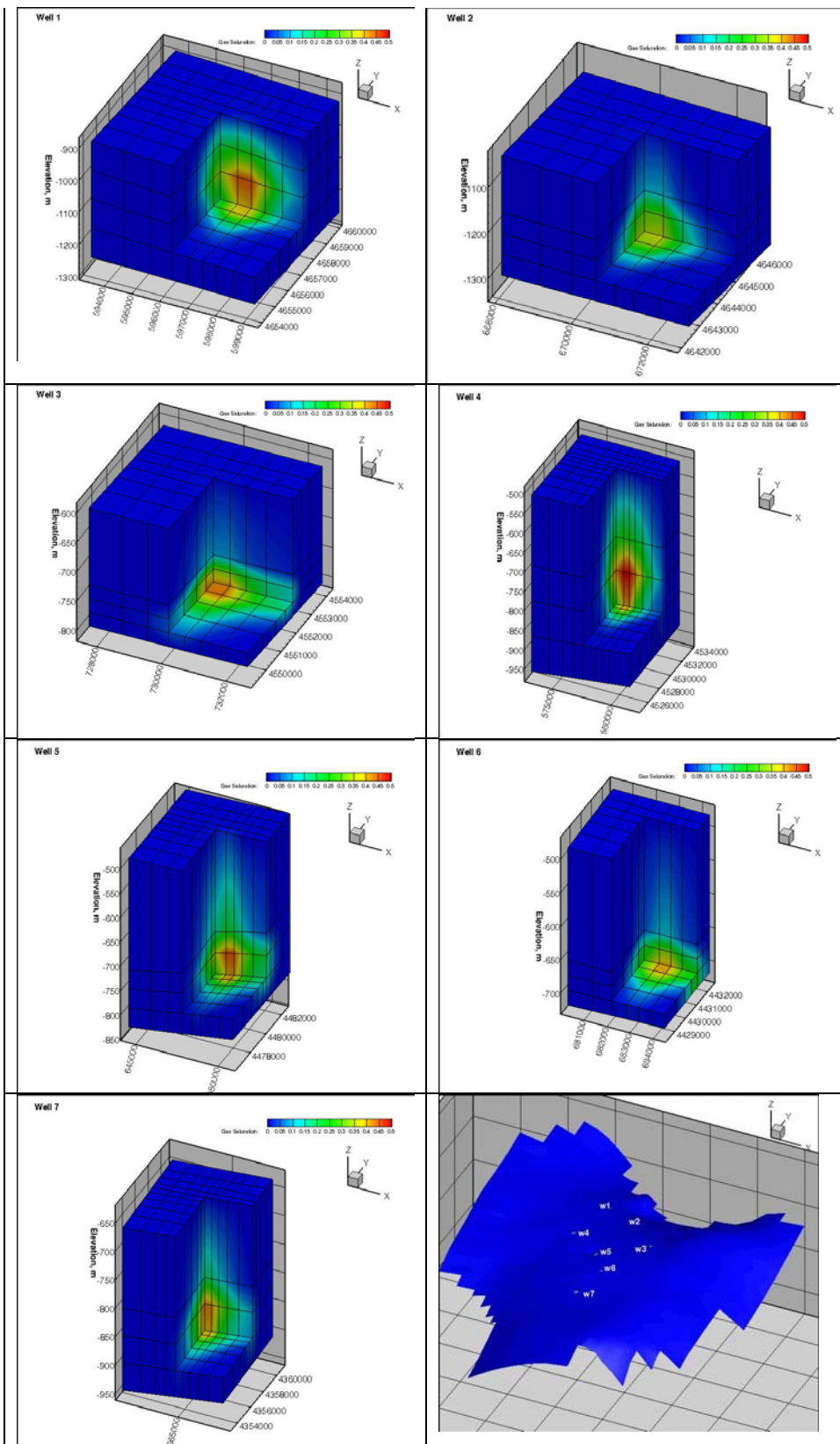


Figure 4-15. Gas Saturation in the Area Near Each Injection Location After 15 Years of CO₂ Injection

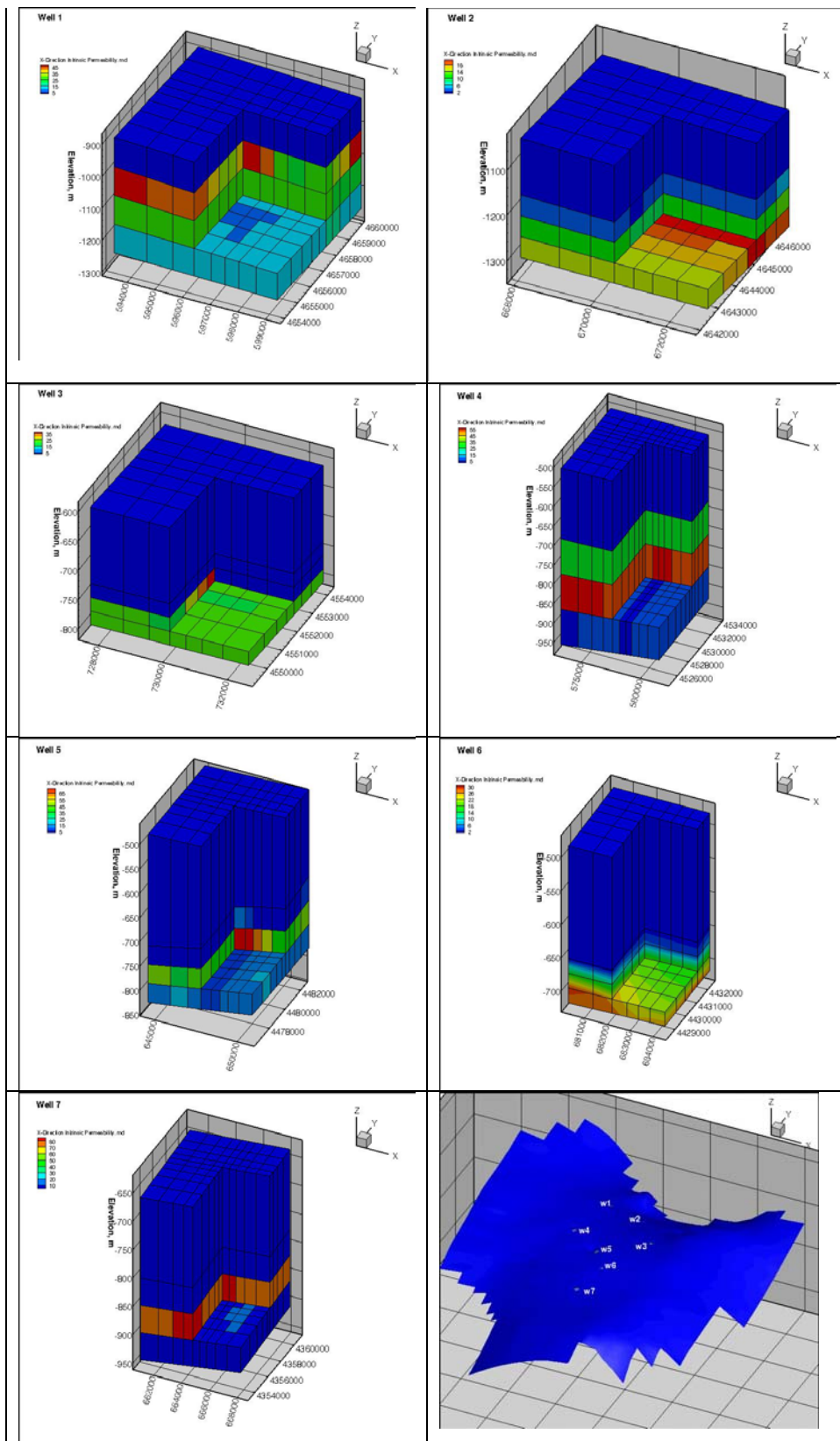


Figure 4-16. Intrinsic Permeability in the Area Near Each Injection Location

Section 5.0: CONCLUSIONS

A variety of scoping-level simulations was conducted successfully to help determine suitable model domains and input data for the Arches Province numerical simulations. Three main tasks were completed for the variable density modeling:

- Single-phase groundwater flow modeling,
- Scoping level multi-phase simulations, and
- Preliminary basin-scale multi-phase simulations.

Data from the geocellular model developed earlier in the project were translated into preliminary numerical models. These models calibrated to observed conditions in the Mt. Simon, suggesting a suitable geologic depiction of the system.

Initial single-phase flow simulations were developed for the Arches Province based on the geocellular model dataset. The single-phase flow simulations were completed with the computer codes MODFLOW (McDonald and Harbaugh, 1988) and SEAWAT (Langevin et al., 2007). These single-phase simulations helped provide guidance on input parameters for the more complex multiple-phase simulations. The model results indicate suitable calibration to observed reservoir pressure, flow budget, and flow vectors in the Mt. Simon.

The SEAWAT model suggests fairly high resolution grid spacing is necessary around the injection wells to capture CO₂ injection processes. Grid cell spacing less than 500 m by 500 m X-Y spacing is likely necessary around injection wells. Otherwise, the cells are too large to accurately simulate changes in saturation. Well modules are another option for simulating near-well processes. However, the coarser grid spacing appears sufficient to simulate pressure changes on a basin scale.

Scoping level simulations were run with the multi-phase code STOMP in 2D mode. The first set of simulations was completed based on general conditions in the model domain for 5 by 5, 6 by 6, and 7 by 7 well clusters at several injection rates. Simulation results were analyzed for injection potential and pressure buildup. The second set of simulations was based on site-specific conditions at seven potential regional storage sites identified in the pipeline routing study. These simulations were used to evaluate the range of conditions expected within the Arches Province. The simulations were also used to assess effects of relative permeability curves based on Leverett J-function fit of mercury injection capillary pressure test data on Mt. Simon rock cores completed in association with the Arches Province. In general, the simulations seemed insensitive to capillary pressure relationships, suggesting these processes may not be critical for basin-scale models. The local-scale column models were useful for establishing the expected magnitude of plume movement and pressure buildup in the near-field. Furthermore, using representative columns from proposed regional storage sites aided in estimating plume size and pressure buildup at each site. The simulations also provided a basis for balancing injection rates across sites to maximize sweep efficiency and balance pressures in the near-field.

The preliminary basin-scale multi-phase simulations indicate that more grid refinement and material property evaluation is needed near the injection areas to capture the impacts of injecting a significant amount of mass into a regional reservoir. With the current model, the effects are too localized and probably not representative of the regional effect of multiple injection areas with large amounts of total injected mass. The next steps will be to refine the grid further, particularly in the vertical direction and use a number of wells within each injection area to inject the CO₂. A network of wells within each injection area will provide a more representative model and distribute the CO₂ more reasonably into the

reservoir. In addition, the regional model will be used to establish boundary conditions for submodels where the grid resolution and injection scenarios can be constructed in a more realistic manner. The model has several inherent assumptions and limitations related to depicting the nature of deep rock formations. This is a basin-scale simulation study, and many trends in geology and input parameters were generalized. The variable density models were created with fairly coarse grid spacing and many of the complicated processes related to CO₂ storage. The simulation results are intended to provide general guidance for a large region of the Midwestern U.S. A CO₂ storage project would require field work such as seismic surveys, drilling, geophysical logging, reservoir tests, detailed reservoir modeling, and system design. The results of this report shall not be viewed or interpreted as a definitive assessment of suitability of candidate geologic CO₂ storage formations, the presence of suitable caprocks, or sufficient injectivity to allow CO₂ sequestration to be carried out in an economical manner.

Section 6.0: REFERENCES

Battelle. 2010. *Data Package Summary Report for Simulation Framework for Regional Geologic CO₂ Storage Along Arches Province of Midwestern United States*. Topical Report Prepared for USDOE/NETL Award# DE-FE0001034 and Ohio Dept. of Development Grant CDO/D-10-03.

Battelle. 2011. *Conceptual Model Summary Report for Simulation Framework for Regional Geologic CO₂ Storage Along Arches Province of Midwestern United States*. Topical Report Prepared for USDOE/NETL Award# DE-FE0001034 and Ohio Dept. of Development Grant CDO/D-10-03.

Clifford, M.J. 1973. Hydrodynamics of Mt. Simon Sandstone, Ohio and Adjoining Areas. *Underground Waste Management and Artificial Recharge*, Vol. 1, p. 349-356.

Eberts, S.M. and L.L. George. 2000. "Regional Ground-Water Flow and Geochemistry in the Midwestern Basins and Arches Aquifer System in Parts of Indiana, Ohio, Michigan, and Illinois," U.S. Geological Survey Professional Paper 1423-C. 103 p.

Gupta, N, and E.S. Bair. 1997. Variable-Density Flow in the Mid-Continent Basins and Arches Region of the United States. *Water Resources Research*, v. 33, no. 8, p. 1785-1802.

Langevin, C.D., D.T. Thorne, Jr., A.M. Dausman, M.C. Sukop, and Weixing Guo, 2007. SEAWAT Version 4: A Computer Program for Simulation of Multi-Species Solute and Heat Transport: U.S. Geological Survey Techniques and Methods Book 6, Chapter A22, 39 p.

Leverett. M.C. 1941. "Capillary Behaviour in Porous Solids". *Transactions of the AIME* (142): 159–172.

McDonald, G. and A.W. Harbaugh. 1988. "A Modular Three-Dimensional Finite-Difference Ground Water Flow Model." *Techniques of Water Resources Investigations of the U. S. Geological Survey*, Book 6, Chapter A1.

Nicot, J.P., S. Hovorka, and J. Choi, 2009. "Investigation of Water Displacement Following Large CO₂ Sequestration Operations". *Energy Procedia* 1, 2009, p. 4411-4418.

Person, M., A. Banerjee, J. Rupp, C. Medina, P. Lichtner, C. Gable, R. Pawar, M. Celia, J. McIntosh, and V. Bense, 2010. "Assessment of Basin-Scale Hydrologic Impacts of CO₂ Sequestration, Illinois Basin," *International Journal of Greenhouse Gas Control*, v. 4, p. 840-854.

U.S. Department of Energy (U.S. DOE). 2008. Carbon Sequestration Atlas of the United States and Canada. National Energy Technology Laboratory, Pittsburgh, PA, USA.

White, M.D. and M. Oostrom. 2000. *STOMP Subsurface Transport Over Multiple Phases, Version 2.0, Theory Guide*. PNNL-12030, UC-2010, Pacific Northwest National Laboratory, Richland, Washington.

White, M.D. and M. Oostrom. 2006. *STOMP Subsurface Transport Over Multiple Phases, Version 4.0, User's Guide*. PNNL-15782, Pacific Northwest National Laboratory, Richland, Washington.

White, M.D. and B.P. McGrail. 2005. *STOMP Subsurface Transport Over Multiple Phases, Version 1.0, Addendum: ECKEChem Equilibrium-Conservation-Kinetic Equation Chemistry and Reactive Transport*. PNNL-15482, Pacific Northwest National Laboratory, Richland, Washington.

White, S.K., and Zang, Z.F. 2011. *Draft Report: Impacts of Well Spacing and Reservoir Heterogeneity on the Extent of the Injected CO₂ Plume*, FutureGen Industrial Alliance. Report No. PNWD-4289.

Zhou, Q., J.T. Birkholzer, E. Mehnert, Y.-F. Lin, and K. Zhang. 2010. “Modeling Basin- and Plume-Scale Processes of CO₂ Storage for Full-Scale Deployment;” *Ground Water*, v. 48, p. 494-514.